



universität
wien

MASTERARBEIT

Titel der Masterarbeit

„Characterization of the *fdx* promoter for establishment of an expression system as well as the construction and analysis of a *pibD* deletion mutant of *Natrialba magadii*”

verfasst von

Agnes Kogler, BSc

angestrebter akademischer Grad

Master of Science (MSc)

Wien, 2015

Studienkennzahl lt. Studienblatt:

A 066 830

Studienrichtung lt. Studienblatt:

Masterstudium Molekulare Mikrobiologie und Immunbiologie

Betreut von:

Ao. Univ.-Prof. Dipl.-Biol. Dr. Angela Witte

TABLE OF CONTENTS

1. INTRODUCTION	10
1.1. Halophilic <i>Archaea</i>	10
1.1.1. Adaptations to an extreme environment.....	12
1.1.2. Polyploidy	14
1.1.3. Transcription	15
1.1.3.1. Gene expression systems.....	16
1.1.4. Archaeal flagella.....	17
1.1.4.1. Characteristics	17
1.1.4.2. Components and assembly	18
1.1.4.3. The peptidase FlaK/PibD	19
1.2. The haloalkaliphilic archaeon <i>Natrialba magadii</i>	20
1.2.1. General characteristics.....	20
1.2.2. Laboratory strains	21
1.2.3. Transformation	21
1.2.4. Shuttle vectors.....	22
1.2.5. Gene expression systems for <i>N. magadii</i>	23
1.2.6. Flagellum of <i>N. magadii</i>	24
1.3. Viruses of halophilic <i>Archaea</i>	26
1.3.1. The virus Φ Ch1	27
1.3.1.1. General features	27
1.3.1.2. Life cycle.....	28
1.3.1.3. Genome organization	28
1.3.1.4. Tail-fibre protein	30
2. MATERIAL	32
2.1. Strains	32
2.1.1. <i>Escherichia coli</i>	32
2.1.2. <i>Natrialba magadii</i>	32

2.2.	Media	32
2.2.1.	Bacterial media	32
2.2.2.	Archaeal media.....	33
2.3.	Antibiotics	34
2.3.1.	<i>E. coli</i>	34
2.3.2.	<i>N. magadii</i>	35
2.4.	Primer	35
2.5.	Plasmids	36
2.6.	Kits.....	37
2.7.	Nucleotides.....	38
2.8.	Size markers	38
2.8.1.	DNA – Agarose gels.....	38
2.8.2.	Protein – SDS-PAGE.....	38
2.9.	Enzymes	39
2.9.1.	Restriction enzymes.....	39
2.9.2.	DNA polymerases.....	39
2.9.3.	DNA-modifying enzymes.....	40
2.10.	Antibodies.....	40
2.11.	Buffers and Solutions	40
2.11.1.	DNA Gel Electrophoresis.....	40
2.11.2.	Competent cells	41
2.11.2.1.	<i>E. coli</i>	41
2.11.2.2.	<i>N. magadii</i>	41
2.11.3.	Southern Blot.....	42
2.11.4.	Isolation of Φ Ch1	43
2.11.5.	SDS-PAGE and Western Blot.....	44
2.11.6.	BgaH-measurements	45
3.	METHODS.....	46
3.1.	DNA methods	46
3.1.1.	Agarose gel electrophoresis.....	46
3.1.2.	Polymerase chain reaction	46

3.1.3.	Plasmid isolation	48
3.1.4.	DNA purification.....	48
3.1.5.	DNA modifications.....	48
3.1.5.1.	Restriction	48
3.1.5.2.	Ligation.....	49
3.1.5.3.	Fill-in of 5'- overhangs.....	49
3.1.5.4.	Digestion of 3'- overhangs.....	49
3.1.6.	Transformation of <i>E. coli</i>	49
3.1.6.1.	Competent cells.....	49
3.1.6.2.	Transformation	50
3.1.6.3.	Screening	50
3.1.7.	Transformation of <i>N. magadii</i>	51
3.1.7.1.	Competent cells.....	51
3.1.7.2.	Transformation	51
3.1.7.3.	Screening	52
3.1.8.	Isolation of chromosomal DNA of <i>N. magadii</i>	52
3.1.9.	Southern Blot.....	53
3.1.9.1.	Synthesis of the probe	53
3.1.9.2.	Blotting of DNA, probe-hybridization and development.....	53
3.1.10.	Homozygation of a <i>N. magadii</i> deletion mutant.....	54
3.2.	ΦCh1 methods	54
3.2.1.	Isolation of virus particles	54
3.2.2.	Virus titre assay	55
3.3.	Protein methods.....	56
3.3.1.	Preparation of crude cell extracts.....	56
3.3.2.	Precipitation of proteins from supernatant.....	56
3.3.3.	SDS-PAGE	56
3.3.4.	Western Blot	57
3.3.5.	Measurements of <i>bgaH</i> -expression.....	58
3.4.	Motility assay for <i>N. magadii</i>	59
3.5.	Cloning Strategies.....	60
3.5.1.	pRo-5-fdx- <i>bgaH</i>	60

3.5.2.	pKSII-pib1-4 NovR.....	60
3.5.3.	pNB102-pibD	61
4.	RESULTS AND DISCUSSION.....	62
4.1.	Analysis of the ferredoxin promoter.....	62
4.1.1.	Aim.....	62
4.1.2.	Experimental setup	63
4.1.3.	Determination of promoter strength.....	64
4.1.4.	Influence of Iron-Concentration	67
4.1.5.	Discussion	67
4.2.	Generation and analysis of <i>N. magadii</i> L13:: <i>pibD</i> - a peptidase deletion mutant.....	69
4.2.1.	Aim.....	69
4.2.2.	Experimental setup to create a <i>pibD</i> deletion mutant.....	70
4.2.2.1.	Transformation of <i>N. magadii</i> L13.....	70
4.2.2.2.	Screening of the clones.....	72
4.2.2.3.	Passaging of candidates	72
4.2.3.	Attempt to create a deletion mutant with pKSII-pib1-4 NovR forward	73
4.2.4.	Creation of a <i>pibD</i> deletion mutant with pKSII-pib1-4 NovR reverse	75
4.2.4.1.	Confirmation with Southern Blot.....	78
4.2.5.	Complementation of <i>N. magadii</i> L13:: <i>pibD</i> mutant strain.....	80
4.2.6.	Phenotypical analysis of the <i>N. magadii</i> L13:: <i>pibD</i> mutant strain	82
4.2.6.1.	Growth behavior	82
4.2.6.2.	Western Blot.....	83
4.2.6.3.	Motility assay	84
4.2.6.4.	Surface adhesion.....	85
4.2.6.5.	Virus titre assay.....	86
4.2.7.	Discussion	87
5.	REFERENCES.....	91
6.	LIST OF FIGURES AND TABLES.....	97
7.	ABSTRACT	98

8. ZUSAMMENFASSUNG	99
9. APPENDIX.....	100
9.1. Acknowledgement.....	100
9.2. Curriculum vitae	101

1. INTRODUCTION

1.1. Halophilic *Archaea*

In 1977, Woese and Fox proposed a new model of taxonomy, where all organisms can be classified into the following groups: *Archaea*, *Bacteria* and *Eukarya* (1). Later on, Woese *et al.* introduced the new term “domain” to describe these very distinct groups, with each domain including two or more kingdoms/phyla (2). Besides the two main phyla *Euryarchaeota* and *Crenarchaeota*, the domain *Archaea* consists of the phyla *Aigarchaeota*, *Thaumarchaeota*, *Korarchaeota* and *Nanoarchaeota* (see Figure 1) (3).

Archaea are unique organisms and their classification as the third domain of life has been justified many times. Nevertheless, *Archaea* share some features exclusively with *Bacteria* or *Eukarya*. On the one hand, the size and organization of their genome is similar to that of *Bacteria*, for example, the presence of polycistronic transcription units or the utilization of Shine-Dalgarno sequences for translation-initiation. Moreover, a more apparent resemblance concerns the morphology of *Archaea* and *Bacteria*. On the other hand, however, *Archaea* share some features with *Eukarya*, e.g. homologous transcription factors, the presence of TATA-box promoters or multi-subunit RNA polymerases. Concerning the level of complexity of the molecular systems, *Archaea* lie in between *Bacteria* and *Eukarya* (4) (5).

Archaea can thrive in environments with extreme conditions, for example high or low temperature, high pressure, high or low pH or high salinity, albeit they are not restricted to such habitats (6). One group living in extreme environments are halophilic *Archaea*. They are most abundant among the *Halobacteria* within the phylum of *Euryarchaeota* (7). Some members of the family of *Halobacteriaceae*, which belongs to the class of *Halobacteria*, are: *Haloarcula*, *Halobacterium*, *Haloferax*, *Halococcus*, *Haloquadratum*, *Halorubrum*, *Natrialba*, *Natronobacterium*, *Natronococcus*, *Natronomonas* and *Natronorubrum* (8).

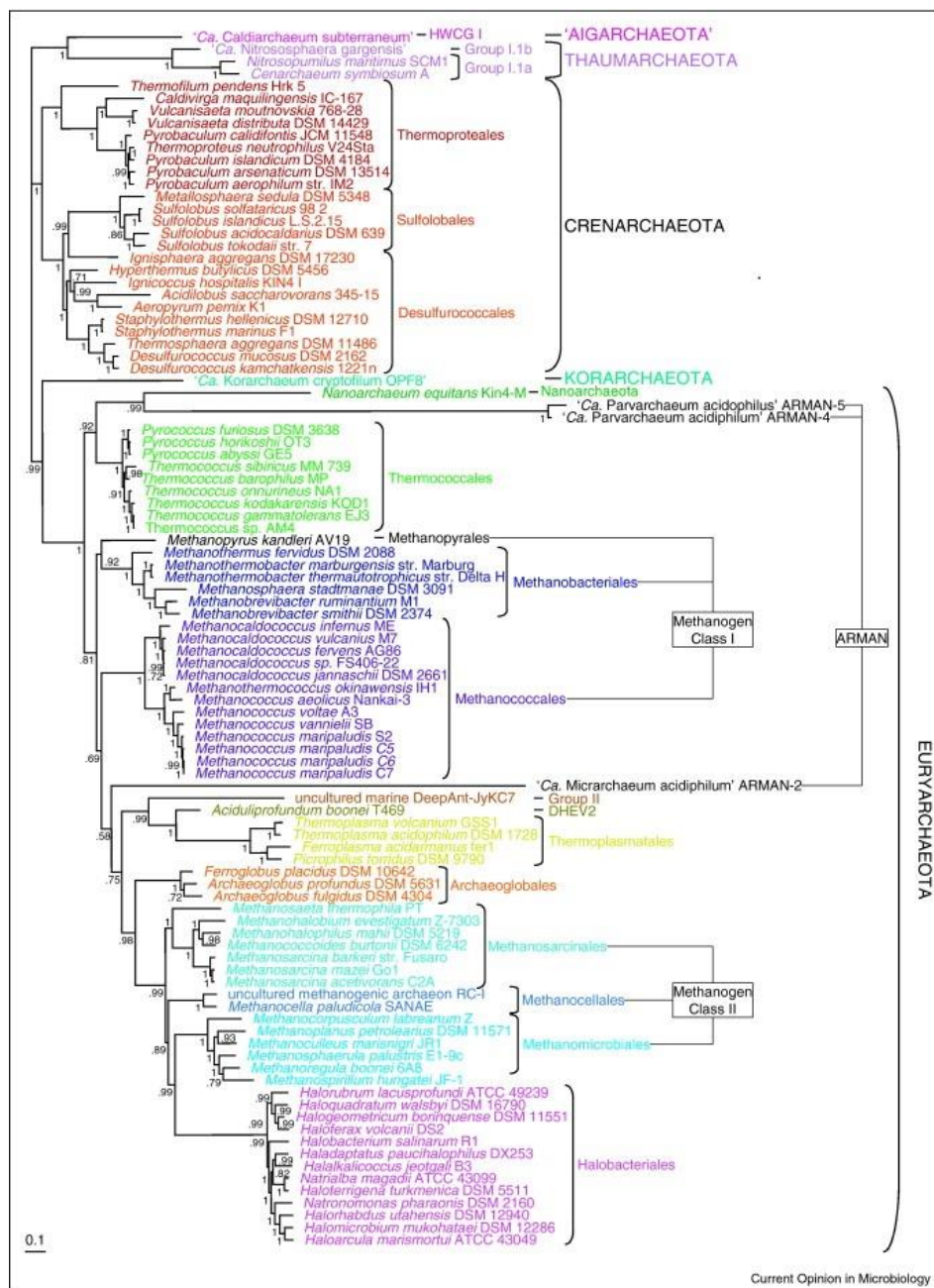


Figure 1: Overview of the domain Archaea

Archaea are a monophyletic group, constituting one of the three domains of life. Currently six phylogenetically distinct subgroups are acknowledged: the phyla *Euryarchaeota*, *Nanoarchaeota*, *Korarchaeota*, *Crenarchaeota*, *Thaumarchaeota* and *Aigarchaeota*. The classification is based on the analysis of ribosomal proteins. Adapted from Brochier-Armanant *et al.*, 2011 (3).

Halophiles are organized into different categories depending on their salt tolerance and -optimum. By the definition of Kushner, the following groups are distinguished: extreme halophiles, requiring 2.5 - 5.2 M salt for growth, borderline extreme halophiles, which grow best at salt concentrations between 1.5 - 4.0 M, moderate halophiles, which need 0.5 - 2.5 M salt for growth and halotolerant microorganisms, which do not depend on

higher salt concentrations for growth, but still are able to tolerate salt concentrations up to 2.5 M (9).

Halophilic organisms live in hypersaline environments, such as natural brines, saline lakes, marine solar salterns or saline soils. One of their habitats, referred to as thalassohaline environment, is of marine origin and arises from the evaporation of seawater. Therefore, the salt composition in thalassohaline habitats is similar to that of seawater and in addition such habitats feature a neutral to slightly alkaline pH. Contrary, athalassohaline environments are terminal lakes, where the ionic composition differs from that of seawater, e.g. the Dead Sea (10) (11) (12).

Haloalkaliphilic strains belong to one subgroup of halophiles, which does not only require high salt concentrations for growth, but also alkaline pH. Such organisms thrive in alkaline soda lakes where the pH value is 11 or higher, e.g. Lake Magadi, Kenya, Lonar Lake, India or Mono Lake, USA (13). In addition to their need for high salt concentrations and a high pH, haloalkaliphilic *Archaea* only require low amounts of the divalent cations Mg^{2+} and Ca^{2+} , which reflects the scarcity of these ions in alkaline soda lakes (10) (14). Soda Lakes are often colored red or pink, due to the prevalence of halophilic *Archaea*. As a protection against the strong sunlight, which is characteristic for such habitats, halophilic *Archaea* incorporate carotenoids and bacterioruberin (or its derivatives) into their membranes, which confers the distinctive color (5) (10).

1.1.1. Adaptations to an extreme environment

In order to survive in a high-salt environment, microorganisms have developed some adaptations so that their cytoplasm is at least iso-osmotic with the surrounding medium. Two strategies are used by halophiles to accomplish this: the “high-salt-in”-strategy and the “organic-solutes-in”-strategy. Most halophilic *Archaea* employ the first strategy, which describes the accumulation of potassium and chloride in the cell, in order to balance the osmotic pressure with the environment. However, due to the high intracellular salt concentrations this strategy requires adaptations of the enzymatic machinery in order to maintain protein function. Thus, such organisms are usually unable to survive in a low-salt environment. The second mechanism, the “compatible-solutes-in”-

strategy, is based on the biosynthesis and accumulation of organic osmotic solutes, which are mainly based on amino acids, amino acid derivatives, sugars and sugar alcohols (e.g. β -glutamine, Ectoine, 2-sulfothrehalose). Organisms employing this strategy exclude as much salt as possible from their cytoplasm and therefore only require a few protein adaptations. Such organisms are able to adapt to a broad range of salt concentrations (7) (10).

In general, the cytoplasmic membrane of *Archaea* consists mainly of glycerol phosphate phospholipids. Unlike in *Bacteria*, where the phospholipids are linked via an ester bond, the membrane lipids of *Archaea* are connected via ether bonds. Among a great diversity of archaeal lipids regarding the length, configuration and composition of the side chains (for example see Figure 2), the most common core lipid in *Archaea* is *sn*-2-3-diphytanylglycerol diether, also known as archaeol (6) (15).

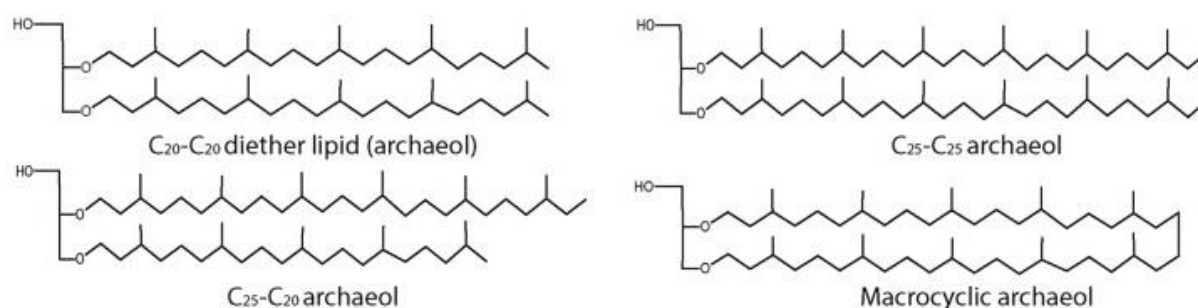


Figure 2: Structures of several membrane lipids in *Archaea*

Archaeol (*sn*-2,3-diphytanylglycerol) is the most common archaeal core lipid. It can vary in chain length and may contain macrocyclic ring structures. Archaeol can be modified, for example by hydroxylation or condensation and is especially abundant among the phylum of *Euryarchaeota*. Adapted from Jain *et al.*, 2014 (15).

A further difference between the archaeal and bacterial cell wall composition is the lack of peptidoglycan in *Archaea*. Instead, a pseudo-crystalline surface layer (S-layer), which is often highly glycosylated, encloses the archaeal cytoplasm membrane. It is assumed, that the S-layer maintains the cell shape and serves as a protection against the extreme environments that *Archaea* often face (6).

Unfortunately, only little is known about the adaptations of *Archaea* to an alkaliphilic environment. In *Natronococcus* species, for example, a prevalence of acidic residues in the S-layer is predicted to attract cations and repel anions, thus stabilizing the cell shape in

the alkaliphilic environment. Moreover, *Natronococcus* species utilize C25-C20 core lipids, which contain asymmetric phytanyl chains. Therefore, they are assembled in a zip-like structure, which leads to an enhancement of plasma membrane stiffening (14).

As mentioned before, most halophilic *Archaea* use the “salt-in-strategy” to cope with the osmotic pressure. Consequently, their enzymes require or tolerate 4 – 5 M salt concentrations, owing to some adaptations in the composition of the proteome. Halophilic proteins contain large numbers of acidic residues, while basic residues are scarce, which provides them with a negative charge. In addition, they contain less bulky hydrophobic side chains, such as phenylalanine, isoleucine or leucine, which makes them more flexible (16).

1.1.2. Polyploidy

While polyploidy is widely distributed among eukaryotes, e.g. fish, amphibian or plants, prokaryotes are generally thought to be monoploid. However, individual organisms belonging to the phylum of *Bacteria* and *Archaea* are di-, oligo- or polyploid (17). One representative of an oligoploid bacterium is the radio-resistant species *Deinococcus radiodurans*, which contains 8 chromosomal copies (18). Among the *Archaea*, an organism that has been shown to be diploid is *Archaeoglobus fulgidus* (19). Moreover, the hyperthermophilic *Methanococcus jannaschii* and the extreme halophile *Halobacterium cutirubrum* possess multiple genome copies (20) (21). Two other members of the class of *Halobacteria*, *Halobacterium salinarum* and *Haloferax volcanii*, have not only been reported to be highly polyploid, but in addition maintain a growth-phase dependent regulation of ploidy. *H. salinarum* contains around 30 genome copies per cell during exponential growth phase, but down-regulates its genome copies upon entering stationary growth phase to 10 copies per cell. For *H. volcanii*, similar observations were made; it maintains approximately 20 genome copies during exponential growth phase, but only around 12 copies in stationary phase (17).

The fact that until now, no monoploid haloarchaeal species has been described, leads to the speculation, that polyploidy may constitute a common trait of these organisms (22). One advantage of polyploidy is that wildtype genome copies can be used to repair mutated

genome copies, which results in a low mutation rate and consequently favors survival in extreme conditions. It has also been speculated, that DNA might serve as a storage polymer for phosphate, carbon and/or nitrate in polyploid organisms (23). As a member of the haloalkaliphilic *Archaea*, the species *Natrialba magadii* is also polyploid, with an estimated genome copy number of up to 50 (24).

1.1.3. Transcription

In 1979, Zillig *et al.* were the first to characterize an archaeal RNA polymerase, in particular that of the crenarchaeal *Sulfolobus acidocaldarius*. Their studies revealed a high similarity with the eukaryotic RNA polymerase II regarding subunit composition, even though the archaeal transcription machinery is much more simple (25) (26). The proteins TBP (TATA-box-binding protein) and TFB (homologue of eukaryotic transcription factor TFIIB) together with the archaeal RNA polymerase constitute the minimal requirements for the initiation of transcription in *Archaea*. TBP recognizes the TATA-box, which is located approximately 30 bp upstream of the initiation site, whereas TFB binds to the BRE (B-recognition element) located upstream of the TATA-box, thereby signifying the direction of the promoter (27). Both genetic elements, the TATA-box and BRE, are well conserved in archaeal promoters and mediate the recruitment of the RNA polymerase to the initiation site and subsequent transcription (26). In contrast to the basal transcription machinery including the general transcription factors, most of the specific transcription factors of *Archaea* resemble those of *Bacteria* (28). These specific regulators are referred to as bacterial/archaeal (BA) regulators and several of these molecules have been characterized at the molecular level, e.g. MDR1 of *A. fulgidus* or Lrs14 from *Sulfolobus solfataricus* (26).

1.1.3.1. Gene expression systems

Unlike for *Bacteria*, only a few gene expression systems have been established for *Archaea* until now. Two constitutively active promoters used in halophilic expression systems are the *fdx* and the *bop* promoter, which regulate genes encoding ferredoxin and bacterioopsin, respectively. A few inducible promoters, which allow to switch on or off the gene expression by changing the conditions, are applied in gene expression systems as well, for example heat-inducible chaperonin promoters, the tryptophanase promoter *ptna* or the potassium-responsive promoter *pkdp* (29).

A common reporter gene for promoter studies in halophilic *Archaea* is the β -galactosidase gene *bgaH*. This gene was isolated from a “superblue” mutant strain of *Haloferax alicanteii* as a 5.4 kb long DNA fragment, including three other open-reading frames (ORFs) as well. The *bgaH* gene encodes a protein comprised of 665 amino acids, resulting in a molecular mass of 74.5 kDa. This protein is extremely halophilic, thus its activity is highest at 4 M NaCl. Furthermore, it was shown to be highly specific for β -D-galactosides, e.g. ortho-Nitrophenyl- β -galactoside (ONPG) or lactulose (30) (31). Enzymatic activity of the β -galactosidase can be quantified using a spectrometric assay, due to its ability to hydrolyze ONPG into galactose and the chromogenic compound ortho-nitrophenol. If ONPG is available at excess, the amount of ortho-nitrophenol directly reflects the enzymatic activity of BgaH, which then allows further conclusions about the promoter activity (30). Studies by Patenge *et al.* in *H. salinarum* confirmed, that *bgaH*-transcript levels correspond to the enzymatic activity of the BgaH protein, indicating that no regulatory steps interfere with the assay (32). Several studies demonstrated, that the *bgaH* gene is suitable for the use as a reporter gene to analyze transcriptional regulation in various halophilic organisms, e.g. *Haloferax mediterranei*, *H. volcanii* or *H. salinarum* (31) (32) (33). A prerequisite for the use of *bgaH* as reporter gene however is that the model organisms do not encode a β -galactosidase themselves.

1.1.4. Archaeal flagella

Motility is widely spread among prokaryotes and a great diversity exists regarding the employed mechanisms. Microorganisms may move through swimming, swarming, twitching, gliding or floating. Motility is mediated either via surface structures, e.g. flagella or pili, or via internal structures, like gas vesicles or the cytoskeleton (34).

Archaea possess diverse surface structures, e.g. flagella, pili, hami or cannulae; but flagella are by far the most extensively studied (35) (36). Swimming motility, mediated via flagella, is common with *Archaea* belonging to both *Crenarchaeota* and *Euryarchaeota*. Although archaeal and bacterial flagella carry out the same function, they are very distinct regarding their composition and assembly. In fact, all three domains of life, *Archaea*, *Bacteria*, and *Eukarya*, possess unique flagella (36) (37). Besides conferring motility, flagella might be involved in other processes as well, such as surface adhesion, cell-cell contacts or the formation of biofilms.

In 1984, Alam and Oesterhelt were the first to study archaeal flagella, in particular those of *H. salinarum* (38). In the meantime, the flagella of several archaeal species have been studied intensively, e.g. *S. solfataricus*, *S. acidocaldarius*, *Methanococcus maripaludis*, *Methanococcus voltae*. More and more studies revealed, that the assembly of the archaeal flagellum strongly resembles that of type-IV-pili (T4P) in *Bacteria* (35) (36) (37).

1.1.4.1. Characteristics

Archaeal as well as bacterial flagella are rotating structures with a filament and a hook, yet the archaeal filament is much thinner with a diameter of 11-14 nm as compared to 20 nm in the bacterial filament (35) (36). In contrast to most bacterial flagella, the helical filaments of *Archaea* are right-handed. Another important difference is the mode of action: unlike in *Bacteria*, where the motor of the flagella is driven by proton-motive force, the motor of archaeal flagella is powered through ATP-hydrolysis (35) (37). The flagellum of *Archaea* lacks a central channel, which in *Bacteria* enables its assembly. Assembly of the archaeal flagellum is presumably facilitated through the addition of subunits to the

base of the growing flagellum, whereas in *Bacteria* the subunits travel to the tip of the flagellum for assembly (35) (36).

1.1.4.2. Components and assembly

While in *Bacteria* flagella usually are composed of only one type of flagellin, in *Archaea* several flagellins contribute to the mature flagellum structure. The only exception of this rule discovered until now are species of the genus *Sulfolobales* (35). In general, the flagellin operon in *Archaea* is comprised of genes encoding the structural proteins of the flagellum, termed flagellins (*flaA* and/or *flaB*), and various *fla*-associated genes (*flaC* to *flaJ*), which are encoded downstream of the flagellins and are co-transcribed (35) (37). Archaeal flagellins are built as pre-proteins with a signal peptide and are often modified by glycosylation on the N-terminus, just the same as bacterial type-IV-pilins. The *fla*-associated genes *flaF*, *flaG*, *flaH*, *flaI* and *flaJ* are conserved among the *Archaea* and although their specific functions are not elucidated in detail, each of them is required for flagellation. Analysis and comparison of various archaeal *fla* operons revealed differences between the two major phyla of the *Archaea*: the genes *flaCE* and *flaD* are only present in *Euryarchaeota*, whereas *flaXY* is unique for *Crenarchaeota* (35) (37). Figure 3 shows an illustration of the archaeal flagellum.

The proteins FlaI, FlaJ and PibD/FlaK, which are involved in flagellum assembly, share great homology with components of the bacterial T4P assembly systems. The ATPase FlaI displays homology to the T4P components PilB/PilT, which are involved in assembly and disassembly of the pilus. Next, the membrane protein FlaJ exhibits similarity to the inner membrane protein PilC in the T4P-system. It contains two well-conserved cytoplasmic loops and is predicted to form the central core complex, together with FlaI. This complex then may facilitate the interaction with other components and serves as a platform for the assembly of the whole flagellum. Finally, the peptidases PibD/FlaK resemble the prepilin peptidase PilD involved in T4P assembly (35).

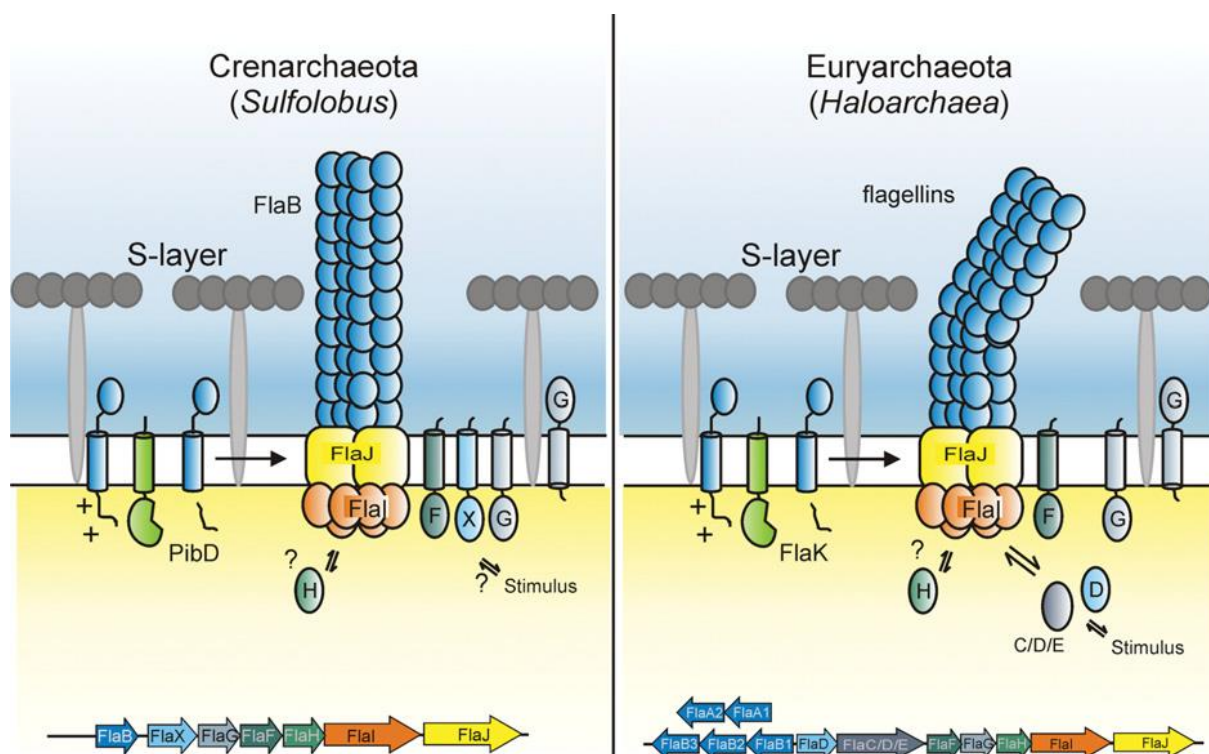


Figure 3: Structure of the archaeal flagellum and organization of the *fla* operon

On the left side, the crenarchaeal flagellum is depicted; the euryarchaeal flagellum is displayed on the right side. Several components are conserved among *Archaea*; however, FlaXY only exists in *Crenarchaeota*, whereas FlaCE and FlaD are only present in *Euryarchaeota*. The flagellum of *Euryarchaeota* is composed of several types of flagellins, whereas the flagellum of *Sulfolobales* is only composed of one type of flagellin. The conserved proteins FlaJ and FlaI build the central core complex, with FlaI constituting an ATPase and FlaJ building an anchor for the flagellum. The homologous peptidases PibD and FlaK process the preflagellins and enable the assembly of the flagellum. Proteins FlaF and FlaG may play a role in anchoring the flagellum in the membrane. The proteins FlaCE and FlaD are involved in signal transduction. The concrete functions of FlaH as well as FlaXY are currently unknown. Both the genes for the flagellins as well as the *fla*-associated genes are encoded by the *fla* operon. Adapted from Gosh and Albers, 2011 (35).

The protein FlaH possesses an incomplete ATPase like domain and is the only other cytoplasmic component besides FlaI. Although its function is not studied in detail, it is speculated that FlaH might modulate the activity of FlaI (35) (37). The components FlaF and FlaG are monotopic membrane proteins, which may be involved in the anchoring of the flagellum into the archaeal cell envelope (37).

1.1.4.3. The peptidase FlaK/PibD

FlaK/PibD belong to the type IV prepilin peptidases and contain two conserved aspartic acid residues in their catalytical core (Asp¹⁸ and Asp⁷⁹ in FlaK and Asp²³ and Asp⁸⁰ in PibD), which enable recognition and processing of the pre-flagellins (39) (40).

Proteolytical removal of the positively charged N-terminal signal sequences on the flagellins facilitates the assembly of the flagellum (35). In general, the signal peptide of preflagellins in *Archaea* has a length of 6 to 12 amino acids (41). In *M. voltae*, the glycines at position -1 and +3, as well as the lysines at positions -2 and -3 are mandatory for cleavage by FlaK (42). The peptidase FlaK from *M. maripaludis* and *M. voltae* require a minimal signal peptide length of at least 5 amino acids, whereas the peptidase PibD of *S. solfataricus* recognizes signal peptides as short as 3 amino acids (41) (43). The more flexible nature of PibD compared to FlaK correlates with its broad substrate range, whereas FlaK is predicted to solely cleave pre-flagellins (43) (44).

1.2. The haloalkaliphilic archaeon *Natrialba magadii*

1.2.1. General characteristics

The haloalkaliphilic archaeon *N. magadii* was isolated from Lake Magadi, Kenya, by Tindall *et al.* in 1984 (45). At first, it was placed into the genus *Natronobacterium*, but due to comparative 16s rRNA analysis, it was later transferred to the genus *Natrialba* (46). *N. magadii* is a member of the family of *Halobacteriaceae* within the phylum of *Euryarchaeota*. Its cells are rod-shaped with a dimension of 0.5 -1.0 x 1.0 - 5.0 μm (47). As a haloalkaliphilic organism, *N. magadii* requires 4 M NaCl and pH-conditions between 8.5 and 10.5 for optimal growth. Since *N. magadii* is rated among the extremely halophilic organisms, it is not able to withstand sodium chloride concentrations lower than 2 M. Furthermore, *N. magadii* is sensitive to low temperatures and prefers temperatures between 37 and 42 °C. Typical for haloalkaliphilic *Archaea*, it only requires low Mg^{2+} concentrations (below 10 mM). Even if optimal growth conditions prevail, *N. magadii* has a generation time of 9 hours in logarithmic growth phase. Physiologically, *N. magadii* is a strict aerob and chemoorganotrophic organism, which grows proteolytically and consequently uses amino acids and peptides instead of carbohydrates as carbon and energy source (45).

1.2.2. Laboratory strains

In 1997, a virus termed Φ Ch1 was isolated from *N. magadii* upon spontaneous lysis. So far, *N. magadii* is the only known host for this temperate virus. Repeated subculturing and subsequent testing of single colonies yielded in the generation of a non-lysogenic *N. magadii* strain, termed *N. magadii* L13. An additional strain was acquired by infection of L13 with isolated virus particles. This strain, termed *N. magadii* L11, carries the provirus integrated in its genome, equally as the original isolate from Lake Magadi. Both strains, *N. magadii* L11 and *N. magadii* L13, were confirmed to belong to the species *N. magadii* and are used in our laboratory ever since (48). Electron micrographs of both strains *N. magadii* L11 and *N. magadii* L13 are depicted in Figure 4.

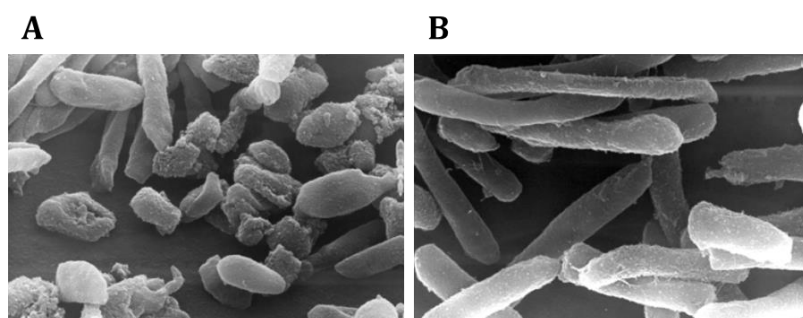


Figure 4: Morphology of *N. magadii*

Electron micrographs show the *N. magadii* L11 strain carrying the provirus in **A** and the *N. magadii* L13 strain, which is cured of the virus in **B**. Adapted from Iro, 2006 (49).

1.2.3. Transformation

Cline and Doolittle were the first to transfect a member of the *Archaea* with DNA. They used ethylenediaminetetraacetic acid (EDTA) for the removal of the paracrystalline glycoprotein S-layer, resulting in spheroblastic cells. Transfection of these competent cells was then achieved by coupling of the DNA to polyethylenglycol (PEG)-600 (50). Since this method is not applicable for *N. magadii*, a transformation procedure including some alterations has been established only recently. For transformation of *N. magadii*, cells are treated with the antibiotic bacitracin, which prevents glycosylation of the S-layer. In addition, incubation of the cells with proteinase K leads to a partial digestion of the S-layer, giving rise to spheroblastic cells. These competent cells can then be transformed

with foreign DNA by use of PEG-600. With this method, a transfection efficiency of 10^4 PFU/ μg DNA can be obtained for *N. magadii* cells when incubated with ΦCh1 DNA. Although this transfection efficiency is lower compared to other halophilic strains, the establishment of a transformation system for *N. magadii* still is a breakthrough for future studies on ΦCh1 and its host *N. magadii* (51).

1.2.4. Shuttle vectors

In addition to the development of a transformation procedure, the establishment of shuttle vectors that work for *N. magadii* as well as for *Escherichia coli* is substantial for scientific progress.

Two selectable markers are commonly used for the work with *N. magadii*: novobiocin and mevinolin. The antibiotic novobiocin interferes with the DNA-supercoiling activity of the B-subunit of DNA gyrase (GyrB), thereby inhibiting its ATPase activity (52). Holmes *et al.* were able to isolate a mutated *gyrB* variant from a member of the genus *Haloferax*. Subsequent comparative studies with the wildtype *gyrB* gene revealed, that the isolate contained three point mutations, resulting in a resistance against novobiocin (53). The other compound, mevinolin, inhibits the HMG-CoA reductase, which is responsible for the synthesis of mevalonate. In halophiles, mevalonate is an essential compound of the isoprenoid side chains of lipids. A mutated version of the gene coding for the HMG-CoA reductase was isolated from *H. volcanii*, which confers tolerance against mevinolin by producing the enzyme at excess (54).

For halophilic *Archaea*, the *repH* gene and an AT-rich region located upstream of the gene constitute the minimal replication origin (55). ORF53 and ORF54 of the virus infecting *N. magadii*, ΦCh1 , show high similarity to the *repH* gene, therefore they were used for the construction of a shuttle vector (51). Distinct parts of ORF53 and ORF54 were cloned into the vector pNov-1, which was generated by introducing the mutated *gyrB* gene from *H. alicantei* into pBluescript II KS⁺. These plasmids, termed pRo-1 to pRo-11, were then analyzed regarding their ability for autonomous replication after transformation into *N. magadii* L13. With a transformation rate of 10^3 CFU/ μg DNA, the shuttle vector pRo-5 gave the best result and is employed for transformation of *N. magadii* ever since (51).

The plasmid pNB102 is applied as a shuttle vector for the transformation of *N. magadii* as well. This plasmid originates from plasmid pNB101, which was isolated from a haloalkaliphilic archaeon. To enable replication in *E. coli*, the ColE1 origin of replication of *E. coli* was inserted into pNB101, as well as two selectable markers providing resistance against mevinolin and ampicillin (56).

1.2.5. Gene expression systems for *N. magadii*

So far, no gene expression system within *N. magadii* could be established. Therefore, over-expression of proteins from *N. magadii* or Φ Ch1 is achieved using a gene expression system of *E. coli*. Due to the pronounced differences in physiology and growth conditions between these two organisms, archaeal proteins produced in *E. coli* are not equivalent to intrinsically produced ones. To overcome the problems caused by heterologous gene expression, for example improper folding of the proteins, the establishment of an expression system in *N. magadii* is a necessity. Two approaches are currently pursued: on the one hand, the development of an expression system using the tryptophanase promoter (*ptnaN*) is in progress, and on the other hand, the ferredoxin promoter (*pfdx*) is a potential candidate for usage in an expression system.

The inducible *ptnaN* of *N. magadii*, which regulates the tryptophanase-gene (*tnaA*), was characterized in 2011 by Alte (57). It was shown, that gene expression can be switched on after induction with 2 mM tryptophan. The possibility to switch on gene expression from *ptnaN* at a desired time point is a big benefit for the use in an expression system. On the downside, however, the activity of *ptnaN* is rather low, making it difficult to express proteins with a satisfactory yield (57). Nevertheless, the development of an expression system using *ptnaN* was further driven by the construction of a *N. magadii* L13 *tnaA* deletion mutant (*N. magadii* L13::*tnaA*). This strain lacks *tnaA*, which degrades the inducer tryptophan upon gene expression, thereby eliminating the need to add the inducer on a daily basis (58). Further studies with *N. magadii* L13::*tnaA* will show, whether efficient gene expression from constructs using *ptnaN* is possible.

The ferredoxin gene (*fdx*) of *H. salinarum*, which is a so-called house-keeping gene, was first isolated in 1993 by Pfeifer *et al.* (59). Following studies on the ferredoxin promoter

(*pfdx*) in *H. volcanii* using the *bgaH* reporter-gene revealed that the promoter is strong and constitutively active. High levels of BgaH activity were observed during exponential as well as stationary phase, albeit the activity was slightly reduced during stationary growth phase (60). However, trials to use *pfdx* of *H. salinarum* for the expression of gp34 of Φ Ch1 in *N. magadii* did not result in an enhancement of gene expression compared to the endogenous promoter. It was speculated that the transcriptional machinery of *N. magadii* might not recognize *pfdx* as good, considering that the two organisms belong to different genera and inhabit different environmental niches (61).

1.2.6. Flagellum of *N. magadii*

N. magadii is motile owing to its polar flagella, which are 10 nm in diameter and were shown to consist of four subunits, termed FM1 to FM4 or FlaB1-FlaB4 (62) (63) (64). Table 1 summarizes the different nomenclatures for the flagellins of *N. magadii* and their molecular masses as estimated by SDS-PAGE and calculated from genome sequencing, respectively.

	estimated by SDS-PAGE	calculated from genome sequencing
FlaB1/FM4	45	21.4
FlaB2/FM2	60	26.5
FlaB3/FM1	105	41.7
FlaB4/FM3	59	27.0

Table 1: Molecular masses of subunit flagellins of *N. magadii*

The four subunit flagellins of *N. magadii* can be described by different terms, namely FlaB1 to FlaB4 or FM1 to FM4, the corresponding subunits are indicated. Molecular masses were estimated from SDS-PAGE by Fedorov *et al.* (62) and calculated from genome sequencing by Serganova *et al.* (64). Molecular masses are given in kDa.

As can be seen from Table 1, the molecular masses estimated from SDS-PAGE (62) are 2 - 2.5 times larger than calculated from genome-sequencing (64). Firstly, this can be explained by the large amounts of acidic amino acids in the flagellins of *N. magadii*, which

alter the migration behavior of the proteins. Secondly, posttranslational modifications of the flagellins contribute to the poor agreement of the data. In particular, FlaB1 and FlaB2 are modified by N-glycosylation (64). The two subunits FlaB2 and FlaB4 share a high sequence homology and are distributed uniformly in the flagellum filament (62) (63). Detailed analysis of the composition of the filament revealed that it is built of several longitudinal rows, which each consist of one type of flagellin. It is speculated, that the analogical FlaB2/FlaB4 and FlaB1 determine the helical shape of the filament, whereas FlaB3 plays an auxiliary role in the biogenesis of the flagellar filament (63) (64). This theory is based on two observations: Unlike the other flagellins, FlaB3 harbors an insertion in its middle region, which significantly increases its size. In addition, it is less abundant than the other three types of flagellins (63) (64).

The four flagellins of *N. magadii* are located in an operon, as shown in Figure 5. The flagellins FlaB1 to FlaB4 are encoded by ORF1 to ORF4, whereas ORF5 might encode a homologue of FlaF from *M. voltae* and *M. jannaschii*.

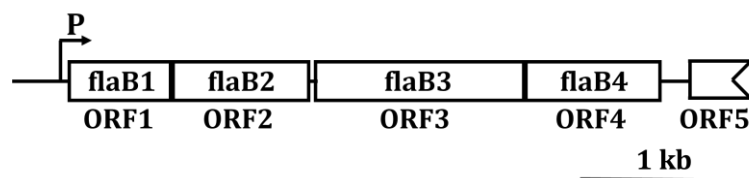


Figure 5: Illustration of the *flaB* genes of *N. magadii*

The four flagellins FlaB1 to FlaB4 are encoded by ORF1 to ORF4. The operon further contains an additional ORF, which might code for a homologue of FlaF. The scale represents 1 kb.

Contrary to the C-terminal amino acids of *N. magadii* flagellins, the N-termini were shown to be highly conserved among *Archaea*. They encode the signal peptide, which is most likely cleaved between glycine and glutamine in the RGQ sequence. The length of the signal peptide varies between the flagellins; in FlaB1, the signal peptide consists of 11 amino acids (43) (64).

1.3. Viruses of halophilic *Archaea*

The first archaeal virus was described in 1970, even before *Archaea* were phylogenetically separated from *Bacteria* (65). Since then, intense research on archaeal viruses discovered nearly 130 viruses, 90 of which infect halophilic *Archaea* (66). Contrary to bacterial viruses, which contain either DNA or RNA, all archaeal viruses studied so far utilize DNA to store their genetic material. Although more than half of all studied archaeal viruses belong to the phylum of *Euryarchaeota*, broader morphological diversity is displayed by crenarchaeal viruses (65). Based on their morphology, the known archaeal viruses were grouped into 16 different types, many of which are unique for archaeal viruses, e.g. pleiomorphic and lemon-shaped viruses (65) (66). Head-tail viruses infect *Archaea* as well as *Bacteria* and belong to the order *Caudovirales*. The tail morphology further allows the distinction of three families: *Myoviridae* feature long and contractible tails, whereas *Siphoviridae* possess long, but non-contractible tails and the family of *Podoviridae* exhibits short, non-contractible tails (67). The majority of archaeal viruses described so far belongs to the family of *Myoviridae*, which solely infect member of the *Euryarchaeota* (66) (65). Furthermore, they are especially abundant among halophilic *Archaea* and often feature a broad host range (66). Viruses infecting halophilic *Archaea* are often dependent on high salt concentrations to maintain infectivity. However, even after the exposure to a low salt environment, they can regain infectivity when high-salt conditions are rehabilitated (65). Until now, the genomic sequences of 17 halophilic head-tail viruses have been resolved, all of which feature circularly permuted or non-permuted dsDNA molecules with direct terminal repeats. Moreover, the average GC content of these resolved genomes was above 50%, which is a common trait of halophiles (67).

1.3.1. The virus Φ Ch1

1.3.1.1. General features

As mentioned before, the virus Φ Ch1 was isolated upon spontaneous lysis of *N. magadii* batch cultures in 1997. According to its morphology, Φ Ch1 belongs to the family of *Myoviridae*. It has a head-tail structure, with a total length of approximately 200 nm. The icosahedral head of the virus spans 70 nm, whereas the contractible tail is 130 nm long and approximately 20 nm wide (see Figure 6) (48).

Super-infection of the *N. magadii* L11 strain is not possible, but the cured strain *N. magadii* L13 can be infected with virus particles, therefore it serves as an indicator strain. Various attempt to infect other members of the haloalkaliphilic *Archaea* like *Natronobacterium pharaonis*, *Natronobacterium gregoryi* and *Natronococcus occultus* with Φ Ch1 failed, leaving *N. magadii* the only known host of Φ Ch1 (48).

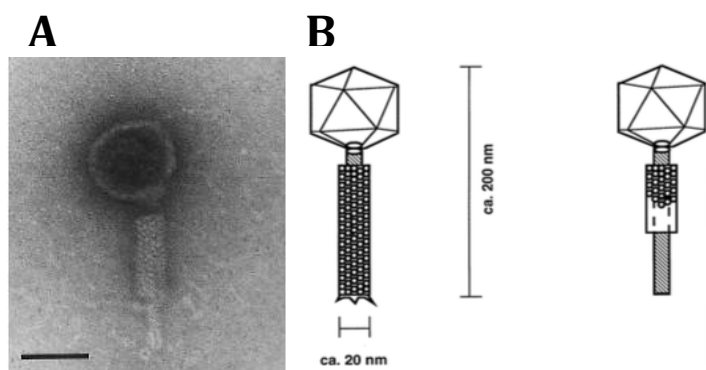


Figure 6: Electron micrograph and illustration of virus Φ Ch1

In **A** an electron micrograph of purified Φ Ch1 particles, stained with phosphotungstate is shown; with the bar representing 50 nm. In **B**, a graphical illustration of the virus particle is depicted, including its dimensions. Adapted from Witte *et al.*, 1997 (48).

A close relative of Φ Ch1 is the halovirus Φ H, which infects *H. salinarum* (68). Even though only parts of its genome have been sequenced, Φ H is the best studied halovirus so far. Same as Φ Ch1, Φ H is a temperate, head-tail virus with a 59 kb dsDNA genome (69). Comparison of the central part of the Φ Ch1-genome with the so-called L-fragment of Φ H revealed a sequence similarity of 50-95 % (70). This is a surprising observation, considering that the two hosts reside in different habitats and in particular require different pH-conditions for growth (69) (70).

Φ Ch1 is highly adapted to the physiology of *N. magadii*. Equal to its host, the virus is dependent on high ionic strength and is not able to tolerate NaCl-concentrations below 2 M without losing its structural stability and infectivity (48).

Similar to other halophiles, the proteome of Φ Ch1 is mainly acidic with isoelectric points between 3.3 and 5.2 (48). Due to their negative charge, the affinity of acidic amino acids to sodium-dodecylsulfat is reduced. This in turn results in a slower migration of acidic proteins during SDS-PAGE, which leads to a discrepancy with the molecular masses which can be calculated from the amino acid sequence (71).

1.3.1.2. Life cycle

Φ Ch1 is a temperate virus, thus it maintains a lytic as well as a lysogenic state. In the early logarithmic growth phase, Φ Ch1 remains integrated into the chromosome of *N. magadii* as a provirus. The production of virus particles starts at the transition to late logarithmic growth phase, which is why the lysis of *N. magadii* L11 cultures can be described as growth-phase dependent. Finally, after approximately 4 days of growth and when the burst size of approximately 150 virus particles per cell is reached, lysis of the cell starts and virus particles are released (48). Two regulators of this transition have already been revealed: ORF48 and ORF49 (see Figure 7) (72) (73).

1.3.1.3. Genome organization

The icosahedral head of the virus contains the genome, consisting of linear DNA as well as RNA. Upon experimental analysis, the 58498 bp long DNA of Φ Ch1 exhibit a GC-content of 62 %, which is in agreement with the calculated content based on the genomic sequence (48) (70). The 80 - 700 bp long RNA-species are presumably encoded by the host *N. magadii* and were speculated to be involved in DNA-packaging (48). Φ Ch1 DNA has been shown to be terminally redundant and circularly permuted, hence it is estimated that the packaging of DNA into the viral heads is facilitated via the “headful” mechanism (70).

The complete genome-sequence of Φ Ch1 was resolved in 2002. Subsequent analysis of the sequence revealed 570 ORFs, 98 of which are protein-coding genes. Almost every protein-coding ORF starts with an ATG; only four ORFs are initiated by a GTG. A map displaying the protein-coding ORFs and the verified or putative functions of their gene products can be viewed in Figure 7.

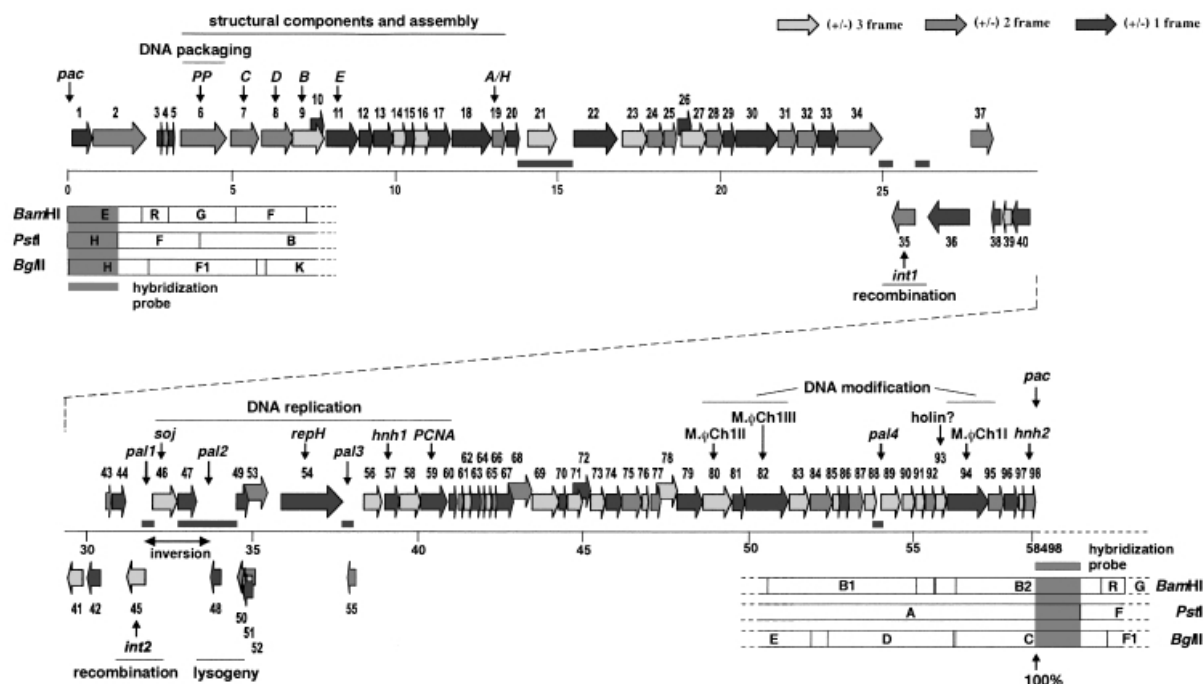


Figure 7: Genome organization of the virus Φ Ch1

Genome sequencing of Φ Ch1 DNA displayed 98 protein-coding ORFs, which are depicted as arrows; putative or determined functions of the gene products are given. The genome can be organized in three parts: the left part encodes structural proteins, the central part contains genes that are involved in DNA replication and regulation of gene expression and the right part encodes proteins that play a role in DNA modification. Adapted from Klein *et al.*, 2002 (70).

The genome is organized in transcriptional units, thereby enabling an optimal timing of gene expression. The genome can be divided into three parts: the left part codes for structural proteins, the middle part is comprised of genes involved in DNA replication and the right part harbors genes that play a role in the modification of DNA. Interestingly, the left and the right part exclusively contain rightward-transcribed genes, whereas the middle part encodes rightward- as well as leftward-transcribed genes (70).

The capsid of the virus is composed of four major proteins (termed A, E, H and I) and five minor proteins (termed B, C, D, F and G) (48). Detection with α - Φ Ch1 antiserum showed, that the capsid proteins B, C and D, which are encoded on ORFs 9, 7 and 8 respectively, are expressed at a much lower extent than proteins A and E (70). The most extensively studied capsid protein is the 35.8 kDa major protein E, which is encoded by ORF11. In the lysogenic strain, the mRNA transcribed from ORF11 can be detected approximately 20 hours before onset of lysis, which is in good agreement with its involvement in the composition of the viral capsid. Protein E is associated with the membrane and presumably plays a role in the packaging of virus DNA into the capsid (74).

Interestingly, Φ Ch1 DNA is partly methylated, unlike the genome of its host *N. magadii*. Methylation of adenine on dam-like sites (5'-GATC-3') takes place in a fraction of the genome, while the other part remains non-methylated (48). The *mtase* gene (ORF94) was shown to encode a methyltransferase of the β -subgroup of N⁶-adenin methyltransferases, which is termed M. Φ Ch1-I. Since the mRNA of M. Φ Ch1-I is not detectable until 24 hours before onset of lysis, the *mtase* gene is classified as a "late" gene. This is in accordance with the observation that about 50 % of Φ Ch1 genomes from the lysogenic strain are methylated, whereas only 5 % of progeny genomes of a newly infected strain are methylated (75).

1.3.1.4. Tail-fibre protein

ORFs 34, 35 and 36 are located in the middle of the Φ Ch1 genome (see Figure 7) (70). They represent a phase-variation system, which allows the virus to produce different variants of tail-fibre proteins (76). ORF35 encodes an integrase, which is termed Int1. The protein is 25.5 kDa in size and belongs to the λ family of site-specific recombinases (70). In the lysogenic strain *N. magadii* L11, *int1* transcripts are detectable 12 hours after inoculation. It was shown that the integrase is constitutively expressed, albeit expression increases around 72 hours, coinciding with the onset of lysis (76). The fragments IR-R and IR-L, which contain several conserved 30 bp direct repeats, are embedded within the ORFs 34 and 36. The designated gene products of the two ORFs, termed gp34 and gp36, have a molecular weight of 41 - 54 kDa and share a sequence similarity of approximately

33 % (70) (77). Both proteins were shown to be part of the mature virus particle (77). Since a promoter sequence is only encoded upstream of ORF34, but not ORF36, solely ORF34 is transcribed. (76) Upon inversion through Int1, the C-terminal parts of ORF34 and 36 are exchanged, giving rise to diverse variants of tail-fibres. The variants differ in the exact copy number of the repeats and the orientation of the integrase ((+) or (-) direction) (77). One variant representing the (+) orientation is termed gp34₁ and another, carrying the *int1*-gene in (-) orientation is termed gp34₅₂. However, binding studies of purified gp34₁ and gp34₅₂ revealed that only gp34₅₂ is able to attach to *N. magadii* L13. Since the N-terminal part of gp34₅₂ is dispensable for binding, the C-terminal part was further investigated. Both proteins harbor a galactose-binding domain, but conserved amino acid residues that are typical for this kind of domain are only present in gp34₅₂. Indeed, the mutation of a conserved tryptophan residue of gp34₅₂ inhibited binding of the protein to *N. magadii*. Moreover, incubation of gp34₅₂ with ≥ 25 mM α -D-galactose prevented the attachment to the cell surface of *N. magadii*. Even more so, the presence of 50 mM α -D-galactose in the medium resulted in a decrease of Φ Ch1 infectivity towards *N. magadii* L13 by four orders of magnitude. All these findings indicate that the attachment of Φ Ch1 to *N. magadii* is mediated via galactose-residues on its cell surface. There are two structures, which could mediate the attachment of the virus to *N. magadii*: the glycoproteins in the S-layer and the glycosylated flagellum proteins FlaB1 and FlaB2 (76).

2. MATERIAL

2.1. Strains

2.1.1. *Escherichia coli*

Strain	Genotype	Source
XL1-Blue	<i>recA1, endA1, gyrA96, thi-1, hsdR17, supE44, relA1, lac</i> [F', proAB, <i>lacI</i> ^q ZΔM15, Tn 10 (Tet ^r)]	Stratagene

2.1.2. *Natrialba magadii*

Strain	Genotype	Source
L11	wildtype, virus ΦCh1 integrated in genome	Witte <i>et al.</i> , 1997
L13	„cured“ strain, without ΦCh1	Witte <i>et al.</i> , 1997
L13:: <i>pibD</i>	peptidase <i>pibD</i> -deficient strain	this thesis

2.2. Media

2.2.1. Bacterial media

Medium for <i>E. coli</i> (LB)	
Peptone	10 g/l
Yeast extract	5 g/l
NaCl	5 g/l

dissolve components in dH₂O, for solid medium add 15 g/l agar, autoclave

2.2.2. Archaeal media

Medium for <i>N. magadii</i> (NVM⁺)	
Casaminoacids	8.8 g/l
Yeast extract	11.7 g/l
Tri-sodiumcitrate	0.8 g/l
KCl	2.35 g/l
NaCl	235 g/l

dissolve components in dH₂O, adjust pH to 9.0 with NaOH, fill up to final volume of 934 ml, for solid medium add 8 g/l agar, for soft agar add 4 g/l agar, for swimming plates add 2 g/l agar, autoclave

After autoclaving, the medium is complemented with the following:

Na ₂ CO ₃ (dissolved in sterile dH ₂ O)	37 mM
MgSO ₄ (autoclaved)	1 mM
FeSO ₄ (dissolved in sterile dH ₂ O)	20 μM

Mineral medium for <i>N. magadii</i> (NMMb⁺)			
NaCl	3.5 M	Arginine	5 mM
KCl	27 mM	Histidine	5 mM
Na ₂ HPO ₄	2 mM	Lysine	5 mM
NaH ₂ PO ₄	2 mM	Tri-sodiumcitrate	2.7 mM
Alanine	25 mM	Sodiumacetate	20 mM
Leucine	5 mM	Sodiumpyruvate	10 mM

dissolve components in dH₂O, adjust pH between 9.0 and 9.5 with NaOH, fill up to final volume of 900 ml, autoclave

After autoclaving, the medium is complemented with the following:

Na ₂ CO ₃ (dissolved in sterile dH ₂ O)	175 mM
MgSO ₄ (autoclaved)	1 mM
FeSO ₄ (dissolved in sterile dH ₂ O)	5 μM
1000x trace elements	1 ml

1000x trace elements	
MnCl ₃	4 mM
CaCl ₂	3 mM
CuSO ₄	4 mM
ZnSO ₄	3 mM

2.3. Antibiotics

2.3.1. *E. coli*

Substance	Stock concentration	Final concentration	Preparation and storage
Ampicillin	20 mg/ml	100 μg/ml	dissolved in ddH ₂ O, sterile filtered, stored at 4 °C
Tetracyclin	10 mg/ml	10 μg/ml	dissolved in ½ volume ddH ₂ O, completed by addition of ½ volume 96 % EtOH, stored at -20 °C (light protected)

2.3.2. *N. magadii*

Substance	Stock concentration	Final concentration	Preparation and storage
Novobiocin	3 mg/ml	3 µg/ml	dissolved in ddH ₂ O, sterile filtered, stored at -20 °C (light protected)
Mevinolin	10 mg/ml	5.5 µg/ml	isolated from pulverized tablets, dissolved in 96 % EtOH, stored at -20 °C
Bacitracin	7 mg/ml	70 µg/ml	dissolved in ddH ₂ O, sterile filtered, stored at 4 °C

2.4. Primer

Name	Sequence (5' → 3' direction)	Restriction site	T _m [°C]
FdxNab-1	GATTAAGCTTGAGCATCATCGGACTCGG	<i>Hind</i> III	63.3
FdxNab-2	GAACGGATCCCATATGCAACCGGCGCTTCGAGT	<i>Bam</i> HI, <i>Nde</i> I	66.4
BgaH-3i	GAGTGAAAAACCACCCAT		55.9
Pib-1	GATCTCTAGAGATGAGCGTCGCCAGCCCGAT	<i>Xba</i> I	75.4
Pib-2	GTAAGGATCCGCGCGGATCGACGGGAC	<i>Bam</i> HI	71.6
Pib-3	GATCAAGCTTCCAGCGTGTTGCGTCAGCGATC	<i>Hind</i> III	75.0
Pib-4	GATCCTCGAGCGTCGCCTCTCTCGGCCGTG	<i>Xho</i> I	75.6
PibD-5	GATCGGATCCATGTCACTCGCGTTCATCTC	<i>Bam</i> HI	75.0
PibD-3	GATCGGTACCTTAGAAGAGGCCGAGCACG	<i>Kpn</i> I	64.3
Pib-5Ende	GAGATATGGAGCGGAAAACG		62.2
Pib-3Ende	GAGTCGCGCACCGAC		61.7
PibD-Bam	GACAGGATCCATGTCACTCGCGTTCATCTC	<i>Bam</i> HI	57.0

Name	Sequence (5'→3' direction)	Restriction site	Tm [°C]
Comp-1	GATCGAATTCCACCACAGTCGGGCGA	<i>EcoRI</i>	64.9
Comp-2	GAACATCGATCCACTCCTCATCCC	<i>ClaI</i>	64.0
I-Pib-3	GTTTGGTACCTTACCAGACCGTCTCCTTCGT	<i>KpnI</i>	61.7
Nov-12	GCCGGTGAGTACTTAACGC		61.1
Nov-13	GACGCCGAATGGGTAGAC		61.9
NB-1	TCTACCGGGTGCTGAACG		63.7

2.5. Plasmids

Plasmid/Construct	Features	Source
pBAD24	<i>bla</i> , <i>araC</i> , <i>rrnB</i> , mcs, PBAD promoter, pBR322 ori	Guzman <i>et al.</i> , 1995
pBAD24-fdx	pBAD24 with <i>fdx</i> promoter of <i>N. magadii</i>	This thesis
pRV1-pTna	Amp ^R , <i>gyrB</i> (Nov ^R), <i>ptna</i> promoted <i>bgaH</i>	Lund <i>et al.</i> , 2007
pBAD24-fdx-bgaH	pBAD24 with <i>bgaH</i> gene under <i>fdx</i> promoter of <i>N. magadii</i>	This thesis
pRo-5	<i>bla</i> , ColeE1 ori, <i>gyrB</i> (Nov ^R), ΦCh1 derived ori	Mayrhofer-Iro <i>et al.</i> , 2013
pRo-5-fdx-bgaH	pRo-5 with <i>bgaH</i> gene under <i>fdx</i> promoter of <i>N. magadii</i>	This thesis
pBluescript II KS ⁺	mcs, <i>bla</i> , ColeE1 ori, <i>lacZa</i>	Stratagene
pKSII-pib-1-2	pBluescript II KS ⁺ with upstream-flank of <i>pibD</i> gene	This thesis
pKSII-pib-1-4	pBluescript II KS ⁺ with up- and downstream-flank of <i>pibD</i> gene	This thesis

Plasmid/Construct	Features	Source
pKSII-pib1-4 NovR forward	pBluescript II KS ⁺ with up- and downstream-flank of <i>pibD</i> gene, novobiocin-resistance cassette in between in forward direction	This thesis
pKSII-pib1-4 NovR reverse	pBluescript II KS ⁺ with up- and downstream-flank of <i>pibD</i> gene, novobiocin-resistance cassette in between in reverse direction	This thesis
pNB102	<i>bla</i> , ColE1 ori, <i>hmg</i> (Mev ^R), pNB101 ori	Zhou <i>et al.</i> , 2004
pNB102-pibD	pNB102 with internal sequence of <i>pibD</i> gene	This thesis

2.6. Kits

Name	Company	Product number
GeneJET Plasmid Miniprep Kit	Thermo Scientific	#K0502
GeneJET PCR Purification Kit	Thermo Scientific	#K0701
SuperSignal™ West Pico Chemiluminescent Substrate	Thermo Scientific	#34080
QIAquick Gel Extraction Kit	Qiagen	#28704
Phototope™-Star Detection Kit for Nucleic Acids	New England Biolabs	#N7020S

2.7. Nucleotides

Name	Company	Product number
dNTP Mix	Promega	U1511
Biotin-11-dUTP	GeneON	110

2.8. Size markers

2.8.1. DNA – Agarose gels

Name	Size of fragments (in bp)	Company	Product number
GeneRuler 1 kb DNA Ladder	10.000, 8.000, 6.000, 5.000, 4.000, 3.500, 3.000, 2.500, 2.000, 1.500, 1.000, 750, 500, 250	Thermo Scientific	#SM0311
2-Log DNA Ladder	10.000, 8.000, 6.000, 5.000, 4.000, 3.000, 2.000, 1.500, 1.200, 1.000, 900, 800, 700, 600, 500, 400, 300, 200, 100	New England Biolabs	#N3200S

2.8.2. Protein – SDS-PAGE

Name	Size of fragments (in kDa)	Company	Product number
Pierce™ Unstained Protein MW Marker	116.0, 66.2, 45.0, 35.0, 25.0, 18.4, 14.4	Thermo Scientific	#26610

2.9. Enzymes

2.9.1. Restriction enzymes

Name	Company	Product number
<i>Bam</i> HI	Thermo Scientific	#ER0051
<i>Hind</i> III	Thermo Scientific	#ER0501
FastDigest <i>Bam</i> HI	Thermo Scientific	#FD0054
FastDigest <i>Bsu</i> 15I	Thermo Scientific	#FD0143
FastDigest <i>Eco</i> RI	Thermo Scientific	#FD0274
FastDigest <i>Eco</i> 32I	Thermo Scientific	#FD0303
FastDigest <i>Hind</i> III	Thermo Scientific	#FD0504
FastDigest <i>Kpn</i> I	Thermo Scientific	#FD0524
FastDigest <i>Nde</i> I	Thermo Scientific	#FD0583
FastDigest <i>Nhe</i> I	Thermo Scientific	#FD0973
FastDigest <i>Sma</i> I	Thermo Scientific	#FD0663
FastDigest <i>Xba</i> I	Thermo Scientific	#FD0684
FastDigest <i>Xho</i> I	Thermo Scientific	#FD0694

2.9.2. DNA polymerases

Name	Company	Product number
<i>Pfu</i> DNA Polymerase	Promega	#M7741
<i>GoTaq</i> ® Green Master Mix	Promega	#M7122
T4 DNA Polymerase	Thermo Scientific	#EP0061

2.9.3. DNA-modifying enzymes

Name	Company	Product number
T4 DNA Ligase	Promega	#M1801
Klenow Fragment	Thermo Scientific	#EP0051

2.10. Antibodies

Name	Target	Dilution	Source
α -FlaB1 (from rabbit)	FlaB1 of <i>N. magadii</i>	1 : 500	Till, 2011
α -rabbit IgG, horseradish peroxidase linked (from donkey)	rabbit IgG	1 : 5000	GE Healthcare

2.11. Buffers and Solutions

2.11.1. DNA Gel Electrophoresis

50x TAE	
Tris/HCl, pH 8.2	2 M
Acetic acid	1 M
EDTA	0.1 M

5x DNA Loading Dye	
Tris/HCl, pH 8.2	50 mM
Sucrose	25 %
SDS	0.1 %
Bromphenol blue	0.05 %
Xylene cyanol	0.05 %

2.11.2. Competent cells

2.11.2.1. *E. coli*

MOPS I	
MOPS	100 mM
CaCl ₂	10 mM
RbCl	10 mM

adjust pH to 7 with KOH

MOPS II	
MOPS	100 mM
CaCl ₂	70 mM
RbCl	10 mM

adjust pH to 6.5 with KOH

MOPS IIa	
MOPS	100 mM
CaCl ₂	70 mM
RbCl	10 mM
Glycerol	15 %

adjust pH to 6.5 with KOH

2.11.2.2. *N. magadii*

Buffered, high-salt spheroblasting solution with glycerol	
Tris/HCl, pH 9.5	50 mM
NaCl	2 M
KCl	27 mM
Glycerol	15 %

after autoclaving, add 15 % sucrose (sterile filtered)

Buffered, high-salt spheroblasting solution without glycerol	
Tris/HCl, pH 8.0	50 mM
NaCl	2 M
KCl	27 mM

after autoclaving, add 15 % sucrose (sterile filtered)

Unbuffered, high-salt spheroblasting solution	
NaCl	2 M
KCl	27 mM

after autoclaving, add 15 % sucrose (sterile filtered)

2.11.3. Southern Blot

10x SSC	
NaCl	3 M
Sodiumcitrate	0.3 M

adjust pH to 7.2, autoclave

50x Denhardt's Solution	
Ficoll 400	1 g
Polyvinylpyrrolidone	1 g
BSA	1 g

fill up with ddH₂O to 100 ml

1x Wash Solution I	
1 : 10 dilution of Blocking Solution	

10x Wash Solution II	
Tris	100 mM
NaCl	100 mM
MgCl ₂ , hexahydrate	10 mM

adjust pH to 9.5

Hybridization Buffer	
20x SSC	25 ml
50x Denhardt's Solution	10 ml
BSA 10 %	5 ml
Na ₂ HPO ₄ , 1 M	5 ml
SDS 20 %	500 µl
EDTA, 0.5 M	200 µl
ddH ₂ O	55 ml

Blocking Solution	
NaCl	125 mM
Na ₂ HPO ₄	17 mM
NaH ₂ PO ₄	8 mM
SDS	0.5 %

adjust pH to 7.2

2.11.4. Isolation of Φ Ch1

High-salt alkaline solution	
NaCl	4 M
Tris/HCl, pH 9.5	50 mM

1.5 CsCl-solution	
CsCl	135 g
NaCl	23.4 g
Tris/HCl, pH 9.5	50 mM

fill up with ddH₂O to 200 ml

1.3 CsCl-solution	
CsCl	90 g
NaCl	23.4 g
Tris/HCl, pH 9.5	50 mM

fill up with ddH₂O to 200 ml

1.1 CsCl-solution	
CsCl	20 g
NaCl	23.4 g
Tris/HCl, pH 9.5	50 mM

fill up with ddH₂O to 200 ml

2.11.5. SDS-PAGE and Western Blot

Separating Gel Buffer	
Tris/HCl, pH 8.8	1.5 M
SDS	0.4 %

autoclave

Stacking Gel Buffer	
Tris/HCl, pH 6.8	0.5 M
SDS	0.4 %

autoclave

30 % Acrylamid	
Acrylamid	29 %
N, N' -methylenebisacrylamid	1 %

10x SDS-PAGE Running Buffer	
Glycine	1.92 M
Tris	0.25 M
SDS	1 %

5 mM Sodiumphosphate Buffer	
NaH ₂ PO ₄ , 0.2M	2.55 ml
Na ₂ HPO ₄	2.45 ml

fill up with ddH₂O to 200 ml

2x Laemmli Buffer	
Tris/HCl, pH 6.8	60 mM
SDS	2 %
Glycerol	10 %
β-mercaptoethanol	5 %
Bromphenol blue	0.01 %

Transfer buffer	
Tris	48 mM
Glycine	39 mM
SDS	0.037 %
Methanol	20 %

10x TBS	
Tris/HCl, pH 8.0	0.25 M
NaCl	1.37 M
KCl	27 mM

autoclave

Coomassie staining solution	
Methanol	25 %
Acetic acid	10 %
Coomassie Brilliant Blue R250	0.15 %

Coomassie destaining solution	
Methanol	25 %
Acetic acid	10 %

Ponceau S staining solution	
Ponceau S	0.5 %
Trichloroacetic acid	3 %

2.11.6. BgaH-measurements

BgaH-buffer	
NaCl	2.5 M
Tris/HCl, pH 7.2	50 mM
MnCl ₂	10 μ M
β -mercaptoethanol	0.1 %

ONPG solution
8 mg/ml dissolved in BgaH-buffer

3. METHODS

3.1. DNA methods

3.1.1. Agarose gel electrophoresis

For the separation of DNA fragments by size, a 0.8 % agarose gel was prepared. The appropriate amount of agarose was melted in 1x TAE (see 2.11.1), then cooled down and poured into the apparatus. When being solid, the gel was covered with 1x TAE and after loading the samples the DNA fragments were separated with an applied voltage of 100 V. When separation was completed, the gel was put into an ethidium-bromide bath and DNA fragments were visualized using UV-light.

3.1.2. Polymerase chain reaction

For a preparative polymerase chain reaction (PCR) the *Pfu*-Polymerase of *Pyrococcus furiosus* (see 2.9.2), which possesses 3'-5' exonuclease activity, was used. Since great precision is not a priority for analytical PCRs, a polymerase lacking the 3'-5' exonuclease activity but instead being capable of synthesizing DNA faster, the *GoTaq*-Polymerase of *Thermus aquaticus* (see 2.9.2), was used. In the case of *E. coli* templates were gained using plasmid DNA isolation from liquid cultures (see 3.1.3). In order to generate templates from *N. magadii*, 50 µl of a dense liquid culture were centrifuged for 3 minutes at 13.000 rpm and room temperature and the pellet was solved in 100 µl ddH₂O.

Batch for preparative PCR	
forward primer (0.1 µg/µl)	5 µl
reverse primer (0.1 µg/µl)	5 µl
dNTPs, 2 mM	10 µl
10x <i>Pfu</i> -reaction buffer	10 µl
template	1 µl
<i>Pfu</i> -Polymerase	2 µl
ddH ₂ O	67 µl

Batch for analytical PCR	
forward primer (0.1 µg/µl)	2.5 µl
reverse primer (0.1 µg/µl)	2.5 µl
2x <i>GoTaq</i> Green Master Mix	12.5 µl
template	1 µl
ddH ₂ O	6.5 µl

PCR-Program			
Step	Temperature (°C)	Duration (minutes)	Number of cycles
Initial Denaturation	95	5	1
Denaturation	95	1	35 (preparative) 20 (analytical)
Annealing	X	1	
Extension	72	Y	
Final Extension	72	5 / at the least Y * 2	1

The annealing temperature X is dependent on the melting temperature of the used primers. To calculate the annealing temperature 4 °C were subtracted from the melting temperature of the primer with the lower melting temperature (calculated with GeneRunner (Version 3.05, Hastings Software Inc.)).

The elongation time Y is dependent on which polymerase is employed and the length of the desired PCR-product. *Pfu*-Polymerase is able to add 500 bp per minute, whereas *GoTaq*-Polymerase is capable of attaching 1000 bp per minute.

3.1.3. Plasmid isolation

Plasmid isolation of bacterial cultures was achieved using the GeneJet Plasmid Miniprep Kit (see 2.6.). All steps were performed as described in the manufacturer's protocol, with exception of the DNA elution step, which was carried out with ddH₂O instead of elution buffer. Afterwards, the yield of the plasmid isolation was controlled by measuring the amount of DNA with NanoDrop 2000.

3.1.4. DNA purification

After PCR as well as after plasmid restriction, DNA was purified using the GeneJet PCR Purification Kit (see 2.6.). In cases where a specific DNA-fragment of a particular size had to be purified, gel elution with the QIAquick Gel Extraction Kit (see 2.6) was performed. All steps were done according to the manufacturer's protocol, with one exception: elution of the DNA was carried out with ddH₂O instead of elution buffer.

3.1.5. DNA modifications

3.1.5.1. Restriction

DNA restrictions were performed using endonucleases from Thermo Scientific (see 2.9.1). Depending on the conditions, either FastDigest Enzymes (double digests) or conventional enzymes were used. For both types of endonucleases, all steps were performed as described in the manufacturer's protocol, with the following exception: reactions with FastDigest enzymes were incubated at 37°C for 1 hour and reactions using conventional enzymes were done at 37°C for 3 hours or over night.

3.1.5.2. Ligation

Ligation of DNA fragments was achieved using T4 DNA Ligase from Promega (see 2.9.3). The optimal amount of vector and insert to be used in the reaction was calculated as suggested in the manufacturer's protocol, using an insert-to-vector ratio of 3:1. Sticky-end ligation reactions were performed at 4 °C over night or at room temperature for 3 hours, respectively. Blunt-end ligation reactions were incubated at 16 °C over night.

3.1.5.3. Fill-in of 5'- overhangs

In some cases, the 5'- overhang resulting from restriction had to be filled in to generate a blunt end. Therefore, the Klenow fragment from Thermo Scientific (see 2.9.3) was applied according to the manufacturer's protocol. Inactivation of the enzyme was achieved by heating to 75 °C for 10 minutes.

3.1.5.4. Digestion of 3'- overhangs

For generation of a blunt end from a 3'- overhang, the 3'-5' exonuclease activity of T4 DNA Polymerase from Thermo Scientific (see 2.9.2) was used. Since the desired result was the digestion of the overhang, the batch without nucleotides was used as described in the manufacturer's protocol.

3.1.6. Transformation of *E. coli*

3.1.6.1. Competent cells

For the preparation of competent *E. coli* cells, 100 ml LB-medium, supplemented with the appropriate antibiotics (see 2.3.1), were inoculated with a dense *E. coli* culture to an optical density at 600 nm (OD₆₀₀) of 0.1. The culture was then incubated at 37 °C with agitation until an OD₆₀₀ of 0.6 was reached. At this time point, the cells were harvested by

centrifugation at 10.000 rpm at 4 °C for 10 minutes. The pelleted cells were then resuspended carefully in 40 ml MOPS I solution (see 2.11.2.1) and incubated on ice for 10 minutes. After another centrifugation step at 10.000 rpm and 4 °C for 10 minutes, the pelleted cells were resuspended in 40 ml MOPS II solution (see 2.11.2.1) and incubated on ice for 30 minutes. Then, the cells were centrifuged one last time at 10.000 rpm and 4 °C for 10 minutes. The pelleted cells were taken up in 2 ml MOPS IIa solution (see 2.11.2.1) before they were aliquoted (100 µl) and stored frozen at -80 °C.

3.1.6.2. Transformation

For the transformation of competent *E.coli* cells, an aliquot was taken from -80 °C and thawed on ice for 10 minutes. After adding the DNA of interest it was incubated for 30 minutes on ice. The next step was a heat-shock, where the cells were put on 42 °C for 2 minutes, before being put on ice again. Then, 300 µl LB-medium were added to the cells and they were put on 37 °C for 30 minutes in order to regenerate. The cells were then plated on LB-plates with the suitable antibiotics and incubated at 37 °C over night. Single colonies were incubated in 5 ml LB-medium with the appropriate antibiotics over night.

3.1.6.3. Screening

For screening of individual colonies the quick prep method was used. Therefore, 300 µl of the over-night culture were centrifuged for 5 minutes at 13.000 rpm and room temperature. The pellet was then resuspended in 30 µl of 5x DNA Loading Dye (see 2.11.1) and 14 µl of a 1:1 Phenol/Chloroform solution. After proper vortexing, centrifugation at 13.000 rpm and room temperature for 5 minutes was performed. 12 µl of the supernatant were loaded onto an agarose gel for screening. Putative positive clones were then analyzed with an analytical PCR (see 3.1.2).

3.1.7. Transformation of *N. magadii*

3.1.7.1. Competent cells

For the preparation of competent *N. magadii* cells, 60 ml NVM⁺-medium, supplemented with 70 µg/ml bacitracin (see 2.3.2) were incubated with a dense *N. magadii* culture to an OD₆₀₀ of 0.5-0.6. At this time point, the cells were harvested by centrifugation at 6.000 rpm and room temperature for 15 minutes. The pelleted cells were resuspended carefully in 30 ml buffered, high-salt spheroblasting solution with glycerol (see 2.11.2.2) and 0.1 % proteinase K were added. The cells were incubated at 42 °C with agitation, until the rod-shaped cells had become spheroblastic cells.

3.1.7.2. Transformation

1.5 ml of the spheroblastic cells were centrifuged for 3 minutes at 10.000 rpm and room temperature. The pellet was resuspended very carefully in 150 µl buffered, high-salt spheroblasting solution without glycerol (see 2.11.2.2) and 15 µl of 0.5 M EDTA were added. After incubation of the cells at room temperature for 10 minutes, the DNA of interest was added to the cells. After 5 minutes at room temperature, 150 µl of 60 % PEG-600 (prepared by mixing 600 µl PEG-600 with 400 µl of unbuffered, high-salt spheroblasting solution without glycerol (see 2.11.2.2)) were added to the cells and incubated for 30 minutes at room temperature. Then, 1 ml of NVM⁺-medium was added and the cells were collected at 10.000 rpm and room temperature for 5 minutes. The supernatant was discarded and the pelleted cells were carefully resuspended in another 1 ml of NVM⁺-medium. After repeating the last centrifugation step, the cells were taken up in 1 ml NVM⁺-medium and kept at 37 °C with agitation until they regenerated to rod-shaped cells. Then, they were plated on NVM⁺-plates with the appropriate antibiotics and were incubated on 42 °C until colonies appeared.

3.1.7.3. Screening

To analyze whether the transformation was successful, individual colonies were picked and inoculated in 700 μ l NVM⁺-medium without antibiotics. Since *N. magadii* is an obligate aerobic organism, every day the cultures had to be provided with fresh air. Once the cultures were dense, they were tested by analytical PCR (see 3.1.2).

3.1.8. Isolation of chromosomal DNA of *N. magadii*

500 ml of a *N. magadii* culture with an OD₆₀₀ of at least 0.6 was centrifuged for 20 minutes at 8.000 rpm and room temperature. The pelleted cells were resuspended completely in high-salt alkaline solution (see 2.11.4). The suspension was transferred into two 50 ml centrifugation tubes. Per tube, 2.5 ml 14 mM desoxycholate were added and the tubes were rotated until the content was mixed well. 7.5 ml sterile ddH₂O were added per tube and again the tubes were rotated until the cell suspension was mixed completely. Then, 12.5 ml of a 1:1 Phenol/Chloroform-Solution were added per tube and the tubes were inverted carefully until all compounds were homogeneously mixed. After that, the tubes were centrifuged for 30 minutes at 10.000 rpm and 4°C. The supernatant was transferred into a 100 ml Erlenmeyer-flask and isopropanol was added until the layer was approximately 1 cm thick. The DNA was fished from the solution with a sterile Pasteur pipette and was solved in 5 ml sterile ddH₂O. Sterile EDTA was added to a final concentration of 10 mM. 1.5 g CsCl were added per ml of solved DNA and the tubes were inverted carefully until it was solved. Afterwards, 15 μ l ethidium bromide were added. The solution was filled in Quick-Seal tubes, which were then sealed from air. The tubes were centrifuged at 60.000 rpm for at least 16 hours at room temperature. The pink DNA band was collected using a needle and a syringe, and was then transferred into a 1.5 ml Eppendorf reaction tube. The ethidium bromide was removed by a water-saturated butanol extraction. In order to get rid of the CsCl, the chromosomal DNA was dialyzed against sterile ddH₂O for 1 hour, and after changing the sterile ddH₂O it was dialyzed over night.

3.1.9. Southern Blot

3.1.9.1. Synthesis of the probe

Synthesis of the probe was carried out using PCR and marking of the probe was achieved by adding biotinylated dUTP (see 2.7) to the PCR batch. The *N. magadii* template for the PCR-reaction was generated as described in 3.1.2.

PCR Batch for probe synthesis	
<i>GoTaq</i> Green Mastermix	50 µl
forward primer (0.1 µg/µl)	10 µl
reverse primer (0.1 µg/µl)	10 µl
biotinylated dUTP	2.5 µl
ddH ₂ O	26.5 µl
template	1 µl

For the PCR-Program see 3.1.2.

3.1.9.2. Blotting of DNA, probe-hybridization and development

The sample designated for Southern Blot analysis was separated on an agarose gel and visualization was achieved by ethidium bromide staining and exposure to UV-light. After taking a picture, the gel was drowned in 0.25 M HCl for 30 minutes. As a next step, the gel was put into 0.4 M NaOH / 0.6 M NaCl for 30 minutes and into 1.5 M NaCl / 0.5 M Tris/HCl pH 7.5 for another 30 minutes. Blotting of the gel onto a nylon membrane (Amersham Hybond-N+, GE Healthcare Life Sciences) took place over night via capillary blotting. After blotting, the membrane was soaked in 0.4 M NaOH for 1 minute and afterwards in 0.2 M Tris/HCl pH 7.5 for 1 minute. The DNA on the membrane was then fixed by UV-crosslinking. Blocking of the membrane took place at 65 °C for 3 hours with 0.1 mg/ml

salmon sperm in 12 ml hybridization buffer while rotating. Prior to hybridization, the probe was denatured for 5 minutes at 95 °C. Afterwards, the probe was added to the membrane and hybridization took place over night. After hybridization, the membrane was washed several times: two times with 2x SSC / 0.1 % SDS for 5 minutes at room temperature, and two times with pre-warmed 0.1x SSC / 0.1 % SDS for 15 minutes at 65°C. Then, the membrane was put into blocking solution for 5 minutes before developing the blot with Phototope™-Star Detection Kit for Nucleic Acids. Visualization was achieved by exposure to an X-ray film (Amersham Hyperfilm™ ECL, GE Healthcare Life Sciences).

3.1.10. Homozygation of a *N. magadii* deletion mutant

For the construction of a *N. magadii* deletion mutant, a *N. magadii* L13 strain was transformed with a plasmid carrying a novobiocin-resistance cassette in place of the gene to be deleted. Since *N. magadii* has up to 50 copies of its genome in one cell, the transformation itself is not sufficient to generate a homozygous deletion mutant. By applying a constant selection pressure to the heterozygous mutants, over many passages they should become homozygous. For passaging, 200 µl of a dense culture were inoculated in 20 ml NVM⁺-medium containing novobiocin, thus selecting for transformed cells. After every 5th passage, an analytical PCR (see 3.1.2) was performed to detect the homozygation status.

3.2. ΦCh1 methods

3.2.1. Isolation of virus particles

For the isolation of ΦCh1 a *N. magadii* L11 culture was inoculated at an OD₆₀₀ of 0.1 and incubated at 37 °C with agitation. The lysis of *N. magadii* is marked by a decrease in the optical density, which was therefore monitored over several days. After lysis of the culture, it was centrifuged at 6.000 rpm and room temperature for 20 minutes. The

supernatant was stirred over night with 10 % PEG-6000. The PEG-6000-coated virus particles were then harvested by centrifugation at 6.000 rpm and room temperature for 20 minutes. The resulting pellet was resuspended in as little as possible of high-salt alkaline solution (see 2.11.4). For purification of the virus particles, a discontinuous CsCl-Gradient was prepared, consisting of 2 ml 1.5 CsCl-Solution, 5 ml 1.3 CsCl-Solution (see 2.11.4) and 5.5 ml virus-suspension. For balancing, 1.1 CsCl-Solution (see 2.11.4) was used if necessary. After centrifugation at 30.000 rpm and room temperature for 20 hours, the virus-containing, blue glimmering band was sampled. For further purification, a continuous gradient was done subsequently. Therefore, the probe isolated from the discontinuous gradient was mixed with 1.3 CsCl-Solution and again centrifuged at 30.000 rpm and room temperature for 20 hours. For further use of the virus particles it is essential to get rid of the CsCl, which is why the concentrated virus particles were dialyzed for 1 hour against high-salt alkaline solution, and after changing the buffer they were dialyzed over night.

3.2.2. Virus titre assay

Infectivity of the virus Φ Ch1 is analyzed by determination of the virus titre using *N. magadii* L13 as an indicator strain. A *N. magadii* culture was grown until the stationary growth phase and the isolated virus particles were diluted with NVM⁺-medium in the following way: 10^{-2} , 10^{-4} , 10^{-6} , 10^{-8} , 10^{-10} . 300 μ l of the culture were added to 5 ml of soft-agar, prior to adding 100 μ l of the virus-dilution and pouring it on a thin plate of NVM⁺-agar. After letting it solidify over night, the plates were incubated at 37 °C for one week. Then, plaques were counted and plaque-forming units (PFU) per ml virus were calculated.

3.3. Protein methods

3.3.1. Preparation of crude cell extracts

To generate samples of *N. magadii* for SDS-PAGE and Western Blot, 1.5 ml culture were centrifuged for 3 minutes at 13.000 rpm and room temperature. The resulting pellet was covered with X μ l 5 mM sodium phosphate buffer (see 2.11.5) and X μ l 2x Laemmli buffer (see 2.11.5). X was calculated as follows: OD_{600} of the culture * 75 = X. Due to the high DNA-content in *N. magadii* cells, the sample was very viscous at this stage and not suitable for further applications. Therefore, the DNA had to be degraded by incubating the sample at 37 °C until the pellet was resolved.

3.3.2. Precipitation of proteins from supernatant

Proteins were precipitated from the supernatant using trichloroacetic acid. 1.5 ml of the culture were centrifuged for 3 minutes at 13.000 rpm and room temperature and the supernatant was transferred into a fresh tube. Proteins were precipitated by the addition of 5 % trichloroacetic acid for 1 hour on ice. Centrifugation was used to collect the precipitated proteins for 30 minutes at 13.000 rpm and 4 °C. The resulting pellet was resuspended in 5 mM sodium phosphate Buffer and 2x Laemmli Buffer as described above (see 3.3.1). The sample was then incubated at 37 °C until the pellet was resolved. Adjustment of pH was done by pipetting ammonia vapor over the sample until the color turned from yellow to blue.

3.3.3. SDS-PAGE

Analysis of crude cell extracts and precipitated proteins was done with sodium-dodecylsulfate polyacrylamide gel electrophoresis (SDS-PAGE). Through covering up the proteins' charges with SDS, they were separated according to their size. The separating gel contained 12 % acrylamid, whereas the stacking gel contained 4 %.

Separating gel, 12 %	
Separating gel buffer, pH 8.8	1.25 ml
Acrylamid, 30 %	2 ml
ddH ₂ O	1.75 ml
APS, 10 %	60 µl
TEMED	20 µl

Stacking gel, 4 %	
Stacking gel buffer, pH 6.8	0.5 ml
Acrylamid, 30 %	267 µl
ddH ₂ O	1.25 ml
APS, 10 %	20 µl
TEMED	5 µl

The separating gel was mixed on ice and cast between two glass plates. Immediately after pouring the gel, it was covered with isopropanol, in order to get a clear line. When being solid, the isopropanol was removed, the stacking gel was mixed on ice, poured on top of the separating gel and the comb was inserted rapidly. When the gel was polymerized, it was put into the apparatus, covered with 1x SDS page running buffer (see 2.11.5) and the comb was carefully removed. After loading the samples, the gel was connected to electricity. Until the samples had migrated properly into the slots, 40 V were applied. For the migration through the stacking gel, the current voltage was turned up to 60 V. Finally, when the samples reached the separating gel, it was run with 80 V. When separation was completed, the gel was stained with Coomassie staining solution (see 2.11.5) until the whole gel appeared stained. Then, the gel was covered with Coomassie destaining solution (see 2.11.5) until the background was completely destained and the bands were visible.

3.3.4. Western Blot

For the detection of specific proteins with antibodies, the samples were separated using SDS-PAGE as described above. Instead of staining the gel with Coomassie staining solution, the gel was used for transferring the proteins onto a nitrocellulose membrane (Amersham Protran 0.2 NC, GE Healthcare Life Sciences). In this case, an electro-blot was used. Therefore, 3 layers of Whatman™ 3MM chromatography paper (cut to the same size as the gel) were soaked with transfer buffer (see 2.11.5). Next, the membrane was

soaked in transfer buffer and put on top of the Whatman™ papers. Then, the gel was placed on top of the membrane and covered with 3 more layers of soaked Whatman™ paper. Transfer took place at 20 V for 20 minutes. When the transfer was finished, the membrane was stained with Ponceau-S solution (see 2.11.5). Therefore, it was covered with the staining solution for some minutes, prior to being destained with ddH₂O until only the marker bands were visible. They were marked with a pencil and the membrane was fully destained afterwards. Unspecific binding of the antibodies was prevented by blocking free sites on the membrane with 5 % milk powder in 1x TBS (see 2.11.5) over night at 4 °C. The next day, the membrane was washed with 1x TBS for at least 15 minutes before incubating it with the primary antibody for 1 hour at room temperature. After incubation, the membrane was washed three times for 10 minutes with 1x TBS. Then, incubation with the secondary antibody was done for 1 hour at room temperature. Again, the membrane was washed three times for 10 minutes with 1x TBS. Finally, the blot was developed using the SuperSignal™ West Pico Chemiluminescent Substrate (see 2.6). Visualization was achieved by exposing the blot onto an X-ray film (Amersham Hyperfilm™ ECL, GE Healthcare Life Sciences).

3.3.5. Measurements of *bgaH*-expression

In order to determine the strength of a promoter, a reporter-gene is needed. For halophilic promoters, the *bgaH* gene is a common reporter-gene. The BgaH-protein is the halophilic equivalent of β -galactosidase, which is also capable of cleaving ortho-Nitrophenyl- β -galactoside (ONPG) to galactose and ortho-nitrophenol. Because of its yellow color, the amount of ortho-nitrophenol and therefore indirectly the amount of BgaH can be monitored by measuring its absorption at 405 nm.

For the measurement of BgaH levels in a culture, 700 μ l of BgaH buffer (see 2.11.6) were provided in a clean plastic-cuvette. Then, 100 μ l of fresh culture (diluted if necessary) were added and the cuvette was vortexed for 3 seconds. In order to lyse the cells, 100 μ l of a 2 % Triton X-100 solution (prepared in ddH₂O) were added to the cuvette and vortexing for 10 seconds took place. The reaction was then started by adding 100 μ l of ONPG solution (see 2.11.6). After vortexing the cuvette for another 3 seconds, absorption

at 405 nm was measured every 20 seconds over a two-minute time span. In addition, the OD_{600} of the culture was determined in a separate measurement.

The specific activity (SA) of BgaH in the culture was then calculated with the following formula:

$$SA = \frac{\Delta A_{405}}{\Delta t * V * OD_{600}} * 1000$$

Variable	Meaning
ΔA_{405}	change in absorption at 405 nm
Δt	time-span of change of the absorption (in minutes)
V	volume of culture (in ml)
OD_{600}	optical density at 600 nm

3.4. Motility assay for *N. magadii*

Since *N. magadii* possesses flagella and pili, it is a motile organism. For analysis of movement through flagella, swimming-plates were used. Therefore, NVM⁺-plates with very low agar-concentration (0.2 %, see 2.2.2) were poured. Once the plates cooled down, a 5 μ l droplet of culture was placed into the middle of the plate. Importantly, the optical density of different cultures to be analyzed was adapted first. The plates were then incubated at 37 °C in a styrofoam-box that contained a cup of water, providing a moist environment for the plates and preventing them from drying out. After four days the plates were analyzed and photographed.

3.5. Cloning Strategies

3.5.1. pRo-5-fdx-bgaH

The *fdx* promoter was amplified from *N. magadii* L13 with the primers FdxNab-1 and FdxNab-2 (see 2.4). Both the *fdx* promoter and vector pBAD24 (see 2.5) were restricted with *Bam*HI and *Hind*III and ligated, giving rise to the plasmid pBAD24-fdx. The *bgaH* gene was isolated from vector pRV1-pTna after restriction with *Bam*HI and *Nde*I and purified by gel elution. The plasmid pBAD24-fdx was also restricted with *Bam*HI and *Nde*I, prior to ligation with the *bgaH* fragment. The resulting plasmid pBAD24-fdx-bgaH was restricted with *Bam*HI and the generated 5'-overhang was filled in with Klenow fragment (see 3.1.5.3). Afterwards, it was restricted with *Hind*III and the *fdx bgaH* fragment was isolated by gel excision. The vector pRo-5 was restricted with *Kpn*I and the 3'-overhang was digested using T4 DNA Polymerase (see 3.1.5.4) just before being cut with *Hind*III. The vector was then ligated with the *fdx bgaH* fragment, giving rise to the plasmid pRo-5-fdx-bgaH.

3.5.2. pKSII-pib1-4 NovR

The upstream-fragment of the *pibD* gene was amplified with the primers Pib-1 and Pib-2 (see 2.4), prior to being restricted with *Xba*I and *Bam*HI. The plasmid pBluescript II KS⁺ (see 2.5) was also restricted with *Xba*I and *Bam*HI and then ligated with the upstream fragment, resulting in the plasmid pKSII-pib1-2. The downstream fragment of the *pibD* gene was amplified using primers Pib-3 and Pib-4. The fragment then was, equally to plasmid pKSII-pib1-2, restricted with *Hind*III and *Xho*I. The ligation of the downstream fragment with the vector that already contained the upstream fragment, resulted in the plasmid pKSII-pib1-4. The novobiocin resistance (Nov^R) cassette was isolated from the vector pQE30-NovR by use of the restriction enzymes *Sma*I and *Nhe*I. The resulting 5'-overhang was filled in with Klenow Fragment (see 3.1.5.3) and the Nov^R cassette was isolated using gel elution. The plasmid pKSII-pib1-4 was cut open with *Eco*RV and it was ligated with the Nov^R cassette. Since this was a blunt-end cloning, the Nov^R cassette could

be inserted in forward or reverse orientation. Both orientations were created, namely pKSII-pib1-4 NovR forward and pKSII-pib1-4 NovR reverse.

3.5.3. pNB102-pibD

The *pibD* gene was amplified from *N. magadii* L13 by use of the primers Comp-1 and Comp-2 (see 2.4). Then, the fragment and the vector pNB102 (see 2.5.) were restricted with *ClaI* and *EcoRI* and ligated, giving rise to the plasmid pNB102-pibD.

4. RESULTS AND DISCUSSION

4.1. Analysis of the ferredoxin promoter

4.1.1. Aim

For numerous applications, the availability of a reliable gene expression system is crucial to promote scientific progress. For bacteria, in particular for *E. coli*, various expression systems are already available. For *N. magadii* and in general for halophilic archaea, no efficient expression system has been developed up to now (78). In the absence of such a system, heterologous expression of proteins from *N. magadii* or Φ Ch1 is accomplished with an *E. coli* overexpression system. For some applications, the products obtained by this method are of sufficient quality. However, a big disadvantage of heterologous protein expression is that due to their adaptations to the high salt environment, *N. magadii* or Φ Ch1 proteins are not folded correctly in *E. coli* and therefore do not reflect endogenous expression. As this can be a problem for various applications, for example the elucidation of the proteins' function, the development of an expression system for *N. magadii* is indispensable.

In search of a suitable archaeal promoter to conduct homologous gene expression, the tryptophanase promoter of *N. magadii* (*ptnaN*) was discovered and analyzed. This promoter is inducible with tryptophan and regulates the tryptophanase-gene *tnaA*. Analysis of its characteristics and quantification of its activity was accomplished by Alte, 2011 (57). Based on this approach, the *tnaA* deletion mutant strain L13::*tnaA* has been established recently, to overcome the problem that the inducer of gene expression, tryptophan, is degraded upon *tnaA* induction (58). Currently, the development of an expression system using *ptnaN* in the deletion mutant is in progress. However, the strength of the tryptophanase promoter was shown to be rather weak and it is questionable, if the promoter is able to express proteins with a satisfactory yield.

Hence, the search for an appropriate promoter was continued. The ferredoxin promoter (*pfdx*) of *H. salinarum* was described as a very strong promoter in *H. volcanii* transformants. Since the ferredoxin gene is classified as a so-called house-keeping gene, the ferredoxin promoter was found to be constitutively active (60). Trials to express gp34 of Φ Ch1 under the control of *pfdx*, however, did not lead to an enhancement of gene expression in comparison to its endogenous promoter. This could be due to the fact that the ferredoxin promoter originated from a different genus, namely *Halobacterium*, and might be poorly recognized by the transcriptional machinery of *N. magadii* (61). Computational analysis revealed that the *fdx* gene and *fdx* promoter are also encoded within the genome of *N. magadii*.

Therefore, this study examines the suitability of the *N. magadii fdx* promoter for establishment of a gene expression system in *N. magadii*.

4.1.2. Experimental setup

In order to analyze the *fdx* promoter, the promoter-strength has to be monitored in a time-course experiment with a suitable reporter gene. For halophilic archaea, a common reporter gene is the *bgaH* gene, which encodes an enzyme with β -galactosidase activity.

In course of this study, the *fdx* promoter of *N. magadii* was cloned at the 5'-end of the *bgaH* gene on the shuttle vector pRo-5 (see 3.5.1). A graphical presentation can be viewed in Figure 8.

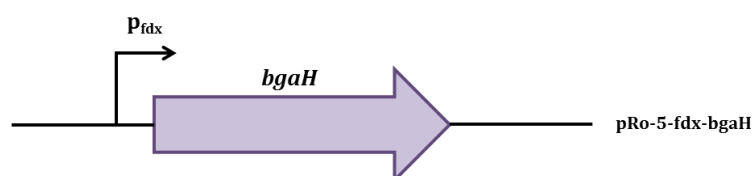


Figure 8: Schematic illustration of construct pRo-5-fdx-bgaH

For determination of the promoter strength of *pfdx* from *N. magadii*, the *bgaH* gene was cloned into the plasmid pRo-5 under control of the ferredoxin promoter.

The promoter activity of *pfdx* can directly be measured by monitoring the enzymatic activity of the BgaH-protein. Like β -galactosidase, BgaH is capable of cleaving ONPG into galactose and ortho-nitrophenol. The amount of released ortho-nitrophenol is

quantifiable by measuring its absorption at 405 nm. This reflects the amount of BgaH in the cell and therefore the activity of the promoter.

The promoter activity of *pdfx* was then compared to the promoter activity of *ptnaN*, which was already characterized by Alte, 2011. For this analysis, *ptnaN* was cloned in front of the *bgaH* gene on the plasmid pRo-5 (see Figure 9) and the plasmid was transformed into *N. magadii* L13 (57).

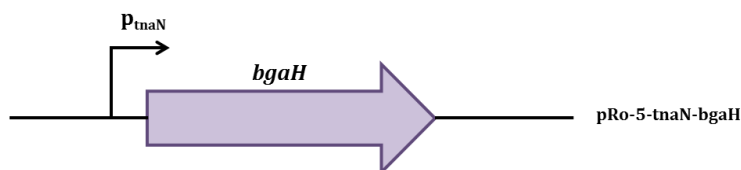


Figure 9: Schematic illustration of plasmid pRo-5-tnaN-bgaH

The promoter *ptnaN* was cloned ahead of the *bgaH* gene on the plasmid pRo-5 to allow quantification of promoter strength. This was carried out by Alte, 2011 (57).

4.1.3. Determination of promoter strength

N. magadii L13 was transformed with the plasmid pRo-5-fdx-bgaH and individual colonies were inoculated in NVM⁺ medium until they reached stationary phase. The candidates were then tested with regard to a positive transformation event by PCR analysis. Therefore, primers FdxNab-1 and BgaH-3i, which have their binding sites on the 5' part of the *fdx* promoter and within the *bgaH* gene, were utilized (primer binding sites are indicated in Figure 10).

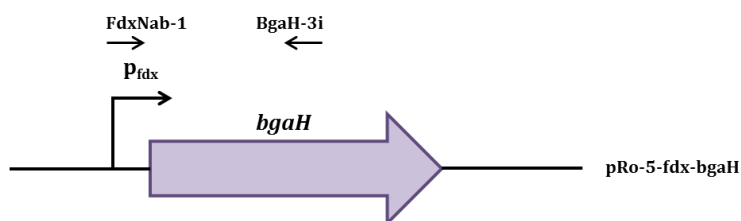


Figure 10: Schematic illustration of primer binding sites on the plasmid pRo-5-fdx-bgaH

PCR-analysis with primers FdxNab-1 and BgaH-3i led to the amplification of a 1200 bp long DNA fragment, if transformation with the plasmid pRo-5-tnaN-bgaH was successful.

As a result, four individual clones were tested positive for the transformation with the plasmid (data not shown). As it cannot be excluded that the different clones succumb to fluctuations regarding the expression of *bgaH*, measurements of the promoter strength

were conducted in parallel with all four clones. For details on BgaH-measurements see 3.3.5. The strains were inoculated to an OD₆₀₀ of 0.1 and measurements were conducted several times per day until late stationary phase was reached. The data depicted in Figure 11 for the *N. magadii* L13 (pRo-5-fdx-bgaH) strain display the average specific activity of all four candidates at the corresponding time points. As a control, BgaH measurements were also performed with the wildtype *N. magadii* L13 strain. For comparison, the data obtained by Alte, 2011 (57) for the *N. magadii* L13 (pRo-5-tnaN-bgaH) strain are also included in Figure 11. Here, in one test series induction of the promoter was achieved with addition of 2 mM tryptophan to the medium on a daily basis. As a control, the second test series was done without tryptophan-addition.

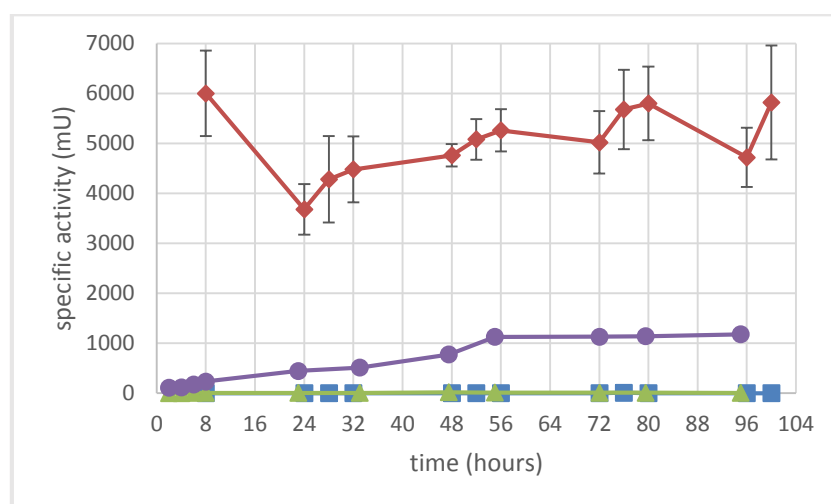


Figure 11: Results from BgaH-measurements of strains *N. magadii* L13 (pRo-5-fdx-bgaH), *N. magadii* L13 (pRo-5-tnaN-bgaH) and *N. magadii* L13

Strains were inoculated to an OD₆₀₀ of 0.1. The data shown for *N. magadii* L13 (pRo-5-fdx-bgaH) is comprised of the average specific activity of all four individual clones at the corresponding time point. Standard deviation is depicted with black bars. The *fdx* promoter is constitutively active with an average specific activity of about 5000 mU. *PtnaN*, however, is inducible by 2 mM tryptophan and shows a specific activity of about 1000 mU at its highest (in stationary growth phase). Both *N. magadii* L13 and *N. magadii* L13 (pRo-5-tnaN-bgaH), which were not induced, did not show any promoter activity.

Blue Line: *N. magadii* L13, **Red Line:** *N. magadii* L13 (pRo-5-fdx-bgaH), **Green Line:** *N. magadii* L13 (pRo-5-tnaN-bgaH) not induced (Alte, 2011 (57)), **Purple Line:** *N. magadii* L13 (pRo-5-tnaN-bgaH) 2 mM tryptophan-induced (Alte, 2011 (57))

The data obtained from BgaH-measurements show, that the *fdx* promoter is indeed a very strong promoter. On average, the *fdx* promoter could yield a specific activity of about 5000 mU. The data obtained from Alte, 2011 (57) show that the *tnaN* promoter yields a

specific activity of about 1000 mU once stationary phase is reached. Both the wildtype *N. magadii* L13 strain and the uninduced *N. magadii* L13 (pRo-5-tnaN-bgaH) strain show no basal activity.

In Figure 12 the corresponding growth curve of *N. magadii* L13 and *N. magadii* L13 (pRo-5-fdx-bgaH) can be seen. As before, the data for the *N. magadii* L13 (pRo-5-fdx-bgaH) strain is shown of the mean value of the four different clones.

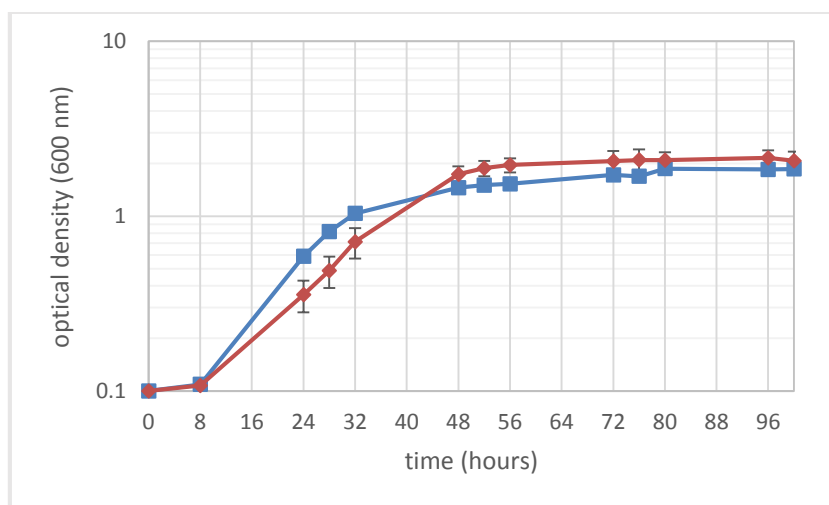


Figure 12: Growth curve of *N. magadii* L13 and *N. magadii* L13 (pRo-5-fdx-bgaH) (data obtained in course of bgaH-measurements)

Comparison of the growth behavior of the *N. magadii* L13 and *N. magadii* L13 (pRo-5-fdx-bgaH) strains show that there is almost no difference between the two strains. The *N. magadii* L13 (pRo-5-fdx-bgaH) strain shows a minimally slower growth rate within the exponential phase than the wildtype *N. magadii* L13 strain.

Blue Line: *N. magadii* L13, **Red Line:** *N. magadii* L13 (pRo-5-fdx-bgaH)

The strains *N. magadii* L13 and *N. magadii* L13 (pRo-5-fdx-bgaH) show no relevant differences regarding their growth behavior. If at all, the *N. magadii* L13 (pRo-5-fdx-bgaH) strain is growing minimally slower at exponential phase than the wildtype. This reflects the increased gene expression inside the cells. One can see in Figure 12 that the *N. magadii* L13 (pRo-5-fdx-bgaH) strain enters exponential growth phase after approximately 8 hours and stationary phase after approximately 48 hours.

Considering Figure 11 and Figure 12, it can be stated that the activity of the *fdx* promoter is higher by trend in stationary phase than in exponential phase.

4.1.4. Influence of Iron-Concentration

Since ferredoxins use iron as a co-factor, it would be conceivable that the regulation of the *fdx* promoter is dependent on the iron-availability in the cell. In order to investigate whether such a correlation exists, BgaH-measurements were repeated for the *N. magadii* L13 (pRo-5-*fdx*-*bgaH*) strain, but the cells were grown in media with different iron-concentrations. One candidate of the above-mentioned four different clones of *N. magadii* L13 (pRo-5-*fdx*-*bgaH*) was inoculated in NVM⁺ media with altered amounts of FeSO₄. Additionally to the usual FeSO₄ concentration of 20 µM, the cells were inoculated in medium containing 40 µM and 80 µM FeSO₄ and one test-series was inoculated in medium without FeSO₄-supplementation.

Preliminary results of this experiment did not show a correlation between intracellular iron-concentration and promoter activity (experiment conducted by Oliver Czerny, data not shown).

4.1.5. Discussion

In course of this study, the *fdx* promoter of *N. magadii* was analyzed regarding its suitability for the establishment of a gene expression system in *N. magadii*. Using the reporter-gene *bgaH*, the activity of the promoter was monitored in a time-course experiment.

It could be shown, that the *fdx* promoter is a very strong promoter (for halophile standards) with an average specific activity of about 5000 mU. In contrast, the inducible *tnaN* promoter displays a specific activity of roughly over 1000 mU at its highest. Hence, it can be said that the *fdx* promoter is 5-times stronger than the *tnaN* promoter, which makes it a good candidate for expressing proteins with a satisfying yield.

BgaH-measurements were also conducted for the wildtype *N. magadii* L13 strain and the *N. magadii* L13 (pRo-5-*tnaN*-*bgaH*) strain without tryptophan induction. Both strains showed no basal activity, which is an important feature for the establishment of a gene expression system.

Comparison of the growth behavior of the wildtype *N. magadii* L13 and the *N. magadii* L13 (pRo-5-fdx-bgaH) strain did not detect any growth defects of the mutant strain.

Further, the differences regarding the regulation of the *fdx* promoter and *ptnaN* are obvious. The *tnaN* promoter is inducible, whereas the *fdx* promoter is constitutively active, even though there are some fluctuations in promoter strength. The drop in promoter activity between 8 hours and 24 hours may be explained by the fact that the cells have to adapt to the new environment before expression is advanced. After 24 hours, promoter activity increases to a constant level of about 5000 mU.

Contrary to the data obtained by Gregor and Pfeifer (60), the highest expression level for the *fdx* promoter was not observed during exponential growth phase, but at the stationary growth phase. This could be due to organism-specific differences in gene-regulation, since Pfeifer *et al.* examined the *fdx* promoter of *H. salinarum* and in this study, the *fdx* promoter of *N. magadii* was analyzed.

It is important to mention, that the four different *N. magadii* L13 (pRo-5-fdx-bgaH) clones all yielded similar BgaH-expression. This indicates a constant promoter activity, which is a desired characteristic of promoters used for protein expression.

A first experiment investigating the role of iron for promoter activity did not show any correlation between intracellular iron-concentration and promoter activity.

To sum it up, it can be said that the *fdx* promoter of *N. magadii* is qualified for the establishment of a gene expression system. However, further experiments have to be conducted to analyze whether the promoter is able to express proteins of *N. magadii* and Φ Ch1.

4.2. Generation and analysis of *N. magadii* L13::*pibD* - a peptidase deletion mutant

4.2.1. Aim

The interaction between the virus Φ Ch1 and its host *N. magadii* has been intensively studied in the past. Yet, the precise mechanism of infection is still unknown. It has been shown that the virus has a head-tail-morphology, with the tail-fibre proteins gp34 and gp36 located at the end of the contractible tail (48) (76). Studies on the invertible region comprising ORF34 and ORF36 showed that Φ Ch1 utilizes a phase variation system, which produces different versions of the tail-fibre proteins gp34 and gp36. One variant, gp34₅₂ (carrying the C-terminus of ORF36₁) has been shown to bind to the cell surface of *N. magadii* L13 via a galactose-binding domain on its C-terminus. Gp34₅₂ contains a conserved amino-acid sequence that is responsible for building the binding pocket for α -D-galactose. Moreover, it was observed that in the presence of ≥ 25 mM α -D-galactose, gp34₅₂ could not bind to the surface of *N. magadii* L13 anymore, indicating that the attachment of the virus to the cell is mediated via galactose residues on the cell surface. Since the S-layer of halophilic archaea consists of glycoproteins, this structure could potentially serve as receptor for viral attachment. Another conceivable receptor would be the glycosylated flagellum proteins of *N. magadii* (76).

To gain insight into the mechanism of viral attachment of Φ Ch1 to *N. magadii*, several attempts have been made to delete the genomic region coding for the flagellum proteins. Unfortunately, due to various reasons, the construction of a homozygous flagellum deletion mutant failed so far (57) (79).

In this thesis, a different approach was chosen to elucidate whether the glycosylated flagella of *N. magadii* serve as receptors for viral attachment. Since the endeavor to delete the flagellin genes directly was fruitless, we searched for an alternative way to disturb flagellum synthesis. The peptidase *pibD* turned out to be a good candidate to intervene at the post-translational level. Since its task is to process the pre-flagellins and subsequently allowing the assembly of the flagellum, by deleting the peptidase it should be possible to

create a mutant strain with a flagellum-deficient phenotype. Analyzing the infectivity of Φ Ch1 towards flagellum-deficient *N. magadii* cells will shed light on the interaction mechanisms between virus and host.

4.2.2. Experimental setup to create a *pibD* deletion mutant

Several deletion mutants of *N. magadii* have already been created (24) (58) (80). A suitable method to delete a gene of interest is to transform cells with a suicide plasmid, which harbors up- and downstream fragments of the gene of interest, flanking a novobiocin resistance (Nov^R) cassette. Upon homologous recombination, the gene of interest is replaced by the resistance-cassette. The term suicide plasmid originates from its inability to replicate in the target organism. In this case, *E. coli* was used for cloning of the corresponding up- and downstream fragments and the resistance cassette into the plasmid pBluescript II KS+, which can be replicated in *E. coli*, yet lacks an archaeal origin of replication. After transformation into *N. magadii* and potential homologous recombination, the plasmid is unable to propagate and gets lost over time.

In course of this thesis the *pibD* gene of *N. magadii* (genome position 1785014 – 1786072R) was deleted following the subsequent work steps: First, a suitable suicide plasmid was cloned, which was then transformed in *N. magadii*. Positive transformants were screened for homologous recombination and subsequently passaged until a homozygous deletion of the *pibD* gene was achieved.

4.2.2.1. Transformation of *N. magadii* L13

The suicide plasmids pKSII-pib1-4 NovR forward and pKSII-pib1-4 NovR reverse (see 3.5.2) were cloned in *E. coli* XL1-Blue. Both plasmids contain a 837 bp long fragment originating from the upstream-region of the *pibD* gene and a 889 bp fragment which is derived from the downstream-region of the gene. Centered in between these two flanking regions, the Nov^R cassette was introduced, once in forward direction and once in reverse

direction of the *pibD* gene. The attempt to create a deletion mutant was conducted with both variants, because the Nov^R cassette was cloned without a terminator sequence and the influence of the transcription of the resistance cassette on surrounding gene-elements could not be predicted.

N. magadii L13 cells were transformed with either of the two plasmids and plated on selective agar plates. Via the annealing of the up- and downstream fragment of the *pibD* gene on the plasmid with their counterparts on the chromosome, homologous recombination was facilitated, resulting in either a single-crossover or a double-crossover recombination event. The desired product is obtained by a double-crossover recombination event between the 5' and 3' flanks, leading to the replacement of the *pibD* gene by the Nov^R cassette. A schematic illustration of a double-crossover recombination event can be seen in Figure 13.

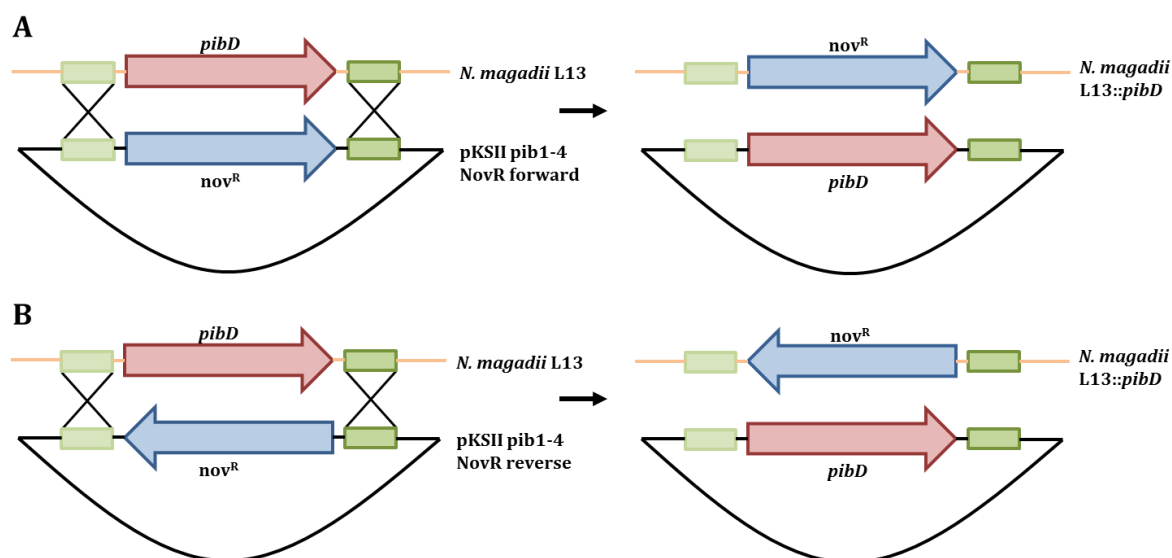


Figure 13: Schematic illustration of a double-crossover event

Homologous recombination of the suicide plasmids with the wildtype *N. magadii* L13 chromosome is shown for pKSII-pib1-4 NovR forward in **A** and for pKSII-pib1-4 NovR reverse in **B**. In both cases, the occurrence of a double-crossover is depicted, which leads to replacement of the *pibD* gene on the chromosome by the Nov^R cassette.

In the case of a single-crossover recombination event, only one of the two flanks (up- or downstream-fragment) anneals to its pendant on the chromosome. The result would be the incorporation of the whole plasmid into the chromosome and the *pibD* gene would still be intact. The fact that such clones would also carry the Nov^R cassette impedes a

distinction between cells with a single- or double- crossover based on their ability to tolerate novobiocin.

4.2.2.2. Screening of the clones

After transformation, single colonies were grown in NVM⁺ medium until they reached the stationary phase. Next, they were examined for the uptake of the plasmid, and if positive, they were further screened if a double-crossover event took place during homologous recombination.

For the verification that the cells had taken up the plasmids, a primer set was necessary, with one primer binding in the 5' flank or the 3' flank respectively and the other primer binding inside the Nov^R cassette. To test whether a double-crossover had occurred, two primer sets were necessary: one primer each had to bind upstream of the 5' flank or downstream of the 3' flank respectively, and the other primer had to bind inside the Nov^R cassette. In case of a single-crossover event, only one of the two primer sets would lead to the amplification of a DNA fragment. Only when both primer sets give rise to PCR products of a certain length, the occurrence of a double-crossover event can be confirmed.

4.2.2.3. Passaging of candidates

As mentioned in 1.1.2 *N. magadii* is a polyploid organism and it is estimated that it carries up to 50 copies of its genome in one cell. This implies that a transformant that was tested positive for a double-crossover recombination event may carry the deletion of the gene on several of its copies, but there may be also several copies with an intact *pibD* gene. Only if the deletion of the gene is homozygous a proper study on the phenotype can be pursued. To create a homozygous deletion mutant, the transformants have to be passaged several times (see 3.1.10). Since cells that harbor the gene deletion on more genome copies than others are selected for by the use of novobiocin, mutants with multiple deletions are enriched and over time, a homozygous deletion mutant should be obtained. The presence of genome copies carrying the wildtype *pibD* gene can be monitored by analytical PCR. If

the *pibD* gene cannot be amplified anymore, this is an indication that the candidate is homozygous for the deletion.

4.2.3. Attempt to create a deletion mutant with pKSII-pib1-4 NovR forward

After transformation of *N. magadii* L13 cells with pKSII-pib1-4 NovR forward, individual clones were tested regarding the uptake of the plasmid with analytical PCR. For this reaction the primers Pib-4 and Nov-13 were used, which have their binding sites at the 3' end of the downstream-fragment of *pibD* and inside the Nov^R cassette. Primer binding sites are presented in Figure 14. Only after screening of 108 individual clones, a successfully transformed candidate was identified (data not shown). This transformant was then further analyzed with regard to a double-crossover recombination event. To analyze whether recombination at the 5' flank had occurred, primers Pib-5Ende and Nov-12 were used. Primers Pib-3Ende and Nov-13 were utilized to test whether recombination on the 3' end of the *pibD* gene took place. Indeed, both PCRs led to the amplification of the expected DNA fragments (data not shown). Thus, the occurrence of a double-crossover recombination event could be confirmed in this clone.

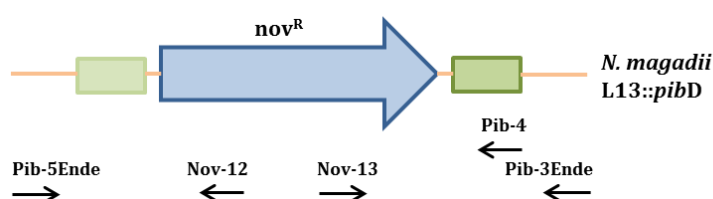


Figure 14: Schematic illustration of pKSII-pib1-4 NovR forward primer binding sites

Candidates were tested regarding a positive transformation with pKSII-pib1-4 NovR forward with the primers Pib-4 and Nov-13. To test whether a double-crossover recombination event had occurred in the transformant, primers Pib-5Ende with Nov-12 and Pib-3Ende with Nov-13 were used. The Nov^R cassette is given as a blue arrow, the up- and downstream sequences of *pibD* as green boxes.

After confirmation of the double-crossover, passaging was conducted. The cells were analyzed regarding the presence of the *pibD* gene every 5th passage using the primers PibD-5 and PibD-3. Previous studies in our laboratory resulted in various *N. magadii* deletion mutants which were shown to be homozygous after at least 20 passages,

provided that the creation of the deletion-mutant was possible in the first place (58) (81). However, even after the 50th passage, the *pibD* gene was still amplified from the candidate and the signal resulting from PCR analysis was even as strong as in the wildtype. The latest PCR analysis of this candidate can be seen in Figure 15.

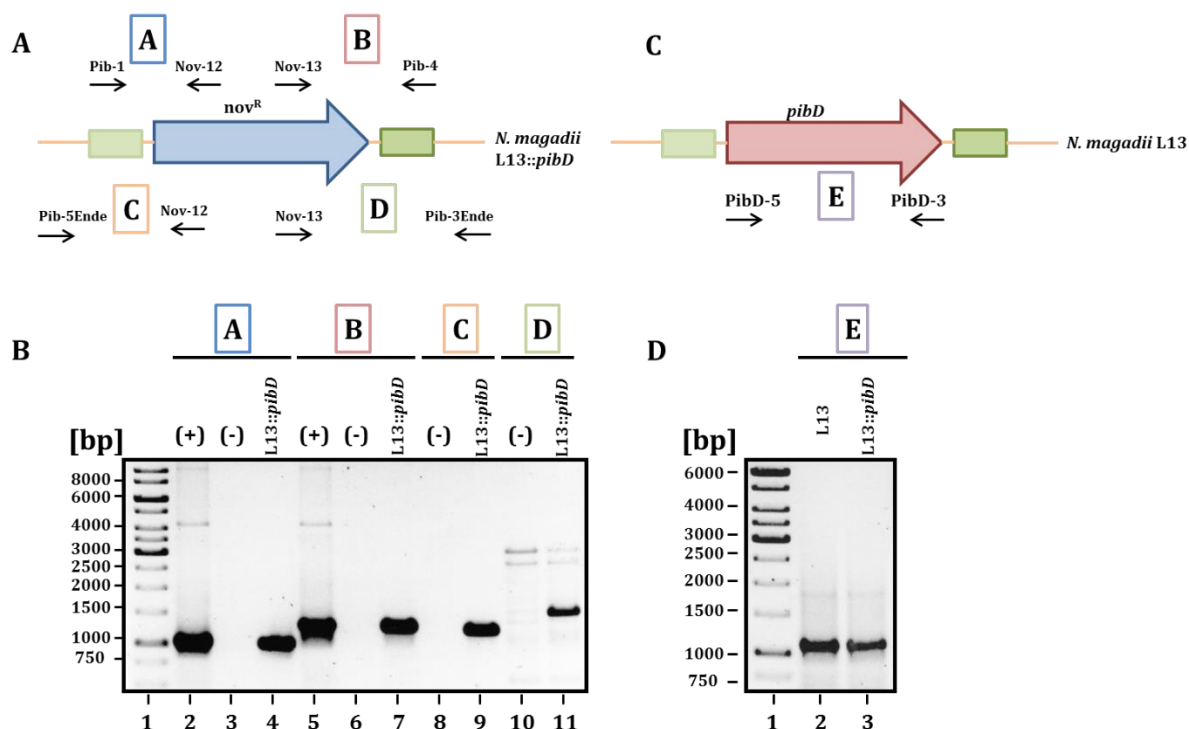


Figure 15: PCR analysis of *N. magadii* L13 (pKSII-pib1-4 NovR forward) candidate after the 50th passage

A: PCR was performed with primer pairs A (Pib-1 and Nov-12) and B (Pib-4 and Nov-13) to verify that the candidate was transformed with the plasmid pKSII-pib-1-4 NovR forward. To prove that a double-crossover recombination event had occurred during homologous recombination, primer pairs C (Pib-5Ende and Nov-12) and D (Pib-3Ende and Nov-13) were used.

B: For the PCR analysis with primer pairs A and B, the plasmid pKSII-pib1-4 NovR forward served as positive control and chromosomal DNA of *N. magadii* L13 served as negative control. Analytical PCR of the candidate with primer pair A gave rise to the 997 bp long fragment and PCR with primer pair B led to a signal at 1126 bp. The light bands at 4000 bp in Lanes 2 and 5 are accounted to unspecific binding of the primers. For the analysis with primer pairs C and D, chromosomal DNA of *N. magadii* L13 was used as a negative control. Both PCRs led to the expected 1229 bp (C) and 1382 bp (D) long fragments.

Lane 1: GeneRuler 1 kb DNA ladder, **Lanes 2-7:** analysis of pKSII-pib1-4 NovR forward, chromosomal DNA of *N. magadii* L13 and candidate with primer pair A (Lanes 2-4) and B (Lanes 5-7) (from left to right), **Lanes 8-11:** analysis of chromosomal DNA of *N. magadii* L13 and candidate with primer pair C (Lanes 8-9) and D (Lanes 10-11) (from left to right)

C: Primer pair E (PibD-5 and PibD-3) was used to detect copies of the wildtype *pibD* gene.

D: Analysis of the wildtype *N. magadii* L13 strain with primer pair E led to the generation of the expected 1056 bp long PCR product from the *pibD* gene. PCR analysis of the candidate led to the amplification of the *pibD* gene fragment as well.

Lane 1: GeneRuler 1 kb DNA ladder, **Lane 2:** chromosomal DNA of *N. magadii* L13, **Lane 3:** candidate

Even though the candidate tested positive for the incorporation of the Nov^R cassette and the occurrence of a double-crossover, a homozygous deletion mutant could not be obtained. This could have its origin in the genetic environment of the *pibD* gene. A possible explanation why the generation of a homozygous deletion mutant by use of the plasmid pKSII-pib1-4 NovR forward failed will be discussed in 4.2.7. In any case, passaging of this candidate was stopped after the 50th passage. From now on, the term *N. magadii* L13::*pibD* refers to the candidate transformed with pKSII-pib1-4 NovR reverse.

4.2.4. Creation of a *pibD* deletion mutant with pKSII-pib1-4 NovR reverse

N. magadii L13 cells were transformed with the plasmid pKSII-pib1-4 NovR reverse. Afterwards, individual candidates were screened for a positive transformation event by analytical PCR with the primers Pib-4 and Nov-12. Pib-4 binds at the 3'-end of the downstream-flank and Nov-12 binds inside the Nov^R cassette (see Figure 16).

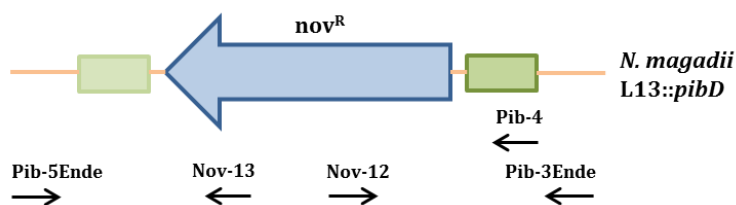


Figure 16: Schematic illustration of pKSII-pib1-4 NovR reverse primer binding sites

In order to test whether the candidates had taken up the plasmid, primers Pib-4 and Nov-12 were used. The primer pair Pib-5Ende and Nov-13 and also Pib-3Ende and Nov-12 were applied to screen transformants for a double-crossover recombination event. The Nov^R cassette is given as a blue arrow, the up- and downstream sequences of *pibD* as green boxes.

The plasmid pKSII-pib1-4 NovR reverse was used as a positive control and chromosomal DNA of *N. magadii* L13 served as a negative control. As can be seen in Figure 17, all of the 10 candidates were tested positive for the transformation with pKSII-pib1-4 NovR reverse.

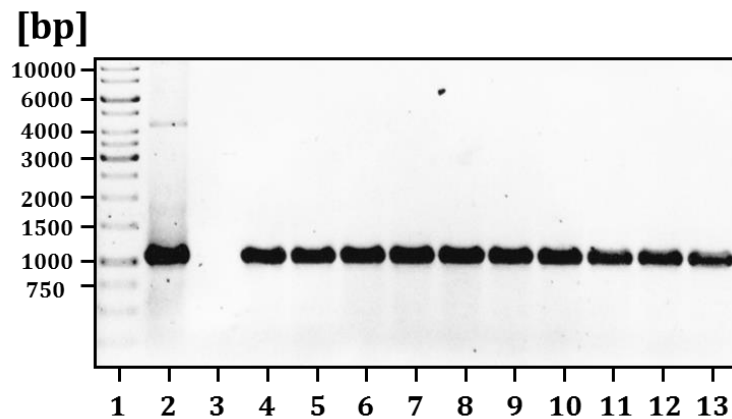


Figure 17: Analysis of *N. magadii* L13 candidates after transformation with pKSII-pib1-4 NovR reverse

PCR analysis with Pib-4 and Nov-12 led to amplification of the 1021 bp long DNA fragment in every candidate that was tested.

Lane 1: GeneRuler 1 kb DNA ladder, **Lane 2:** plasmid pKSII-pib1-4 NovR reverse (positive control), **Lane 3:** chromosomal DNA of *N. magadii* L13 (negative control), **Lanes 4-13:** individual candidates

Next, five of the ten transformants were tested for a double-crossover recombination event. To check whether the 5' flank of *pibD* had recombined, primers Pib-5Ende and Nov-13 were used. To test if recombination took place on the 3'-end, primers Pib-3Ende and Nov-12 were used (for primer binding sites see Figure 16). As a result of this PCR analysis, a double-crossover recombination event could be confirmed for two of the five tested transformants (data not shown).

Passaging was carried out with both clones that were tested positive for a double-crossover. To monitor whether the *pibD* gene was still present on any of the numerous copies of the genome, an analytical PCR using the primers PibD-5 and PibD-3 was performed every 5th passage. Primer binding sites are visualized in Figure 18C. After the 16th passage, amplification of the *pibD* gene was not possible anymore in one of the two candidates, leading to the assumption that this candidate was homozygous for the *pibD* deletion. An exemplary PCR analysis of this transformant can be seen in Figure 18.

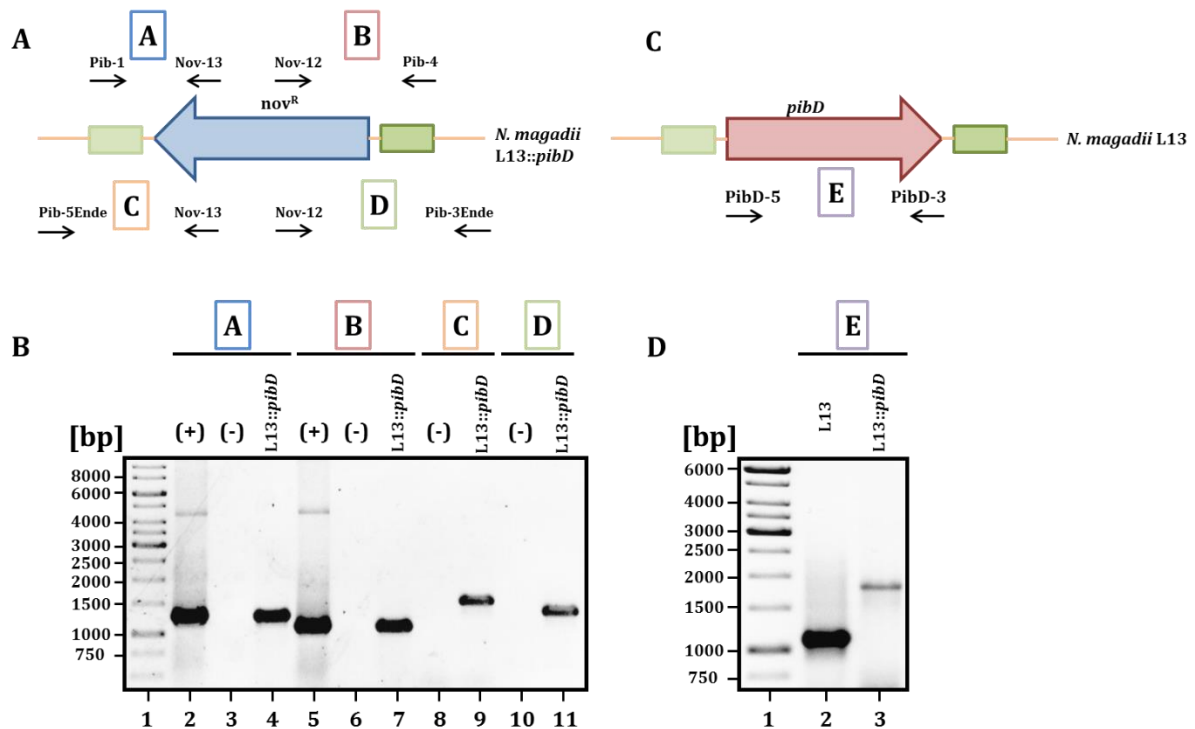


Figure 18: PCR-Analysis of putative deletion mutant *N. magadii* L13::*pibD* after 16 passages

A: Analysis with primer pair A (Pib-1 and Nov-13) and B (Pib-4 and Nov-12) was done to confirm that the Nov^R cassette was inserted into the chromosome in reverse direction. To test whether a double-crossover had taken place during homologous recombination, primer pairs C (Pib-5Ende and Nov-13) and D (Pib-3Ende and Nov-12) were utilized.

B: The plasmid pKSII-pib1-4 Nov^R reverse served as a positive control for analysis with primer pairs A and B; chromosomal DNA of *N. magadii* L13 was used as a negative control for PCR analyses with primer pairs A-D. Analytical PCR of the putative deletion mutant with primer pair A resulted in a 1079 bp long PCR product and primer pair B gave rise to a 1021 bp long PCR fragment. The light bands at 5000 bp in lanes 2 and 5 arise from unspecific binding of the primers to the plasmid. Analytical PCR with primer pairs C and D showed that the 1311 bp (C) and 1277 bp (D) long fragments could both be amplified from the candidate.

Lane 1: GeneRuler 1 kb DNA ladder, **Lanes 2-7:** analysis of pKSII-pib1-4 Nov^R reverse, chromosomal DNA of *N. magadii* L13 and candidate with primer pair A (Lanes 2-4) and B (Lanes 5-7) (from left to right), **Lanes 8-11:** analysis of chromosomal DNA of *N. magadii* L13 and candidate with primer pair C (Lanes 8-9) and D (Lanes 10-11) (from left to right)

C: In order to test if any copies of the wildtype *pibD* gene are present on any of the numerous genome copies of the putative deletion mutant, a PCR using the primers PibD-5 and PibD-3 (primer pair E) was conducted. **D:** For the wildtype *N. magadii* L13 strain, a 1056 bp long fragment of the *pibD* gene could be obtained upon analysis with primer pair E. PCR analysis of the putative deletion mutant with primer pair E did not result in a PCR product of this length. The light signal at approximately 1900 bp in lane 3 is due to unspecific binding of the primers.

Lane 1: GeneRuler 1 kb DNA ladder, **Lane 2:** chromosomal DNA of *N. magadii* L13, **Lane 3:** putative *pibD* deletion mutant strain

Figure 18B shows, that the Nov^R cassette is inserted in reverse direction. In addition, the occurrence of a double-crossover could be confirmed in this candidate. The fact that, even after 50 cycles of PCR, the *pibD* gene could not be amplified any more from the candidate drives the assumption that this strain is homozygous for the deletion of *pibD* (Figure 18D).

4.2.4.1. Confirmation with Southern Blot

Because DNA analysis on base of PCR is not sufficient to confirm that the mutant strain *N. magadii* L13::*pibD* is indeed homozygous for the deletion, an analysis by means of Southern Blot was conducted. A prerequisite for Southern Blot analysis is the preparation of hybridization probes that allow the distinction between wildtype chromosomes and chromosomes carrying the deletion of the gene. The foundation of this analysis is the fact that upon digestion with *EcoRV*, the exchange of the *pibD* gene against the Nov^R cassette in the mutant strain leads to a different restriction pattern than in the wildtype. Two hybridization probes were designed to yield different signals, depending on whether they bind to the wildtype chromosome or the chromosome with the deletion. Because of the great sensitivity of the Southern Blot, the heterogeneity of the mutant strain would be displayed, even if only one copy of the chromosome in the cell would still carry the wildtype *pibD* gene. A graphical declaration of the Southern Blot analysis is depicted in Figure 19.

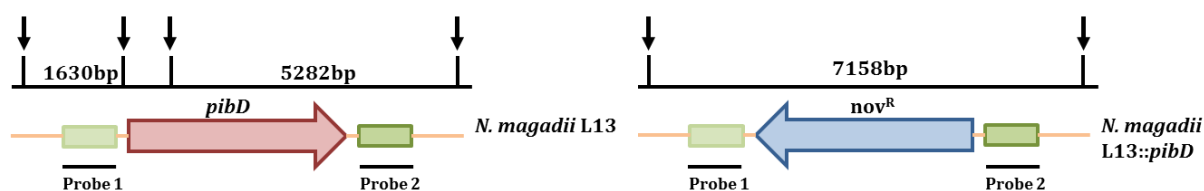


Figure 19: Schematic illustration of experimental setup for Southern Blot analysis

EcoRV restriction sites are marked by an arrow. Due to the replacement of the *pibD* gene with the Nov^R cassette, two *EcoRV* restriction sites are lost in the L13::*pibD* mutant strain. Hybridization of probe 1 to copies of the wildtype *N. magadii* L13 chromosome (restricted with *EcoRV*) leads to a signal at 1630 bp. Upon hybridization of probe 2, a signal at 5282 bp becomes apparent. Conversely, both the hybridization of probe 1 and 2 to *EcoRV* digested chromosomes carrying the deletion lead to a signal at 7158 bp. In the absence of a signal at 1630 bp and 5282 bp, respectively, it can be inferred that the deletion of *pibD* is homozygous.

Chromosomal DNA of *N. magadii* L13 served as a template for the synthesis of the two biotinylated hybridization probes (see 3.1.9.1). Hybridization probe 1 was amplified using the primers Pib-1 and Pib-2. The 836 bp long probe has its binding site upstream of the *pibD* gene. The 888 bp long hybridization probe 2, which was generated using primers Pib-3 and Pib-4, has its binding site at the downstream region of *pibD*. Chromosomal DNA of the putative deletion mutant and the wildtype strain *N. magadii* L13 was isolated,

restricted with *EcoRV* and separated on a 0.8% agarose-gel. Restriction sites and binding sites for the hybridization probes are shown in Figure 19.

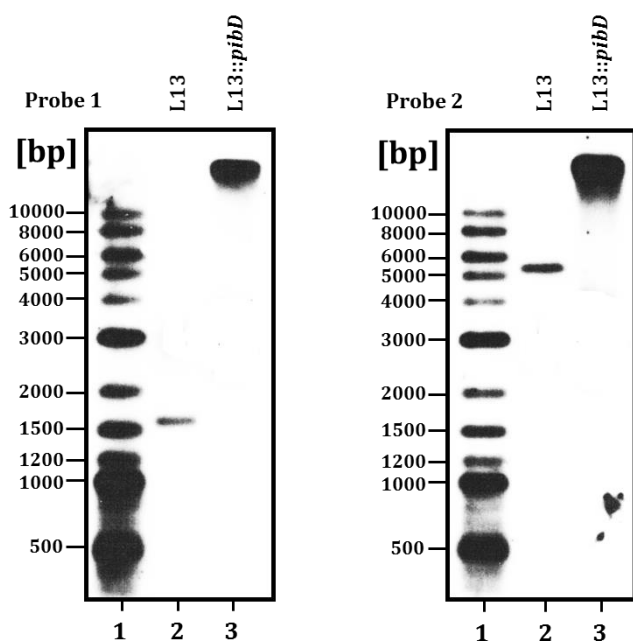


Figure 20: Southern Blot analysis of *N. magadii* L13 and *N. magadii* L13::*pibD*

On the left side, the result from hybridization of probe 1 to fragments of chromosomal DNA of *N. magadii* L13 and the putative *N. magadii* L13::*pibD* deletion mutant can be seen; hybridization with probe 2 is displayed on the right side. Hybridization of probe 1 to restricted chromosomal DNA of *N. magadii* L13 leads to the expected signal at 1630 bp. Also, a signal at 5282 bp can be obtained for the hybridization of probe 2. In the case of the putative *N. magadii* L13::*pibD* deletion mutant, both signals are shifted from the expected 7158 bp to over 10000 bp. No signals associated with the wildtype *N. magadii* L13 chromosome were detected.

Lane 1: 2-Log DNA ladder,
Lane 2: *N. magadii* L13,
Lane 3: *N. magadii* L13::*pibD*

Results from Southern Blot analysis (see Figure 20) showed, that hybridization of probe 1 and 2 to fragmented chromosomal DNA of *N. magadii* L13 yield the expected signal at 1630 bp and 5282 bp, respectively. Hybridization of probes 1 and 2 to fragmented chromosomal DNA of the putative deletion mutant gave a strong signal; unfortunately, this signal seems to be shifted. Instead of the expected 7158 bp a signal at approximately 10000 bp was obtained. Although this phenomenon has been observed before (58), an explanation why the signal shifts could still not be found. Nevertheless, the fact that no signal associated with the wildtype *N. magadii* L13 chromosome could be detected is enough proof to state that the *N. magadii* L13::*pibD* mutant strain is homozygous for the deletion of *pibD*.

4.2.5. Complementation of *N. magadii* L13::*pibD* mutant strain

After construction of the mutant strain *N. magadii* L13::*pibD*, a phenotypical analysis was performed. Additionally, the correlation of the *pibD* deletion with potential phenotypical alterations can be investigated by complementation of the *N. magadii* L13::*pibD* mutant strain in trans. Therefore, the mutant strain was transformed with the plasmid pNB102-*pibD* (for cloning details see 3.5.3). Moreover, the wildtype strain *N. magadii* L13 was transformed with the plasmid pNB102-*pibD*, targeting the over-expression of *pibD*.

After transformation, individual clones were incubated in NVM⁺ medium and after reaching stationary phase, they were analyzed regarding a positive transformation event. Analysis of one candidate each of *N. magadii* L13::*pibD* (pNB102-*pibD*) and *N. magadii* L13 (pNB102-*pibD*) is illustrated in Figure 21. Primers NB-1 and I-Pib-3 were used to confirm the uptake of the plasmid. Here, the primer NB-1 has its binding site on the plasmid pNB102, whereas I-Pib-3 binds inside the *pibD* gene. For this analysis, the plasmid pNB102-*pibD* served as positive control. In a second PCR analysis, both candidates were screened for the wildtype *pibD* gene on the chromosome. For this reason, primers Pib-1 and PibD-Bam, which binds at the 3' end of *pibD*, were utilized. Because primer Pib-1 binds at the upstream region of *pibD*, which is not included on the plasmid pNB102-*pibD*, this PCR is only competent of amplifying the chromosomal version of *pibD*. In a third screening, the candidates were tested regarding the incorporation of the Nov^R cassette on the chromosome. This was performed using primers Pib-1 and Nov-13. *N. magadii* L13 and *N. magadii* L13::*pibD* served as positive or negative control for the screenings, depending on the kind of test. Primer binding sites can be seen in Figure 21A.

As can be seen in Figure 21B transformation with the plasmid could be confirmed for both *N. magadii* L13::*pibD* (pNB102-*pibD*) and *N. magadii* L13 (pNB102-*pibD*). Furthermore, it was shown that the *N. magadii* L13::*pibD* (pNB102-*pibD*) strain carries no version of chromosomal *pibD*, but instead is able to amplify the Nov^R cassette. This verifies in case of *N. magadii* L13::*pibD* (pNB102-*pibD*) the transformation of the *pibD* deletion mutant strain with the plasmid.

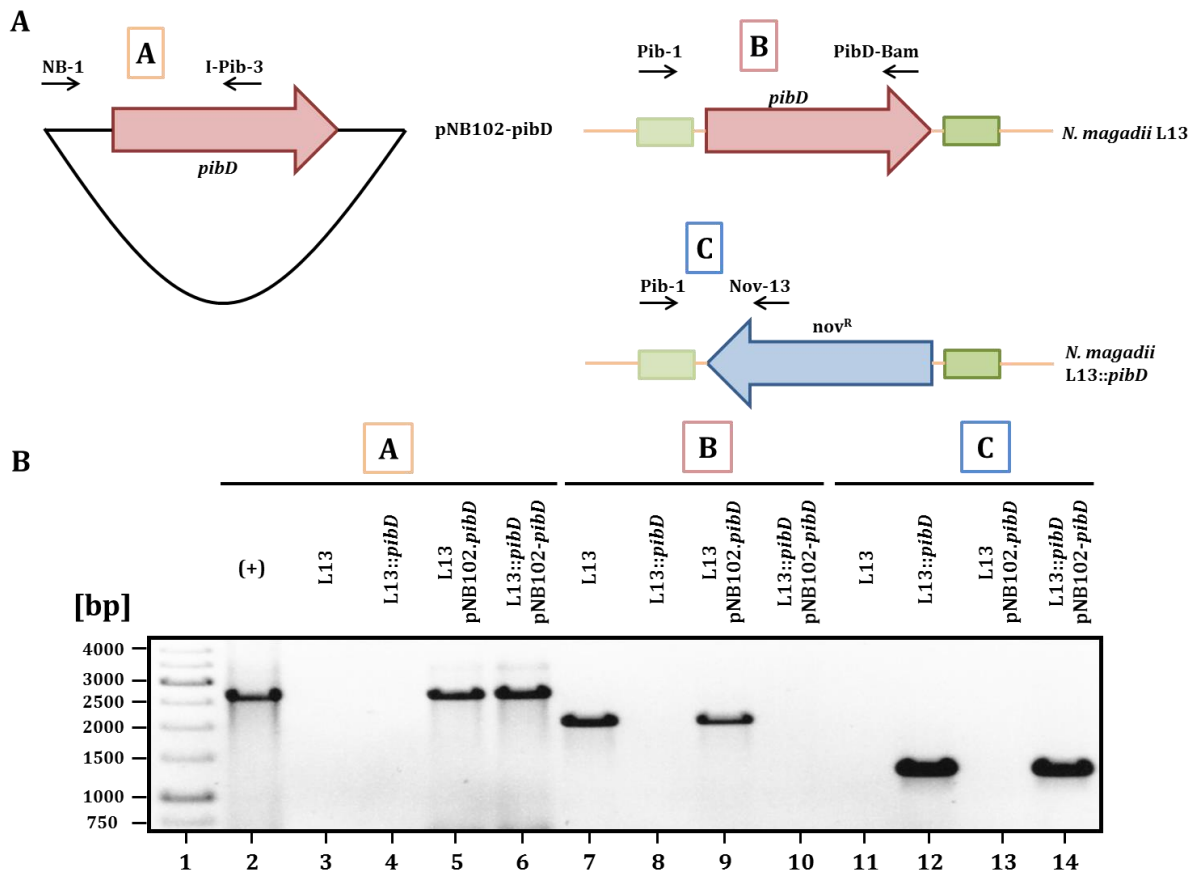


Figure 21: Analysis of candidates after transformation with pNB102-pibD

A: Three different screenings were made: Primer pair A (NB-1 and I-Pib-3) was used to confirm the presence of the plasmid pNB102-pibD in the candidates; Primer pair B (Pib-1 and PibD-Bam) was utilized to amplify the wildtype *pibD* gene from the chromosome; Primer pair C (Pib-1 and Nov-13) was used to amplify a fragment specific for the deletion mutant.

B: Analysis with primer pair A led to the expected 2644 bp long product for the positive control (pNB102-pibD). The fragment could also be obtained for both candidates (*N. magadii* L13 (pNB102-pibD) and *N. magadii* L13::pibD (pNB102-pibD)). PCR analysis with primer pair B resulted in the amplification of the 1977 bp long fragment from the wildtype *pibD* gene in the strains *N. magadii* L13 and *N. magadii* L13 (pNB102-pibD). PCR-analysis with primer pair C led to the amplification of the 1079 bp long DNA-fragment that is specific for the deletion mutant in the strains *N. magadii* L13::pibD and *N. magadii* L13::pibD (pNB102-pibD).

Lane 1: GeneRuler 1 kb DNA ladder, **Lane 2:** PCR analysis of plasmid pNB102-pibD with primer pair A, **Lanes 3-14:** PCR analysis of strains *N. magadii* L13, *N. magadii* L13::pibD, *N. magadii* L13 (pNB102-pibD), *N. magadii* L13::pibD (pNB102-pibD) with primer pair A (Lanes 3-6), B (7-10) and C (11-14) (from left to right)

In strain *N. magadii* L13 (pNB102-pibD), the Nov^R cassette was not integrated in the chromosome, but instead the chromosomal version of *pibD* was amplified. Therefore it could be proven, that the wildtype *N. magadii* L13 strain was successfully transformed with the plasmid.

4.2.6. Phenotypical analysis of the *N. magadii* L13::*pibD* mutant strain

4.2.6.1. Growth behavior

First of all, the growth behavior of the mutant strains *N. magadii* L13::*pibD*, *N. magadii* L13::*pibD* (pNB102-*pibD*) and *N. magadii* L13 (pNB102-*pibD*) was monitored in a time course experiment and compared to the wildtype *N. magadii* L13 strain. The strains were inoculated with an OD₆₀₀ of 0.1 and grown until late stationary phase. To enable the construction of a growth curve and to analyze their growth behavior, the optical density was measured several times per day. In Figure 22 it can be seen, that the mutant strains show no relevant differences regarding their growth behavior when compared to the wildtype. Therefore, the deletion of *pibD* does not lead to any growth defects.

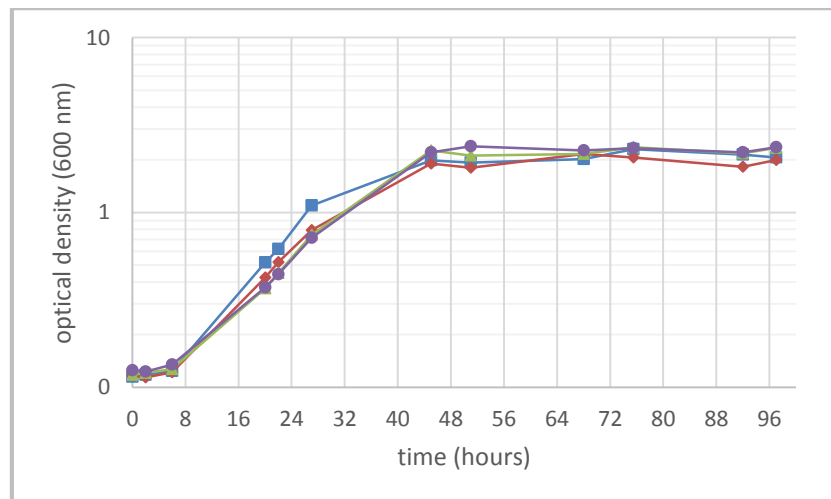


Figure 22: Growth curve of strains *N. magadii* L13, *N. magadii* L13::*pibD*, *N. magadii* L13 (pNB102-*pibD*) and *N. magadii* L13::*pibD* (pNB102-*pibD*)

Strains were inoculated at an OD₆₀₀ of 0.1 and incubated at 37 °C. The comparison of the mutant strains *N. magadii* L13::*pibD*, *N. magadii* L13 (pNB102-*pibD*) and *N. magadii* L13::*pibD* (pNB102-*pibD*) to the wildtype *N. magadii* L13 showed no significant differences in growth behavior.

Blue Line: *N. magadii* L13, **Red Line:** *N. magadii* L13::*pibD*, **Green Line:** *N. magadii* L13 (pNB102-*pibD*), **Purple Line:** *N. magadii* L13::*pibD* (pNB102-*pibD*)

4.2.6.2. Western Blot

After confirming a successful knockout of *pibD* in *N. magadii* L13::*pibD*, its effect on the formation and functionality of flagella can be examined. Since the peptidase *pibD* is responsible for post-translational processing of the flagellins and therefore facilitates subsequent assembly of the flagellum, it is expected that flagellum precursor-proteins are still present in the *N. magadii* L13::*pibD* mutant. However, it is assumed, that due to the disruption in the assembly process, flagellum proteins cannot be detected on the surface of the cell.

Samples from *N. magadii* L13::*pibD* in stationary phase were prepared for protein analysis as described in 3.3.1 and 3.3.2. Not only the pelleted cells were analyzed for proteins, but also precipitation of proteins from the supernatant was performed. Examination of the cell pellet provides insight in the processes inside the cells, whereas membrane-bound proteins, like the flagella, remain in the supernatant. As a control, samples were prepared from *N. magadii* L13 as well. Representatively for all four flagellum proteins, the detection was conducted with the α -FlaB1 antibody established by Till, 2011 (82). Western Blot analysis is shown in Figure 23.

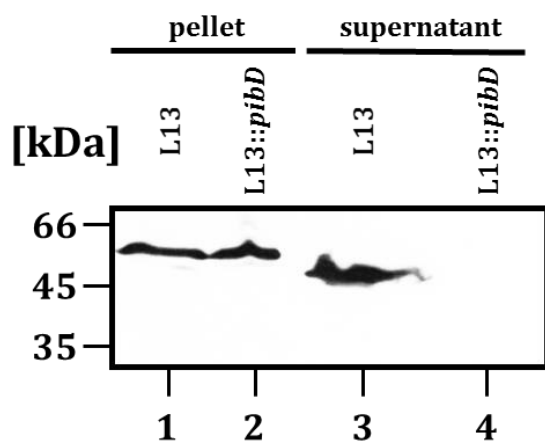


Figure 23: Western Blot of *N. magadii* L13 and *N. magadii* L13::*pibD* samples (pellet and supernatant) with α -FlaB1

Samples from *N. magadii* L13 and *N. magadii* L13::*pibD* were prepared for protein analysis of the pellet as well as the supernatant. Upon incubation with α -FlaB1 antibody and subsequent detection, a signal at approximately 55 kDa was obtained for the pellet sample of *N. magadii* L13 and *N. magadii* L13::*pibD*. For the supernatant sample of *N. magadii* L13, a signal at approximately 50 kDa is visible. However, FlaB1 protein could not be detected in the supernatant sample of *N. magadii* L13::*pibD*.

Lane 1: pellet sample of *N. magadii* L13, **Lane 2:** pellet sample of *N. magadii* L13::*pibD*, **Lane 3:** supernatant sample of *N. magadii* L13, **Lane 4:** supernatant sample of *N. magadii* L13::*pibD*; Molecular weight standard is indicated on the left side. The amount of applied sample was adjusted by means of Coomassie Staining prior to Western Blotting.

The result of the Western Blot verifies the assumption that the deletion of *pibD* leads to a disruption of the flagellum assembly. The α -FlaB1-antibody detects the unprocessed FlaB1 with a molecular weight of approximately 55 kDa inside the cells of the *N. magadii* L13 and *N. magadii* L13::*pibD* strains. However, the absence of FlaB1 protein in the supernatant sample of *N. magadii* L13::*pibD* implies that the *pibD* deletion mutant lacks flagella on its cell surface. By comparison, mature FlaB1 protein with a molecular weight of approximately 50 kDa was detected in the supernatant sample of *N. magadii* L13, indicating its presence on the cell surface of *N. magadii* L13. The shift in molecular weight of the FlaB1 protein from approximately 55 kDa in the pellet sample to approximately 50 kDa in the supernatant sample is due to the fact that the peptidase cleaves off signal peptides from the precursor-proteins.

4.2.6.3. Motility assay

As described before (1.2.6), *N. magadii* possesses polar flagella, which leads to the motility of the organism. As suggested in 4.2.6.2, *N. magadii* L13::*pibD* mutant cells are non-flagellated and are thus expected to be non-motile. Both strains, the wildtype *N. magadii* L13 and the *pibD*-deficient strain, were analyzed regarding their motility. Moreover, for a better understanding of the mode of action of *pibD*, the strains *N. magadii* L13::*pibD* (pNB102-*pibD*) and *N. magadii* L13 (pNB102-*pibD*) were included in the experiment. So-called swimming plates provide information about the ability to move through agar plates by use of flagella. For the preparation of swimming plates and implementation of the motility assay see 3.4. Results of the motility assay are depicted in Figure 24.

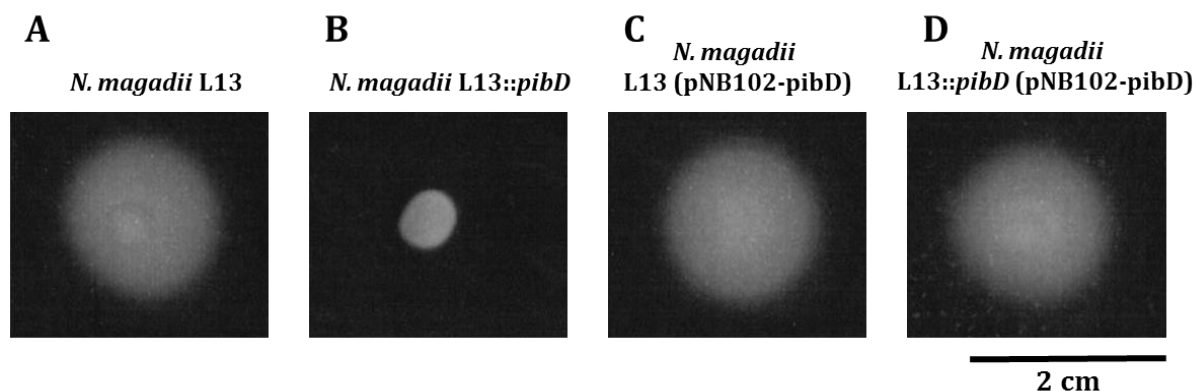


Figure 24: Motility assay with strains *N. magadii* L13, *N. magadii* L13::pibD, *N. magadii* L13 (pNB102-pibD) and *N. magadii* L13::pibD (pNB102-pibD)

Motility assay of **A:** *N. magadii* L13, **B:** *N. magadii* L13::pibD, **C:** *N. magadii* L13 (pNB102-pibD), **D:** *N. magadii* L13::pibD (pNB102-pibD).

On each plate, 5 μ l of the corresponding culture with an OD₆₀₀ of 1.5 was spotted. The plates were incubated at 37°C for 4 days in a styrofoam box, to prevent them from drying out.

As can be seen in Figure 24, the wildtype *N. magadii* L13 strain is able to move through the plate, resulting in a halo around the point of inoculation. According to expectations, the flagellum-deficient mutant strain *N. magadii* L13::pibD cannot swim on the surface of the plate, owing to the loss of flagella in the mutant strain. However, in the complemented mutant strain *N. magadii* L13::pibD (pNB102-pibD), the motility defect is fully rescued compared to the wildtype. Also, the *N. magadii* L13 (pNB102-pibD) over-expression strain is equally motile as the wildtype.

4.2.6.4. Surface adhesion

The role of archaeal flagella in surface adhesion is currently controversial. Different structural proteins are speculated to be involved in surface adhesion. Therefore, it is interesting to explore whether adhesion of *N. magadii* to surfaces, like glass, is mediated via its flagella.

It was observed many times, that wildtype *N. magadii* L13 cultures, incubated in mineral medium (NMMb⁺) with agitation, form a band of cells inside the flask after some time. To examine the role of flagellum-dependent surface adhesion in the formation of this ring, the wildtype and the mutant *N. magadii* L13::pibD strain were inoculated in NMMb⁺

medium with agitation until late stationary phase was reached. A comparative picture can be seen in Figure 25.

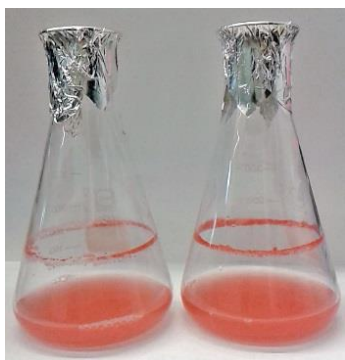


Figure 25: Comparison of flasks after incubation with *N. magadii* L13 and *N. magadii* L13::*pibD*

Left side: *N. magadii* L13, right side: *N. magadii* L13::*pibD*

After incubation of both strains in NMMb⁺ medium at 37 °C with agitation, a picture demonstrating both flasks was taken. It can be seen, that both strains constitute a small band inside the flask.

As a result, it could be observed, that both the wildtype and the mutant strain are able to attach to the glass flask after shaking for several days. However, this simplified examination is not sufficient to draw conclusions on surface adhesion features of the two strains.

4.2.6.5. Virus titre assay

The ultimate goal of this study was to elucidate whether the glycosylated flagellum proteins of *N. magadii* serve as receptors for the attachment of the virus Φ Ch1. Therefore, the infectivity of Φ Ch1 towards the wildtype and the mutant strain was compared in a virus titre assay (see 3.2.2). Not only the strains *N. magadii* L13::*pibD* and the wildtype *N. magadii* L13, but also strains *N. magadii* L13::*pibD* (pNB102-*pibD*) and *N. magadii* L13 (pNB102-*pibD*) were included in the experiment. Results from the virus titre assay are stated in Table 2.

Strain	<i>N. magadii</i> L13	<i>N. magadii</i> L13:: <i>pibD</i>	<i>N. magadii</i> L13:: <i>pibD</i> (pNB102- <i>pibD</i>)	<i>N. magadii</i> L13 (pNB102- <i>pibD</i>)
PFU/ml	1.58x10 ⁹	1.48x10 ⁹	4.5x10 ⁸	1.72x10 ⁹

Table 2: Results from the plaque assay of strains *N. magadii* L13, *N. magadii* L13::*pibD*, *N. magadii* L13 (pNB102-*pibD*) and *N. magadii* L13::*pibD* (pNB102-*pibD*)

Infectivity of the virus is stated as plaque-forming units (PFU) per ml. The results from the plaque-assay show, that the flagella-deficient strain *N. magadii* L13::*pibD* is infected with Φ Ch1 to the same extent than the wildtype. In addition, both strains *N. magadii* L13 (pNB102-*pibD*) and *N. magadii* L13::*pibD* (pNB102-*pibD*) show no significant difference in infectivity when compared to the wildtype.

The results from the plaque assay showed, that all strains are infected with the virus at an equal rate. Importantly, the *pibD* deletion mutant strain shows no difference in the susceptibility to Φ Ch1 infection compared to the wildtype. There is a small drop in PFU/ml for the over-expressed *N. magadii* L13::*pibD* (pNB102-*pibD*) strain. However, this drop is not significant and therefore cannot be accounted to any defect of infectivity. All in all, it was shown that the absence of flagella on the cell surface of the *N. magadii* L13::*pibD* mutant strain does not lead to a loss of infectivity, therefore indicating that the flagella do not serve as receptors for viral attachment.

4.2.7. Discussion

The aim of this study was to analyze the role of flagella upon infection with the virus Φ Ch1. Since the peptidase *pibD* is responsible for flagellin-processing and the assembly of the flagellum, a strain lacking the peptidase is expected to be non-flagellated. For that reason, a *pibD* deletion mutant was constructed. The construction of the deletion mutant was pursued through homologous recombination with a suicide plasmid.

In course of this study, the attempt to create the deletion mutant with the plasmid pKSII-*pib1-4* NovR forward was terminated, because no strain that was homozygous for the deletion could be obtained. The reason for this may be the genetic environment around the *pibD* gene. A uracil-DNA glycosylase is encoded downstream of the *pibD* gene in reverse direction (data obtained from <https://www.halolex.mpg.de/public/>). Since the Nov^R cassette was cloned on the plasmid without a terminator-sequence, transcription continues beyond the Nov^R cassette. During this process, anti-sense RNA of the uracil-

DNA glycosylase might be produced, which then interferes with the translation of the glycosylase and further on obstructs its function. Because the uracil-DNA glycosylase is involved in nucleotide synthesis, its presence in the cell is crucial for survival. Therefore, a possible explanation for the failure to construct a deletion mutant with the plasmid pKSII-pib1-4 NovR forward could be, that during passaging, cells carrying the genome copy with the deletion underlie a negative selection pressure. Over time, more and more genome copies with the deletion are lost and the wildtype genome copies are enriched. The fact that 108 clones had to be screened in order to find a candidate that was in fact transformed with pKSII-pib1-4 NovR forward, as compared to the numerous positive candidates obtained after transformation with pKSII-pib1-4 NovR reverse supports this theory.

Fortunately, the creation of the deletion mutant was also pursued with the pKSII-pib1-4 NovR reverse plasmid, in which there should not be any interference with the uracil-DNA glycosylase. Indeed, a homozygous *pibD* deletion mutant was obtained after only 16 passages and Southern Blot analysis confirmed the lack of wildtype genome copies.

Additionally, this *N. magadii* L13::*pibD* mutant strain was complemented in trans with the plasmid pNB102-pibD. The wildtype *N. magadii* L13 strain was also transformed with this plasmid, targeting an over-expression of the *pibD* gene.

After construction of the deletion mutant, analysis of its phenotype was pursued. It could be observed, that neither the deletion mutant, nor the complemented *N. magadii* L13::*pibD* (pNB102-pibD) or the over-expressed *N. magadii* L13 (pNB102-pibD) strain showed growth defects. This is in accordance with the fact, that the presence of flagella is not crucial for cell viability. Of course, the impact of the *pibD* deletion on the assembly of the flagellum had to be determined. Western Blot analysis with an antibody raised against one of the four flagellum proteins confirmed, that the mutant strain lacks flagella on its cell surface. The precursor-flagellins, however, could be detected inside the cells. This validates the importance of PibD for the maturation and assembly of flagella on the surface of *N. magadii*. Importantly, the construction of a strain that procreates non-flagellated cells could finally be realized, considering that the deletion of the flagellin genes themselves remained unsuccessful in previous attempts. As the

flagella mediate the predominant way of motility, an assay was performed that analyzed the motility of the *N. magadii* L13::*pibD* mutant strain. Contrary to the wildtype *N. magadii* L13 strain, the deletion mutant strain was shown to be non-motile. In addition to the above presented proof on the protein level, that the mutant strain lacks flagella, this constitutes the phenotypical proof for the flagellum-deficiency. Motility assays were also performed with the complemented mutant strain and the *pibD* over-expression-strain. The trans-complemented *N. magadii* L13::*pibD* (pNB102-*pibD*) strain was shown to be motile again and therefore recovers the phenotype of the wildtype. Due to the heterologous expression of *pibD* on the plasmid, processing of the precursor flagellins is conducted and assembly of the flagellum takes place. The motility of the *pibD* over-expression-strain is comparable to the wildtype and the complemented mutant strain. Presumably, since only a limited number of precursor-flagellins are present inside the cell, over-expression of the *pibD* gene does not lead to an increased rate of flagellum assembly.

The connection between flagella and surface adhesion was also briefly analyzed. In a very simplified examination, no differences between the wildtype and the *pibD* deletion mutant strain regarding their ability to bind to glass could be observed. However, this experiment is only preliminary and is not sufficient to draw further conclusions. For *H. volcanii*, a defined binding assay with the wildtype strain and a flagellum deletion mutant was conducted, which showed that both strains were able to attach to glass, therefore in *H. volcanii* surface adhesion is not mediated via flagella. However, a *H. volcanii* *pibD* deletion mutant was unable to adhere to glass, suggesting that *pibD* regulates other processes than pre-flagellar processing as well. (83) In order to make statements regarding the role of PibD in surface adhesion of *N. magadii*, the assay established by Tripepi *et al.* (83) should be performed analogously with the *N. magadii* L13::*pibD* strain.

The main question of this study was, whether the flagella of *N. magadii* serve as receptors for the adhesion of the virus Φ Ch1. To target this issue, the infectivity of Φ Ch1 towards wildtype cells was compared with the infectivity towards the mutant strain *N. magadii* L13::*pibD*. As a matter of fact, the flagellum-deficient strain *N. magadii* L13::*pibD* was equally infected with Φ Ch1 as the wildtype. Also, the complemented and overexpressed strains showed no relevant differences in infectivity.

These results led to the conclusion that the flagella of *N. magadii* do not serve as receptors for viral attachment to the cell. The most likely structures for viral attachment are therefore the S-layer glycoproteins of *N. magadii*. However, further experiments have to be conducted to proof this hypothesis.

The role of PibD in *N. magadii* and the question, which structure serves as the receptor for viral attachment has not yet been solved. In the future, studies on the S-layer as a potential receptor have to be conducted. Binding studies with purified S-layer glycoproteins could shed light on this interesting topic. Furthermore, treatment of *N. magadii* L13 cells with bacitracin, which inhibits glycosylation of the S-layer proteins (84) and subsequent analysis of infectivity could help to understand the process of infection. Also, the availability of an antibody raised against PibD would be of great help in studying the functions of this protein in more detail. Several attempts have been made to purify the protein for subsequent immunization of animals to raise antibodies; unfortunately, none of them was fruitful so far. However, this is definitively an issue worth pursuing. In order to confirm once more that the *pibD* deletion mutant strain lacks flagella on its surface, it would also be beneficial to analyze the mutant strain *N. magadii* L13::*pibD* with electron microscopy. Furthermore, the role of PibD in surface adhesion and in the formation of cell-cell contacts would be interesting to explore.

5. REFERENCES

1. **Woese, C. R. and Fox, G. E.** Phylogenetic structure of the prokaryotic domain: The primary kingdoms. *Proc. Natl. Acad. Sci. USA.* 1977, Vol. 74, pp. 5088-5090.
2. **Woese, C. R., Kandler, O. and Wheelis, M. L.** Towards a natural system of organisms: Porposal for the domains *Archaea*, *Bacteria*, and *Eukarya*. *Proc. Natl. Acad. Sci. USA.* 1990, Vol. 87, pp. 4576-4579.
3. **Brochier-Armanet, C., Forterre, P. and Gribaldo, S.** Phylogeny and evolution of the *Archaea*: one hundred genomes later. *Current Opinion in Microbiology.* 2011, Vol. 14, pp. 274-281.
4. **Gribaldo, S. and Brochier-Armanet, C.** The origin and evolution of *Archaea*: a state of the art. *Phil. Trans. R. Soc. B.* 2006, Vol. 361, pp. 1007-1022.
5. **Fendrihan, S., Legat, A., Pfaffenhuemer, M., Gruber, C., Weidler, G., Gerbl, F. and Stan-Lotter, H.** Extremely halophilic *archaea* and the issue of long-term microbial survival. *Rev. Environ. Sci. Biotechnol.* 2006, Vol. 5, 2-3, pp. 203-218.
6. **Klingl, A.** S-layer and cytoplasmic membrane - exceptions from the typical archaeal cell wall with a focus on double membranes. *Frontiers in Microbiology.* 2014, Vol. 5, 624, pp. 1-6.
7. **Oren, A.** Microbial life at high salt concentrations: phylogenetic and metabolic diversity. *Saline Systems.* 2008, Vol. 4, 2.
8. **Youssef, N. H., Ashlock-Savage, K. N. and Elshahed, M. S.** Phylogenetic Diversities and Community Structure of Members of the Extremely Halophilic *Archaea* (Order *Halobacteriales*) in Multiple Saline Sediment Habitats. *Applied and Environmental Microbiology.* 2011, Vol. 78, 5, pp. 1332-1344.
9. **Kushner, D. J.** Life in high salt and solute concentrations. *Microbial Life in Extreme Environments.* 1978, pp. 317-368.
10. **Oren, A.** Diversity of halophilic microorganisms: Environments, phylogeny, physiology, and applications. *Journal of Industrial Microbiology & Biotechnology.* 2002, Vol. 28, pp. 56-63.
11. **Ventosa, A., de la Haba, R. R., Sánchez-Porro, C. and Papke, R. T.** Microbial diversity of hypersaline environments: a metagenomic approach. *Current Opinion in Microbiology.* 2015, Vol. 25, pp. 80-87.
12. **Andrei, A.-S., Banciu, H. L. and Oren, A.** Living with salt: metabolic and phylogenetic diversity of *archaea* inhabiting saline ecosystems. *FEMS Microbiol Lett.* 2012, Vol. 330, pp. 1-9.
13. **Antony, C. P., Kumaresan, D., Hunger, S., Drake, H. L., Murrell, J. C. and Shouche, Y. S.** Microbiology of Lonar Lake and other soda lakes. *International Society for Microbial Ecology.* 2013, Vol. 7, pp. 468-476.
14. **Banciu, H. L. and Muntyan, M. S.** Adaptive strategies in the double-extremophilic prokaryotes inhabiting soda lakes. *Current Opinion in Microbiology.* 2015, Vol. 25, pp. 73-79.

15. **Jain, S., Caforio, A. and Driessen, A. J. M.** Biosynthesis of archaeal membrane ether lipids. *Frontiers in Microbiology*. 2014, Vol. 5, 641, pp. 1-16.
16. **DasSarma, S. and DasSarma, P.** Halophiles and their enzymes: negativity put to good use. *Current Opinion in Microbiology*. 2015, Vol. 25C, pp. 120-126.
17. **Breuert, S., Allers, T., Spohn, G. and Soppa, J.** Regulated Polyploidy in Halophilic *Archaea*. *PLoS one*. 2006, Vol. 1, 1, p. e92.
18. **Hansen, M. T.** Multiplicity of genome equivalents in the radiation-resistant bacterium *Micrococcus radiodurans*. *Journal of Bacteriology*. 1978, Vol. 134, 1, pp. 71-75.
19. **Maisnier-Patin, S., Malandrin, L., Birkeland, N. K. and Bernander, R.** Chromosome replication patterns in the hyperthermophilic euryarchaea *Archaeoglobus fulgidus* and *Methanocaldococcus (Methanococcus) jannaschii*. *Molecular Microbiology*. 2002, Vol. 45, 5, pp. 1443-1450.
20. **Malandrin, L., Huber, H. and Bernander, R.** Nucleoid structure and partition in *Methanococcus jannaschii*: an archaeon with multiple copies of the chromosome. *Genetics*. 1999, Vol. 152, 4, pp. 1315-1323.
21. **Chant, J., Hui, I., Dejongwong, D., Shimmin, L. and Dennis, P. P.** The protein synthesizing machinery of the Archaeobacterium *Halobacterium cutirubrum* molecular characterization. *Sys Appl Microbiology*. 1986, Vol. 7, 1, pp. 106-114.
22. **Zerulla, K. and Soppa, J.** Polyploidy in haloarchaea: advantages for growth and survival. *Frontiers in microbiology*. Vol. 5, 274, pp. 1-8.
23. **Soppa, J.** Evolutionary advantages of polyploidy in halophilic archaea. *Biochem. Soc. Trans.* 2013, Vol. 41, 1, pp. 339-343.
24. **Derntl, C.** Construction of the first deletion mutant of a haloalkalophilic archaeon and analysis of gene expression of the methyltransferase M.NmaΦCh1I of the halophage ΦCh1. *Diploma thesis*. 2009.
25. **Zillig, W., Stetter, K. O. and Janekovic, D.** DNA-Dependent RNA Polymerase from the Archaeobacterium *Sulfolobus acidocaldarius*. *Eur. J. Biochem.* 1979, Vol. 96, pp. 597-604.
26. **Bell, S. D., Magill, C. P. and Jackson, S. P.** Basal and regulated transcription in *Archaea*. *Biochemical Society Transactions*. 2001, Vol. 29, 4.
27. **Grohmann, D. and Werner, F.** Recent advances in the understanding of archaeal transcription. *Current Opinion in Microbiology*. 2011, Vol. 14, pp. 328-334.
28. **Aravind, L. and Koonin, E. V.** DNA-binding proteins and evolution of transcription regulation in the archaea. *Nucleic Acids Research*. 1999, Vol. 27, 23, pp. 4658-4670.
29. **Farkas, J. A., Picking, J. W. and Santangelo, T. J.** Genetic Techniques for the *Archaea*. *Annu. Rev. Genet.* 2013, Vol. 47, pp. 539-561.
30. **Holmes, M. L., Scopes, R. K., Moritz, R. L., Simpson, R. J., Englert, C., Pfeifer, F. and Dyall-Smith, M. L.** Purification and analysis of an extremely halophilic β-galactosidase from *Haloferax alicantei*. *Biochimica et Biophysica Acta*. 1997, pp. 276-286.

31. **Holmes, M. L. and Dyall-Smith, M. L.** Sequence and expression of a halobacterial β -galactosidase gene. *Molecular Microbiology*. 2000, Vol. 36, 1, pp. 114-122.
32. **Patenge, N., Haase, A., Bolhuis, H. and Oesterhelt, D.** The gene for a halophilic β -galactosidase (*bgaH*) of *Haloferax alicantei* as a reporter gene for promoter analyses in *Halobacterium salinarum*. *Molecular Microbiology*. 2000, Vol. 36, 1, pp. 105-113.
33. **Gregor, D. and Pfeifer, F.** Use of halobacterial *bgaH* reporter gene to analyse the regulation of gene expression in halophilic archaea. *Microbiology*. 2001, Vol. 147, pp. 1745-1754.
34. **Jarell, K. F. and McBride, M. J.** The surprisingly diverse ways that prokaryotes move. *Nature Reviews Microbiology*. 2008, Vol. 6, pp. 466-476.
35. **Ghosh, A. and Albers, S.-V.** Assembly and function of the archaeal flagellum. *Biochemical Society Transactions*. 2011, Vol. 39, pp. 64-69.
36. **Albers, S.-V., Szabó, Z. and Driessen, A. J. M.** Protein secretion in the Archaea: multiple paths towards a unique cell surface. *Nature Reviews*. 2006, Vol. 4, pp. 537-547.
37. **Albers, S.-V. and Jarell, K. F.** The archaeellum: how Archaea swim. *Frontiers in Microbiology*. 2015, Vol. 6, 23, pp. 1-12.
38. **Alam, M. and Oesterhelt, D.** Morphology, function and isolation of halobacterial flagella. *Journal of Molecular Biology*. 1984, Vol. 176, 4, pp. 459-475.
39. **Bardy, S. L. and Jarell, K. F.** Cleavage of preflagellins by an aspartic acid signal peptidase is essential for flagellation in the archaeon *Methanococcus voltae*. *Molecular Microbiology*. 2003, Vol. 50, 4, pp. 1339-1347.
40. **Szabó, Z., Albers, S.-V. and Driessen, A. J. M.** Active-Site Residues in the Type IV Prepilin Peptidase Homologue PibD from the Archaeon *Sulfolobus solfataricus*. *Journal of Bacteriology*. 2006, Vol. 188, 4, pp. 1437-1443.
41. **Ng, S. Y., Chaban, B. and Jarell, K. F.** Archaeal flagella, bacterial flagella and type IV pili: a comparison of genes and posttranslational modifications. *J Mol Microbiol Biotechnol*. 2006, Vol. 11, 3-5, pp. 167-191.
42. **Thomas, N. A., Chao, E. D. and Jarell, K. F.** Identification of amino acids in the leader peptide of *Methanococcus voltae* preflagellin that are important in posttranslational processing. *Arch Microbiol*. 2001, Vol. 175, pp. 263-269.
43. **Ng, S. Y. M., VanDyke, D. J., Chaban, B., Wu, J., Nosaka, Y., Aizama, S.-I. and Jarell, K. F.** Different Minimal Signal Peptide Lengths Recognized by the Archaeal Prepilin-Like Peptidases FlaK and PibD. *Journal of Bacteriology*. 2009, Vol. 191, 21, pp. 6732-6740.
44. **Albers, S.-V., Szabó, Z. and Driessen, A. J. M.** Archaeal Homolog of Bacterial Type IV Prepilin Signal Peptidases with Broad Substrate Specificity. *Journal of Bacteriology*. 2003, Vol. 185, 13, pp. 3918-3925.
45. **Tindall, B. J., Ross, H. N. M. and Grant, W. D.** *Natronobacterium* gen. nov. and *Natronococcus* gen. nov., Two New Genera of Haloalkaliphilic Archaeobacteria. *Syst. Appl. Microbiology*. 5, 1984, pp. 41-57.

46. **Kamekura, M., Dyall-Smith, M. L., Upsani, V., Ventosa, A. and Kates, M.** Diversity of Alkaliphilic Halobacteria: Proposals for Transfer of *Natronobacterium vacuolatum*, *Natronobacterium magadii*, and *Natronobacterium pharaonis* to *Halorubrum*, *Natrialba*, and *Natronomonas* gen. nov., respectively, as *Halorubrum*. *Int. J. Syst. Bacteriol.* 1997, Vol. 47, 3, pp. 853-857.
47. **Kamekura, M. and Dyall-Smith, M. L.** Taxonomy of the family *Halobacteriaceae* and the description of two new genera *Halorubrobacterium* and *Natrialba*. *J. Gen. Appl. Microbiology.* 1995, Vol. 41, pp. 333-350.
48. **Witte, A., Baranyi, U., Klein, R., Sulzner, M., Luo, Ch., Wanner, G., Krüger, D. H. and Lubitz, W.** Characterization of *Natronobacterium magadii* phage Φ Ch1, a unique archaeal phage containing DNA and RNA. *Molecular Microbiology.* 1997, Vol. 23, 3, pp. 603-616.
49. **Iro, M.** Characterisation of the regulatory region of the virus Φ Ch1 infecting *Natrialba magadii*. *Dissertation.* 2006.
50. **Cline, S. W. and Doolittle, W. F.** Efficient Transfection of the Archaeobacterium *Halobacterium halobium*. *Journal of Bacteriology.* 1987, Vol. 169, 3, pp. 1341-1344.
51. **Mayrhofer-Iro, M., Ladurner, A., Meissner, C., Derntl, C., Reiter, M., Haider, F., Dimmel, K., Rössler, N., Klein, R., Baranyi, U., Scholz, H. and Witte, A.** Utilization of Virus Φ Ch1 Elements To Establish a Shuttle Vector System for Halo(alkali)philic *Archaea* via Transformation of *Natrialba magadii*. *Applied and Environmental Microbiology.* 2013, Vol. 79, 8, pp. 2741-2748.
52. **Mizuuchi, K., O'Dea, M. H. and Gellert, M.** DNA gyrase: Subunit structure and ATPase activity of the purified enzyme. *Proc. Natl. Acad. Sci USA.* 1978, Vol. 75, 12, pp. 5960-5963.
53. **Holmes, M. L. and Dyall-Smith, M. L.** Mutations in DNA Gyrase Result in Novobiocin Resistance in Halophilic Archaeobacteria. *Journal of Bacteriology.* 1991, Vol. 173, 2, pp. 642-648.
54. **Lam, W. L. and Doolittle, W. F.** Mevinolin-resistant Mutations Identify a Promoter and the Gene for a Eukaryote-like 3-Hydroxy-3-methylglutaryl-coenzyme A Reductase in the Archaeobacterium *Haloferax volcanii*. *The Journal of Biological Chemistry.* 1992, Vol. 267, 9, pp. 5829-5834.
55. **Ng, W.-L. and DasSarma, S.** Minimal Replication Origin of the 200-Kilobase Halobacterium Plasmid pNRC100. *Journal of Bacteriology.* 1993, Vol. 175, 15, pp. 4584-4596.
56. **Zhou, M., Xiang, H., Sun, C. and Tan, H.** Construction of a novel shuttle vector based on an RCR-plasmid from a haloalkaliphilic archaeon and transformation into other haloarchaea. *Biotechnol. Lett.* 2004, Vol. 26, 4, pp. 1107-1113.
57. **Alte, B.** Konstruktion einer Flagellum-Deletionsmutante in *Natrialba magadii* und Charakterisierung bestehender *Natrialba magadii* Mutanten. *Diploma thesis.* 2011.
58. **Schöner, L.** Construction of different mutants of *N. magadii* and the influence of different Φ Ch1 ORF's on *N. magadii*. *Master thesis.* 2013.
59. **Pfeifer, F., Griffig, J. and Oesterhelt, D.** The *fdx* gene encoding the [2Fe--2S] ferredoxin of *Halobacterium salinarum* (*H. halobium*). *Mol Gen Genet.* 1993, Vol. 239, 1-2, pp. 66-71.
60. **Gregor, D and Pfeifer, F.** In vivo analyses of constitutive and regulated promoters in halophilic *archaea*. *Microbiology.* 151, 2005, pp. 25-33.

61. **Svoboda, T.** Characterization of putative repressors of the temperate phage Φ Ch1 and analysis of the flagellum operon as a putative receptor of Φ Ch1. *Diploma thesis*. 2011.
62. **Fedorov, O. V., Pyatibratov, M. G., Kostyukova, A. S., Osina, N. K. and Tarasov, V. Y.** Protofilament as a structural element of flagella of haloalkalophilic archaeobacteria. *Can J Microbiol.* 1994, Vol. 40, pp. 45-53.
63. **Pyatibratov, M. G., Leonard, K., Tarasov, V. Y. and Fedorov, O. V.** Two immunologically distinct types of protofilaments can be identified in *Natrialba magadii* flagella. *FEMS Microbiology Letters*. 2002, Vol. 212, pp. 23-27.
64. **Serganova I, Ksenzenko V, Serganov A, Meshcheryakova I, Pyatibratov M, Vakhrusheva O, Metlina A, Fedorov O.** Sequencing of Flagellin Genes from *Natrialba magadii* Provides New Insight into Evolutionary Aspects of Archaeal Flagellins. *Journal of Bacteriology*. Vol. 184, No. 1, 2002, pp. 318-322.
65. **Pietilä, M. K., Demina, T. A., Atanasova, N. S., Oksanen, H. M. and Bamford, D. H.** Archaeal viruses and bacteriophages: comparisons and contrasts. *Trends in Microbiology*. 2014, Vol. 22, 6, pp. 334-344.
66. **Atanasova, N. S., Oksanen, H. M. and Bamford, D. H.** Haloviruses of archaea, bacteria, and eukaryotes. *Current Opinion in Microbiology*. 2015, Vol. 25, pp. 40-48.
67. **Sencilo, A. and Roine, E.** A Glimpse of the genomic diversity of haloarchaeal tailed viruses. *Frontiers in Microbiology*. 2014, Vol. 5, 84, pp. 1-6.
68. **Schnabel, H., Zillig, W., Pfäffle, M., Schnabel, R., Michel, H. and Delius, H.** *Halobacterium halobium* phage Φ H. *The EMBO Journal*. 1982, Vol. 1, 1, pp. 87-92.
69. **Dyall-Smith, M., Tang, S.-L. and Bath, C.** Haloarchaeal viruses: how diverse are they? *Research in Microbiology*. 2003, Vol. 154, pp. 309-313.
70. **Klein, R., Baranyi, U., Rössler, N., Greineder, B., Scholz, H. and Witte, A.** *Natrialba magadii* virus Φ Ch1: first complete nucleotide sequence and functional organization of a virus infecting a haloalkaliphilic archaeon. *Molecular Microbiology*. 2002, Vol. 45, 3, pp. 851-863.
71. **Matagne, A., Joris, B. and Frère, J.-M.** Anomalous behaviour of a protein during SDS/PAGE corrected by chemical modification of carboxylic groups. *Biochem. J.* 1991, Vol. 280, pp. 553-556.
72. **Iro, M., Klein, R., Gálos, B., Baranyi, U., Rössler, N. and Witte, A.** The lysogenic region of virus Φ Ch1: identification of a repressor-operator system and determination of its activity in halophilic Archaea. *Extremophiles*. 2007, Vol. 11, pp. 383-396.
73. **Reiter, M.** Gene regulation of Φ Ch1: characterization of ORF49 and further characterization of the origin of replication of the halophage Φ Ch1. *Diploma thesis*. 2010.
74. **Klein, R., Greineder, B., Baranyi, U. and Witte, A.** The Structural Protein E of the Archaeal Virus Φ Ch1: Evidence for Processing in *Natrialba magadii* during Virus Maturation. *Virology*. 2000, Vol. 276, pp. 376-387.
75. **Baranyi, U., Klein, R., Lubitz, W., Krüger, D. H. and Witte, A.** The archaeal halophilic virus-encoded Dam-like methyltransferase M. Φ Ch1-I methylates adenine residues and complements dam mutants in the low salt environment of *Escherichia coli*. *Molecular Microbiology*. 2000, Vol. 35, 5, pp. 1168-1179.

76. **Klein R, Rössler N, Iro M, Scholz H and Witte A.** Haloarchaeal myovirus Φ Ch1 harbours a phase variation system for the production of protein variants with distinct cell surface adhesion specificities. *Molecular Microbiology*. 2012, 83(1), pp. 137-150.
77. **Rössler, N., Klein, R., Scholz, H. and Witte, A.** Inversion within the haloalkaliphilic virus Φ Ch1 DNA results in differential expression of structural proteins. *Molecular Microbiology*. 2004, Vol. 52, 2, pp. 413-426.
78. **Kixmüller, D and Greie, JC.** Construction and Characterization of a Gradually Inducible. *Applied and Environmental Microbiology*. 78, 7, 2012, pp. 2100-2105.
79. **Selb, R.** Construction of mutants of *N. magadii* and Φ Ch1. *Diploma thesis*. 2010.
80. **Hofbauer, C.** The function of gp34 and its regulation by ORF79 of Φ Ch1 as well as the influence of other regulation elements. *Master thesis*. 2015.
81. **Dimmel, K.** Construction of an ORF34 deletion Φ Ch1 strain and secretion of putative tail fibre proteins. *Diploma thesis*. 2013.
82. **Till, P.** Deletion of the tail-fibre protein of Φ Ch1 and further characterization of the inversion within its gene locus. *Diploma thesis*. 2011.
83. **Tripepi M, Imam S and Pohlschröder M.** *Haloferax volcanii* Flagella Are Required for Motility but Are Not Involved in PibD-Dependent Surface Adhesion. *Journal of Bacteriology*. Vol. 192, No. 12, 2010, pp. 3093-3102.
84. **Mescher, M. F. and Strominger, J. L.** Structural (shape-maintaining) role of the cell surface glycoprotein of *Halobacterium salinarium*. *Proc. Natl. Acad. Sci. USA*. 1976, Vol. 73, 8, pp. 2687-2691.

6. LIST OF FIGURES AND TABLES

FIGURE 1: OVERVIEW OF THE DOMAIN <i>ARCHAEA</i>	11
FIGURE 2: STRUCTURES OF SEVERAL MEMBRANE LIPIDS IN <i>ARCHAEA</i>	13
FIGURE 3: STRUCTURE OF THE ARCHAEAL FLAGELLUM AND ORGANIZATION OF THE <i>FLA</i> OPERON	19
FIGURE 4: MORPHOLOGY OF <i>N. MAGADII</i>	21
FIGURE 5: ILLUSTRATION OF THE <i>FLAB</i> GENES OF <i>N. MAGADII</i>	25
FIGURE 6: ELECTRON MICROGRAPH AND ILLUSTRATION OF VIRUS Φ CH1.....	27
FIGURE 7: GENOME ORGANIZATION OF THE VIRUS Φ CH1	29
FIGURE 8: SCHEMATIC ILLUSTRATION OF CONSTRUCT PRO-5-FDX-BGAH.....	63
FIGURE 9: SCHEMATIC ILLUSTRATION OF PLASMID PRO-5-TNAN-BGAH.....	64
FIGURE 10: SCHEMATIC ILLUSTRATION OF PRIMER BINDING SITES ON THE PLASMID PRO-5-FDX-BGAH.....	64
FIGURE 11: RESULTS FROM BGAH-MEASUREMENTS OF STRAINS <i>N. MAGADII</i> L13 (PRO-5-FDX-BGAH), <i>N. MAGADII</i> L13 (PRO-5-TNAN-BGAH) AND <i>N. MAGADII</i> L13	65
FIGURE 12: GROWTH CURVE OF <i>N. MAGADII</i> L13 AND <i>N. MAGADII</i> L13 (PRO-5-FDX-BGAH) (DATA OBTAINED IN COURSE OF BGAH-MEASUREMENTS).....	66
FIGURE 13: SCHEMATIC ILLUSTRATION OF A DOUBLE-CROSSOVER EVENT.....	71
FIGURE 14: SCHEMATIC ILLUSTRATION OF PKSII-PIB1-4 NOVR FORWARD PRIMER BINDING SITES.....	73
FIGURE 15: PCR ANALYSIS OF <i>N. MAGADII</i> L13 (PKSII-PIB1-4 NOVR FORWARD) CANDIDATE AFTER THE 50 TH PASSAGE	74
FIGURE 16: SCHEMATIC ILLUSTRATION OF PKSII-PIB1-4 NOVR REVERSE PRIMER BINDING SITES	75
FIGURE 17: ANALYSIS OF <i>N. MAGADII</i> L13 CANDIDATES AFTER TRANSFORMATION WITH PKSII-PIB1-4 NOVR REVERSE	76
FIGURE 18: PCR-ANALYSIS OF PUTATIVE DELETION MUTANT <i>N. MAGADII</i> L13:: <i>PIBD</i> AFTER 16 PASSAGES	77
FIGURE 19: SCHEMATIC ILLUSTRATION OF EXPERIMENTAL SETUP FOR SOUTHERN BLOT ANALYSIS...78	
FIGURE 20: SOUTHERN BLOT ANALYSIS OF <i>N. MAGADII</i> L13 AND <i>N. MAGADII</i> L13:: <i>PIBD</i>	79
FIGURE 21: ANALYSIS OF CANDIDATES AFTER TRANSFORMATION WITH PNB102-PIBD	81
FIGURE 22: GROWTH CURVE OF STRAINS <i>N. MAGADII</i> L13, <i>N. MAGADII</i> L13:: <i>PIBD</i> , <i>N. MAGADII</i> L13 (PNB102-PIBD) AND <i>N. MAGADII</i> L13:: <i>PIBD</i> (PNB102-PIBD)	82
FIGURE 23: WESTERN BLOT OF <i>N. MAGADII</i> L13 AND <i>N. MAGADII</i> L13:: <i>PIBD</i> SAMPLES (PELLET AND SUPERNATANT) WITH A-FLAB1	83
FIGURE 24: MOTILITY ASSAY WITH STRAINS <i>N. MAGADII</i> L13, <i>N. MAGADII</i> L13:: <i>PIBD</i> , <i>N. MAGADII</i> L13 (PNB102-PIBD) AND <i>N. MAGADII</i> L13:: <i>PIBD</i> (PNB102-PIBD)	85
FIGURE 25: COMPARISON OF FLASKS AFTER INCUBATION WITH <i>N. MAGADII</i> L13 AND <i>N. MAGADII</i> L13:: <i>PIBD</i>	86
TABLE 1: MOLECULAR MASSES OF SUBUNIT FLAGELLINS OF <i>N. MAGADII</i>	24
TABLE 2: RESULTS FROM THE PLAQUE ASSAY OF STRAINS <i>N. MAGADII</i> L13, <i>N. MAGADII</i> L13:: <i>PIBD</i> , <i>N. MAGADII</i> L13 (PNB102-PIBD) AND <i>N. MAGADII</i> L13:: <i>PIBD</i> (PNB102-PIBD).....	87

7. ABSTRACT

The availability of efficient gene expression systems is crucial for scientific progress. Since such a system is missing for the haloalkaliphilic archaeon *Natrialba magadii*, the first part of this thesis focuses on the characterization of the ferredoxin promoter (*pdfx*) and its suitability for the establishment of a gene expression system within *N. magadii*. Analysis of the promoter strength using the reporter gene *bgaH* revealed, that *pdfx* of *N. magadii* is a very strong and constitutively active promoter. Preliminary experiments showed no correlation between the promoter strength and iron-availability. The obtained results indicate, that *pdfx* is suitable for homologous gene expression in *N. magadii*.

The second part of this thesis deals with the question, if the flagella of *N. magadii* could serve as receptors for the attachment of the virus Φ Ch1 to the archaeon. It was already discovered, that the tail-fibre protein gp34₅₂ is responsible for the attachment of the virus particle to *N. magadii* via its galactose-binding domain. Therefore, it is assumed that the virus attaches to glycosylated structures on the cell surface of *N. magadii*. Two structures are worth considering: the glycosylated flagellum- or S-layer proteins. To gain insight into the mechanism of attachment, the flagellum-deficient mutant strain *N. magadii* L13::*pibD* was constructed in the course of this thesis. This was achieved by deleting the peptidase *pibD*, which is responsible for the processing of the pre-flagellins and subsequent assembly of the flagellum. It was shown that the deletion mutant strain is non-motile as a consequence of the lack of flagella. Nevertheless, no decrease in Φ Ch1 infectivity towards the mutant strain compared to the wildtype strain was observed. From this results it can be concluded, that the flagellum proteins of *N. magadii* do not serve as receptors for the attachment of Φ Ch1.

8. ZUSAMMENFASSUNG

Die Verfügbarkeit effizienter Genexpressions-Systeme ist unerlässlich für wissenschaftlichen Fortschritt. Da solch ein System für das haloalkaliphile Archaeon *Natrialba magadii* nicht verfügbar ist, konzentriert sich der erste Teil dieser Masterarbeit auf die Charakterisierung des Ferredoxin-Promoters (*pfdx*) und dessen Eignung für die Entwicklung eines Genexpressions-Systems in *N. magadii*. Die Analyse der Promoter-Stärke mithilfe des Reporter-Gens *bgaH* zeigte, dass *pfdx* ein sehr starker und konstitutiv aktiver Promoter ist. Erste Experimente zeigten keinen Zusammenhang zwischen der Promoter-Stärke und der Eisen-Verfügbarkeit. Die erlangten Ergebnisse zeigen, dass *pfdx* für homologe Genexpression in *N. magadii* geeignet ist.

Der zweite Teil dieser Masterarbeit beschäftigt sich mit der Frage, ob die Flagellen von *N. magadii* möglicherweise als Rezeptoren für die Bindung des Virus Φ Ch1 an die Zelle dienen könnten. Es wurde bereits entdeckt, dass das „tail fibre“ Protein gp34₅₂ mittels seiner Galactose-Bindedomäne für das Anhaften des Virus-Partikels an *N. magadii* zuständig ist. Daher vermutet man, dass der Virus an glycosylierte Strukturen an der Zelloberfläche von *N. magadii* bindet. Zwei Strukturen kommen dabei in Frage: die glycosylierten Flagellum- oder S-layer-Proteine. Um einen Einblick in den Mechanismus des Anhaftens zu bekommen, wurde im Zuge dieser Masterarbeit ein Mutanten-Stamm konstruiert, der keine Flagellen besitzt (*N. magadii* L13::*pibD*). Das wurde erreicht durch die Deletion der Peptidase *pibD*, welche verantwortlich ist für das Prozessieren der Pre-Flagelline und in weiterer Folge die Zusammensetzung des Flagellums ermöglicht. Es wurde gezeigt, dass dieser Deletions-Mutanten-Stamm aufgrund des Fehlens von Flagellen unbeweglich ist. Nichtsdestotrotz konnte keine Verringerung der Infektiosität von Φ Ch1 gegenüber den Mutanten-Stamm im Vergleich zum Wildtyp-Stamm beobachtet werden. Aus diesen Ergebnissen kann man schließen, dass die Flagellum-Proteine nicht als Rezeptoren für das Anhaften von Φ Ch1 dienen.

9. APPENDIX

9.1. Acknowledgement

First of all, I want to thank my supervisor Dr. Angela Witte for her support during the whole time of my study. I learned a lot about microbiology in general and the exciting topic of *Archaea*, but most importantly I was able to improve my scientific skills. I want to thank her for her patience regarding all my questions and the many advices.

Next, I want to express my thankfulness towards my colleagues Christoph Hofbauer and Kathrin Schönfelder. Besides introducing me into our lab, they were substantial for the good working atmosphere; I will always remember the fun times we had. I also want to say thanks to Flora Haider, who helped to improve my teaching skills and showed me the precious sides of teaching.

Special thanks go to my dear friend Maria Schöllner, who was a major help in writing this thesis. A big “thank you” also goes to my close friends Maria Österbauer and Mirjam Zimmermann. They always had time for scientific discussions and supported me with valuable advice regarding my project.

Most important, I want to express my deep gratitude towards my family: my mother Gerda, her partner Christian and my sister Katharina. I appreciate their huge support very much.

Last, I want to thank my partner Andreas for his endless encouragement and support.

This thesis is dedicated to my beloved father Stefan.

9.2. Curriculum vitae

Personal details:

Name: Agnes Kogler
 Date of Birth: 10. November 1990
 Place of Birth: Oberndorf bei Salzburg
 Nationality: Austria

Education:

2014 - 2015 Master thesis: group of Prof. Dr. Angela Witte at the Department of Microbiology, Immunobiology and Genetics at the University of Vienna
 2013 - 2015 Study “Molecular Microbiology and Immunobiology” (Master) with focus on Molecular Microbiology at the University of Vienna
 2009 - 2013 Study “Biology” (Bachelor) with focus on Microbiology and Genetics at the University of Vienna
 2001 - 2009 Bundesrealgymnasium Braunau am Inn, Austria
 1997 – 2001 Volksschule Schalchen, Austria

Working experience:

Summer term 2014 Tutor of students in practical course “Übungen in Molekularer Mikrobiologie” at the University of Vienna
 Summer term 2014 Tutor of students in practical course “Molekularbiologie III LAB” at the FH Campus Wien
 Winter term 2014/2015 Tutor of students in practical course “Übungen in Molekularer Mikrobiologie” at the University of Vienna
 Winter term 2014/2015 Tutor of students in practical course “Molekularbiologie II LAB” at the FH Campus Wien